



DOCTORAL DISSERTATION

TRINH VAN QUYEN

Miskolc - Hungary
2019



UNIVERSITY OF MISKOLC
FACULTY OF EARTH SCIENCE & ENGINEERING
Institute of Raw Material Preparation and Environmental Processing

..... ****



DOCTORAL DISSERTATION

INVESTIGATION OF PRESSURE AGGLOMERATION PROCESS OF BIOMASS

TRINH VAN QUYEN

Scientific supervisors:

Prof. Dr. habil. Barnabás Csőke

Assoc. Prof. Dr. Sándor Nagy

MIKOVINY SÁMUEL DOCTORAL SCHOOL OF EARTH SCIENCES
Head of the Doctoral School: Prof. Dr. habil. Péter Szűcs

Hungary, 2019

DECLARATION

I hereby confirm that this dissertation was composed by myself and that the work contained here is my own, except where clearly stated otherwise. I also wish to state that this work has not been submitted elsewhere for any other degree or professional qualification. All the experiments in this dissertation were carried out at the laboratory of the University of Miskolc from where the data and information presented herein were gotten and I actively participated in the experiment's preparation and execution. The analyses and interpretation of data are entirely mine.

Signed: **Trinh Van Quyen**

Miskolc, January 2019

ACKNOWLEDGEMENTS

I would like to express my gratitude to the following persons for their constant support throughout this research work:

My supervisors Prof. Dr. Barnabás Csőke and Assoc. Prof. Dr. Sándor Nagy for their sincere support, time spent and supervision on this project. My research work would not have been possible without their constant guidance and thoughtful remarks.

Assoc. Prof. Dr. Gábor Mucsi is thanked for his valuable comments and suggestions. Assoc. Prof. Dr. Gombkötő Imre role as Director of Institute of Raw Material Preparation and Environmental Processing for his encouragement all through the PhD program.

Dr. Ádám Rácz and Dr. Tamás Magyar for support during optical microscopy; Viktor Kövesi for manufacturing the single pelletizer unit; Szilveszterné Bernáth, Ferencné Seszták, László Vass for support during labour-work; Gábor Antal for sincere suggestions and comments about pressure distribution; Dr. Vuné Király Ildikó and Msc. Ihemaguba Chukwuemeka for advice during the thesis writing process.

Stipendium Hungaricum Scholarship for funds supporting portions of this project, Nature Gold Farms Ltd. for supporting with spelt chaff raw material.

The described work was carried out as part of the “Sustainable Raw Material Management Thematic Network - RING 2017”, EFOP-3.6.2-16-2017-00010 project in the framework of the Széchenyi 2020 program. The realization of this project is supported by the European Union, co-financed by the European Social Fund.

Family members, friends and colleagues at Quang Ninh University of Industry for their earnest encouragement all through the PhD program.

Very special thanks go to my mother Mrs. Bui Thi Dang, who love me more than herself, and my sweet wife Mrs. Pham Thi Mien for their constant love, encouragement, understanding and sacrifice, which were the source of my motivation for completion of this doctoral dissertation.

TABLE OF CONTENTS

DECLARATION.....	1
ACKNOWLEDGEMENTS	2
TABLE OF CONTENTS.....	3
LIST OF TABLES	7
LIST OF FIGURES.....	8
ABBREVIATIONS.....	11
CHAPTER 1. INTRODUCTION.....	12
CHAPTER 2. LITERATURE OVERVIEW	14
2.1. Processes of agglomeration	14
2.1.1. <i>Pressure agglomeration</i>	14
2.1.2. <i>Growth agglomeration</i>	14
2.1.3. <i>Sintering</i>	14
2.2. Binding mechanism, binding forces, binders and binder-less of agglomeration.....	15
2.2.1. <i>Binding mechanism</i>	15
2.2.2. <i>Binding forces</i>	17
2.2.3. <i>Binders and binder-less of agglomeration</i>	17
2.2.4. <i>Binding process in the case of biomass</i>	18
2.3. Agglomeration of biomass.....	18
2.3.1. <i>Biomass</i>	18
2.3.2. <i>Binding by lignocellulosic</i>	20
2.3.3. <i>Particle shrinkage</i>	20
2.3.4. <i>Particle size distribution</i>	21
2.3.5. <i>Effect of moisture content</i>	21
2.3.6. <i>Effect of temperature</i>	21
2.4. Description of pressure agglomeration.....	21
2.4.1. <i>Pressure agglomeration principle</i>	21
2.4.2. <i>Compressibility - Theoretical background</i>	22
2.4.3. <i>Compactibility</i>	23
2.5. Equipment of pressure agglomeration	24
2.5.1. <i>Piston press</i>	24
2.5.2. <i>Roll press</i>	25

2.5.3. Extrusion (briquetting in open form)	27
2.5.4. Flat die pelletizer	27
2.5.5. Ring die pelletizer.....	29
2.6. Strength of agglomerates	30
2.6.1. Theory of the strength of agglomerates.....	30
2.6.2. Determination of agglomerate strength	30
2.7. Modelling of pelletizer.....	31
2.7.1. Previous research in the press channel model.....	31
2.7.2. Previous research in the applied pressure and backup pressure.....	31
CHAPTER 3. MATERIALS AND METHODS OF RESEARCH WORK.....	33
3.1. Materials	33
3.1.1. Spelt chaff and ground post-agglomerated spelt chaff.....	33
3.1.2. Beech sawdust	34
3.1.3. Acacia mangium sawdust	35
3.1.4. Rice straw	37
3.2. Hydraulic piston press at the University of Miskolc	38
3.3. Flat die pelletizer at the University of Miskolc	39
3.4. Measurement of density	40
3.5. Spring-back ratio.....	40
3.6. Structure of tablets and falling test method	40
CHAPTER 4. DEVELOPMENT OF EQUIPMENT	41
4.1. Single pelletizer unit 1	41
4.1.1. Development of single pelletizer unit 1	41
4.1.2. Determination of compressibility of ground post-agglomerated spelt chaff....	42
4.1.3. Pellet production by flat die pelletizer	43
4.1.4. Pellet production by single pelletizer unit 1.....	44
4.2. Single pelletizer unit 2	45
4.2.1. Development of single pelletizer unit 2	45
4.2.2. Determination of backup pressure distribution procedure	48
4.2.3. Backup pressure and pellet density distribution in the press channel	49
4.3. Evaluation and discussion.....	51
4.3.1. Single pelletizer unit 1	51
4.3.2. Single pelletizer unit 2	52
CHAPTER 5. EFFECT OF MOISTURE CONTENT AND PARTICLE SIZE ON BIOMASS AGGLOMERATION	53

5.1. Experimental procedure	53
5.2. Tablet density.....	53
5.2.1. Tablets made from beech sawdust.....	53
5.2.2. Tablets made from spelt chaff	55
5.3. Spring-back ratio of tablets.....	57
5.3.1. Tablets made from beech sawdust.....	57
5.3.2. Tablets made from spelt chaff	58
5.4. Structure of tablets.....	59
5.4.1. Tablets made from beech sawdust.....	59
5.4.2. Tablets made from spelt chaff	59
5.5. Tablet strength	60
5.6. Evaluation and discussion.....	61
CHAPTER 6. TEMPERATURE, PARTICLE SIZE AND SEASONING EFFECTS ON BIOMASS AGGLOMERATION	62
6.1. Experimental procedure	62
6.2. Tablet density.....	62
6.2.1. Tablets made from beech sawdust.....	62
6.2.2. Tablets made from spelt chaff	64
6.2.3. Tablets made from <i>Acacia mangium</i>	66
6.3. Spring-back ratio of tablets.....	69
6.3.1. Tablets made from spelt chaff	69
6.3.2. Tablets made from <i>A. mangium</i> one month seasoned wood	69
6.4. Structure of tablets.....	70
6.5. Tablet strength	71
6.5.1. Tablets made from <i>Acacia mangium</i>	71
6.5.2. Tablets made from beech sawdust.....	72
6.6. Evaluation and discussion.....	73
CHAPTER 7. CORRELATION OF LIGNIN, CELLULOSE AND STARCH WITH BIOMASS AGGLOMERATION	74
7.1. Determination of ligin, cellulose and starch content	74
7.2. Tablet density.....	74
7.3. Spring-back ratio of tablets.....	77
7.4. Structure of tablets.....	77
7.5. Tablet strength	78
7.6. Evaluation and discussion.....	79

CHAPTER 8. THE APPLICABILITY OF THE RESULTS AND FURTHER DEVELOPMENT OPPORTUNITIES.....	81
8.1. New model single pelletizer unit	81
8.1.1. <i>Single pelletizer unit 1</i>	81
8.1.2. <i>Single pelletizer unit 2</i>	81
8.2. Relationship between moisture content and density of tablets	81
8.3. Relationship between temperature, seasoning and density of tablets	82
8.4. Spring-back ratio, porosity and strength of tablets	82
8.4.1. <i>Spring-back ratio of tablets</i>	82
8.4.2. <i>Porosity of tablets</i>	82
8.4.3. <i>Tablet strength</i>	83
8.5. Correlation of lignin, cellulose and starch with biomass agglomeration.....	83
8.6. Further development opportunities	84
PUBLICATIONS RELATED TO THIS DISSERTATION	85
REFERENCES	87
APPENDIX I: Reproducibility examination.....	96
APPENDIX II: Correlation examination.....	96

LIST OF TABLES

Table 2.1. Lignin and cellulose content in % of beech and spelt chaff..... 19

Table 3.1. Speed of piston 38

Table 4.1. Tablet density values for GPA- spelt chaff with particle size < 1 mm 42

Table 4.2. Measured geometrical parameters and density of pellets..... 43

Table 4.3. Pellet process parameters 44

Table 4.4. Pellet density distribution..... 50

Table 4.5. Relationship between layer number and backup pressure..... 50

Table 4.6. Relationship between density of pellets and backup pressure..... 51

Table 5.1. Constants of Johanson’s equation for beech sawdust with different moisture contents ($x < 1$ mm)..... 54

Table 5.2. Constants of Johanson’s equation for beech sawdust with different moisture contents ($x < 2$ mm)..... 54

Table 5.3. Constants of Johanson’s equation for spelt chaff with different moisture contents ($x < 1.6$ mm) 57

Table 6.1. Constants of Johanson’s equation for beech sawdust with different temperatures ($x < 1$ mm)..... 63

Table 6.2. Constants of Johanson’s equation for beech sawdust with different temperatures ($x < 2$ mm)..... 63

Table 6.3. Constants of Johanson’s equation for spelt chaff with different temperatures .. 65

Table 6.4. Constants of Johanson’s equation for *A. mangium* one month seasoned wood with different temperatures ($x < 0.8$ mm)..... 67

Table 6.5. Constants of the Johanson equation for *A. mangium* one month seasoned wood with different temperatures ($x < 1.6$ mm) 67

Table 6.6. Constants of Johanson’s equation for *A. mangium* six months seasoned wood with different temperatures ($x < 1.6$ mm)..... 68

Table 7.1. Lignin, cellulose, starch content and particle density of biomass materials 74

Table 7.2. Constants of Johanson’s equation for various materials with the same production conditions 76

LIST OF FIGURES

Figure 2.1. Growth agglomeration and its product..... 14

Figure 2.2. Principle of laser sintering 15

Figure 2.3. Binding mechanism between solid particles 16

Figure 2.4. States of liquid bonding in a bulk material; (a) Pendular state; (b) Funicular state; (c) Capillary state..... 17

Figure 2.5. Lignocellulose and its components 19

Figure 2.6. Pressure agglomeration principle 21

Figure 2.7. Sketches explaining the mechanism of pressure agglomeration..... 22

Figure 2.8. Illustration tablet press machine and products 25

Figure 2.9. Roller press technology..... 26

Figure 2.10. Briquetting machine 26

Figure 2.11. Illustration biomass extrusion machine and products 27

Figure 2.12. Roller and flat die..... 28

Figure 2.13. Pellet formation..... 28

Figure 2.14. Compression ratio 28

Figure 2.15. Illustration biomass wood pellet machine..... 29

Figure 2.16. Vertical mounted ring die..... 30

Figure 3.1. Spelt chaff with particle size < 1.6 mm; (left) optical camera; (right) optical microscope: Zeiss AXIO Imager.M2m 33

Figure 3.2. Ground post-agglomerated spelt chaff with particle size < 1 mm; (left) optical camera; (right) optical microscope: Zeiss AXIO Imager.M2m 33

Figure 3.3. Particle size distribution of spelt chaff and GPA-spelt chaff..... 34

Figure 3.4. Beech sawdust with particle size < 2 mm; (left) optical camera; (right) optical microscope: Zeiss AXIO Imager.M2m 34

Figure 3.5. Particle size distribution of beech sawdust 35

Figure 3.6. *A. mangium* sawdust (x < 1.6 mm) in the case of one month seasoned wood; (left) optical camera; (right) optical microscope: Zeiss AXIO Imager.M2m..... 36

Figure 3.7. *A. mangium* sawdust with (x < 1.6 mm) in the case of six months seasoned wood; (left) optical camera; (right) optical microscope: Zeiss AXIO Imager.M2m..... 36

Figure 3.8. Particle size distribution of *A. mangium* sawdust 37

Figure 3.9. Rice straw with (x < 1.6 mm); (left) optical camera; (right) optical microscope: Zeiss AXIO Imager.M2m.....37

Figure 3.10. Hydraulic piston press..... 38

Figure 3.11. Simplified hydraulic circuit diagram of experimental equipment 39

Figure 3.12. Flat die pelletizer (left); hole length (right)..... 39

Figure 4.1. Design of new single pelletizer unit1: press channel (left) and piston (right) .. 41

Figure 4.2. Single pelletizer unit 1 42

Figure 4.3. Applied pressure-tablet density diagram for GPA- spelt chaff ($x < 1$ mm)..... 43

Figure 4.4. Pellets made from spelt chaff raw material by flat die pelletizer..... 43

Figure 4.5. Pellets produced by single pelletizer unit 1 44

Figure 4.6. Relationship between density of pellets and moisture content (left) and temperature (right)..... 45

Figure 4.7. New design press channel of single pelletizer unit 2 46

Figure 4.8. Single pelletizer unit 2 46

Figure 4.9. Air pressure calibration system (left); Calibration results for a PU5402 type pressure transducer (right)..... 47

Figure 4.10. Design of backup pressure measurement disc 47

Figure 4.11. Set up pressure value in the backup pressure measurement disc (left) and hydraulic pressure calibration system (right) 48

Figure 4.12. Calibration results for a backup pressure in the chamber; (left) 0 to 9 bar; (right) 9 to 25 bar 48

Figure 4.13. Jenike shear tester at the University of Miskolc.....49

Figure 4.14. Pellets are produced by single pelletizer unit 2..... 50

Figure 4.15. Pellet density and backup pressure distribution values along the active part at temperature of 60°C 51

Figure 5.1. Tablets made from beech sawdust ($x < 2$ mm) 53

Figure 5.2. Compressibility data for beech sawdust with different moisture content; (left) particle size < 1 mm; (right) particle size < 2 mm 54

Figure 5.3. Tablets made from spelt chaff ($x < 1.6$ mm)..... 56

Figure 5.4. Compressibility data for spelt chaff with different moisture content; $x < 1.6$ mm; temperature of 60°C 56

Figure 5.5. Relationship between spring-back ratio and pressure for different moisture content of beech sawdust ($x < 2$ mm)..... 57

Figure 5.6. Relationship between spring-back ratio and pressure for different moisture content of spelt chaff ($x < 1.6$ mm) 58

Figure 5.7. Cross sectional surface of tablets made from beech sawdust (optical microscope: Zeiss AXIO Imager.M2m) 59

Figure 5.8. Cross sectional surface of tablets made from spelt chaff (optical microscope: Zeiss AXIO Imager.M2m) 60

Figure 5.9. Falling number values in the case of tablets made from beech sawdust with different moisture content and pressure; (left) $x < 1$ mm; (right) $x < 2$ mm	61
Figure 6.1. Tablets made from beech sawdust ($x < 2$ mm)	62
Figure 6.2. Compressibility data for beech sawdust with different temperatures; (left) particle size < 1 mm; (right) particle size < 2 mm	63
Figure 6.3. Tablets made from spelt chaff with different temperatures and $x < 1.6$ mm....	64
Figure 6.4. Compressibility data for spelt chaff with different temperatures ($x < 1.6$ mm)	65
Figure 6.5. Tablets made from <i>A. mangium</i> one month seasoned wood ($x < 1.6$ mm).....	66
Figure 6.6. Compressibility data for <i>A. mangium</i> one month seasoned wood with different temperatures; (left) particle size < 0.8 mm; (right) particle size < 1.6 mm.....	66
Figure 6.7. Compressibility data for <i>A. mangium</i> six months seasoned wood with different temperatures ($x < 1.6$ mm)	68
Figure 6.8. Relationship between spring-back ratio and pressure for the tablets made from spelt chaff at different temperatures ($x < 1.6$ mm)	69
Figure 6.9. Relationship between pressure, spring-back ratio and temperature for the tablets made from <i>A. mangium</i> one month seasoned wood ($x < 1.6$ mm)	70
Figure 6.10. Cross sectional surface of tablets; (a) one month seasoned wood ($T = 100^{\circ}\text{C}$); (c) one month seasoned wood ($T = 20^{\circ}\text{C}$); (b) six months seasoned wood ($T = 100^{\circ}\text{C}$), (optical microscope: Zeiss AXIO Imager.M2m).....	71
Figure 6.11. Relationship between falling number, temperature and pressure for tablets made from <i>A. mangium</i>	72
Figure 6.12. Relationship between falling number, temperature and pressure for tablets made from beech sawdust; (left) particle size < 1 mm; (right) particle size < 2 mm	73
Figure 7.1. Tablets made from various materials and pressure with the same produce conditions ($x < 1.6$ mm; $T = 100^{\circ}\text{C}$; $m = 3$ g; $\text{MC} = 5$ wt.%)	75
Figure 7.2. Compressibility data for various materials with the same production conditions	75
Figure 7.3. Relationship between cellulose content and tablet density	76
Figure 7.4. Spring-back ratio of various materials with the same production conditions...	77
Figure 7.5. Cross sectional surface of tablets: (a) spelt chaff; (b) Rice straw; (c) <i>A. mangium</i> 6 months; (d) GPA-spelt chaff, at $x < 1.6$ mm; $T = 100^{\circ}\text{C}$, $\text{MC} = 5$ wt.%; $m = 3$ g, (optical microscope: Zeiss AXIO Imager.M2m).....	78
Figure 7.6. Falling number of tablets made from various materials with the same production conditions	79
Figure 7.7. Relationship between lignin content and falling number of tablets.....	79

ABBREVIATIONS

SBR	Spring-back ratio [%]
MC or c_w	Moisture content [wt.%]
T	Temperature [°C]
x	Particle size [mm]
SPU	Single pelletizer unit
ρ	Density of tablet [kg/m ³]
ρ_1	Density of pellet [kg/m ³]
$\bar{\rho}_1$	Average pellet density [kg/m ³]
p	Applied pressure [MPa]
p_B	Backup pressure [bar]
U	Voltage [V]
POM	Polyoxymethylene
L	Layer number
L_{max}	Maximum layer
g	Gram
V_s	Spread deviation [%]
R^2	Coefficient of determination
σ	Residual mean square
BPMD	Backup pressure measurement disc
m	Weight of sample [g]
GPA-spelt chaff	Ground post-agglomerated spelt chaff
<i>A. mangium</i>	<i>Acacia mangium</i>
<i>A. mangium 1</i>	<i>Acacia mangium</i> sawdust - one month seasoned wood
<i>A. mangium 6</i>	<i>Acacia mangium</i> sawdust - six months seasoned wood

CHAPTER 1. INTRODUCTION

Environmental issues, the increasing demand for energy and the decreased availability of fossil fuels have all encouraged the development of sustainable technologies based on renewable raw materials. One of the main advantages of biomass as a source of energy is that it is a clean and renewable product. The use of biomass is a good option for domestic heating systems and power plants to reduce net CO₂ emissions. Agglomeration of biomass such as briquetting, extrusion, tableting, pelletizing can increase bulk density, improves storability, reduces transportation costs, makes easy the handling and increase the quality of products.

Wood pellet production in Europe was estimated to be 10 million tonnes (Sikkema et al. 2011) and 6.2 million tonnes for North America (Spelter et al. 2009) for the year 2009. Another study by Cocchi et al. (2011) estimated between 2009 and 2010 global installed production capacity of the pellet industry has recorded 22 % increase reaching over 28 million tonnes. The globally installed pellet production capacity for 2011 was estimated to be about 30 million tonnes. All studies suggest strong growth for both the European and North American pellet markets. The Finnish Pöyry Industry consulting company has predicted growth in global pellet production capacity to 46 million tonnes by 2020 (Pöyry 2011) and 65 million tonnes by 2025 (Strauss 2017).

The parameters of biomass agglomerate production are especially important in aspects related to product quality and economics. On the one hand, the reduction of moisture content and increasing temperature usually results in better quality agglomerates; it is possible to achieve higher density and strength. On the other hand, moisture content reduction (drying) and increasing temperature have a large energy demand. To find the optimal production parameters, the exact relation between moisture content, temperature and briquetability (applied pressure agglomerate density) should be known. The grinding of raw materials also demands a large amount of energy. Optimal particle size should be determined for economical production and for good agglomerate quality.

Pelletizing is currently one of the most frequently used methods for producing agglomerates, using either a ring die or a flat die pelletizer. This process can increase bulk density, reduces storage and transportation costs and makes easy handling of biomass. Briquettes and pellets are often in the stock with a long time before use, so their biological stability is important. While which are increasing in the case of higher density and strength. Raw materials for fuel pellets production can be different types of biomasses from various resources. Also, composition and structural properties of these materials are diverse. This has the consequence that different types of biomass require different processing conditions such as press channel length, moisture content, particle size and temperature. Nowadays, the process optimization is mainly based on expensive and time-consuming “trial and error” experiments and personal experience (Holm et al. 2011). Pressure is an important process parameter that greatly influences the density of biomass pellets.

The aims and novelty of research

The investigated materials are diverse with different kinds of biomass types, which have viscoelastic material properties. Their behavior against mechanical stress are more complex and diverse even between various biomasses than other non-viscoelastic materials. Composition (cellulose, lignin and starch content) and material structure of them are quite various. To demonstrate similar and different behavior according to the above mentioned features, the experimental test is very important, which requires proper experimental procedure and equipment as well as evaluation

method. The development of equipment (single pelletizer units include comparison of laboratory results (SPU1) and measuring backup pressure distribution on the wall of a flat die pelletizer (SPU2)) are one of the main aims of this scientific research work. It was also an objective to use a pilot test method that directly provides data for the process engineering design of biomass pelletization in relation to biomass with granular properties and phase composition. Introduction of examination and evaluation methods (the effects of moisture content, temperature, particle size and main components on biomass agglomeration process) are generally suitable for investigation of behavior of biomass during pressure agglomeration. The equipment of this experimental test was a larger (25 mm diameter) heated pressure channel.

Although many researchers worked on the effect of compaction pressure during the pelletizing process, only few of them, such as Holm et al. 2007 and Stelte et al. 2011b, discussed the backup pressure in the press channel. Hence the objective of the present research is to supplement the measurement method of backup pressure distribution during fuel pellet production from biomass. To achieve this, the backup pressure values along the direction of the applied force was measured at three different positions along the active part length.

There are studies regarding the compaction equation between density and applied pressure. However, no equation was found in the literature that includes the moisture content as a parameter of biomass raw materials. The objective of the current work is also to supplement the original Johanson equation with the moisture content as a parameter. I also tested the spring-back ratio (SBR) and biomass components because they are related to the density and quality of the tablets.

Methods of research work

The spelt chaff pellets were produced by flat die pelletizer, and the results were compared with those of single pelletizer unit 1. During this modelling, the parameters could be changed easily. Single pelletizer unit 2 was developed and used for three positions of backup pressure measurement in the press channel.

Biomasses (including beech sawdust, spelt chaff, ground post-agglomerated spelt chaff, *Acacia mangium* one month seasoned wood, *Acacia mangium* six months seasoned wood and rice straw) were compressed in load cell by hydraulic piston press with 25 mm diameter and compressibility was determined.

Effects of independent variables, including temperature (20 to 120°C), moisture content, the particle size of different raw materials (1 mm and 2 mm) with different cellulose, lignin, starch content and morphology were investigated for pellet properties, pellet densities, strength tablets and expansion of tablets (spring-back ratio).

CHAPTER 2. LITERATURE OVERVIEW

2.1. Processes of agglomeration

The agglomeration is the opposite process of comminution. Agglomeration is the mechanical process when the particle size of solid disperse materials (bulk materials, fine particles of slurry) are increased by bonding forces between the particles (Pietsch 1991).

Processes of agglomeration include pressure agglomeration, growth agglomeration, and sintering. Agglomeration may be due to bonding by solid bridges, the surface and capillary force of freely moving liquids, adhesive and cohesive forces of captive binders, force of attraction between solid particles, suitable shape configurations (Tarján 1986).

2.1.1. Pressure agglomeration

All pressure agglomeration processes have in common that externally provided forces act on particulate solids and that some sort of a tool or die defines the shape of the agglomerated product. Pressure agglomeration includes briquetting, extrusion, tableting, pelletizing (Pietsch 2002).

2.1.2 Growth agglomeration

On adding a little water or other liquid to a mass of dry powder being stirred, some of the powder particles aggregate into balls while the bulk of the powder remains dry (Tarján 1986). Figure 2.1 shows growth agglomeration and its product at the University of Miskolc: Type C35P.48.2, power 1.5 kW.

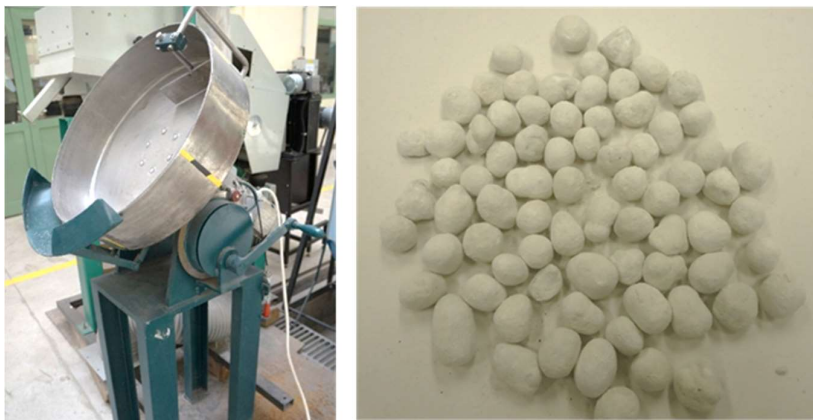


Figure 2.1. Growth agglomeration and its product

2.1.3. Sintering

An operation of agglomeration at high temperature (1100 to 1700°C) forms shapeless large lumps rather than pebbles of uniform size out of the fine particles in contact. The sintering temperature of materials of the heterogeneous composition may remain far below the melting point of the principal component if a component of a lower melting point is present in sufficient abundance: hence, when sintering materials of the high melting point, the dosage of some sintering aid may be indicated (Tarján 1986).

Figure 2.2 shows the typical system components of a laser sintering apparatus used in the described procedure. Each of these described procedure steps has its own requirements on material and system technology. Especially for qualifying a new laser sinter material the understanding of each sub-process and its purpose is essential. The process of laser sintering can be divided into the following sub-processes. The first sub-process is the application of powder. It aims to apply a thin and uniform powder layer with a high density over the whole platform. Afterwards, the newly applied powder has to be heated as fast as possible over the crystallisation temperature of the material (300°C) in order to avoid cooling of the already sintered material, which can cause shrink and deformation of the partly manufactured parts lying in the powder bed (Schmidt et al. 2007).

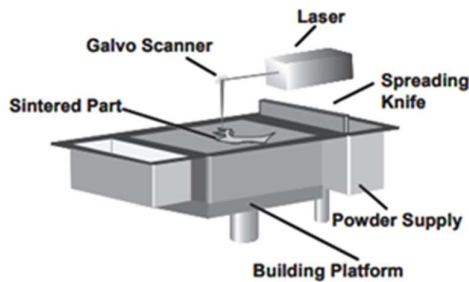


Figure 2.2. Principle of laser sintering

2.2. Binding mechanism, binding forces, binders and binder-less of agglomeration

2.2.1. Binding mechanism

According to Pietsch (2005), the binding mechanisms of size enlargement by agglomeration were first defined and classified by Rumpf (1962), they are divided into five major groups. These are mechanical interlocking bonds, adhesion and cohesion forces, solid bridges, interfacial forces and capillary pressure, and attraction forces between solid particles. Different methods such as covalent bonds between adjacent particles as a result of chemical reactions, mechanical interlocking between fibers and particles and attractive forces, for example, hydrogen bond, van der Waals forces, etc. Furthermore Back (1987) gave a detailed review of binding mechanisms in the production of hardboard, while Kaliyan and Morey (2009), proposed suitable processing conditions, after carrying out a review on the main factors affecting the strength and durability of pellets.

In a separate work by the same author, Kaliyan and Morey (2010), investigation of binding mechanisms in roll-press briquettes made from switch grass and corn stover was carried out, using scanning electron and fluorescence microscopy of the fractured surface of the briquettes, and in conclusion, they affirmed that bonding between particles i.e durable particle-particle bonding occur mainly as result of four solid bridge formation by natural binder (e.g lignin and proteins) that have been softened during the process of pelletizing, in addition, another researcher Stelte et al. 2011, stated that, non-covalent bonds in particular, hydrogen bonds between adjacent hemicelluloses, and/or amorphous cellulose domains having many hydroxyl groups are mainly responsible for inter fiber bonding in wood based material.

Furthermore, Samuelsson et al. 2012 stated that for the production of fuel pellet, it is reasonable to assume similar bonding mechanism, stating that though other mechanisms may

also contribute. The contribution which he said can arise because of the much higher pressure used in pelletizing as compared to hardboard process.

An overview of the binding mechanism between solids particles in a gaseous environment according to Stieß (1997) has already been provided in Figure 2.3.

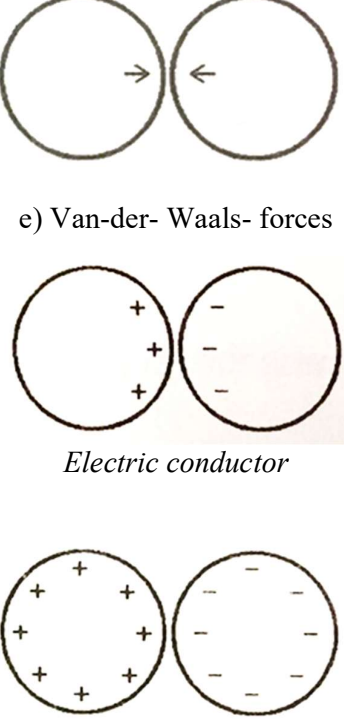
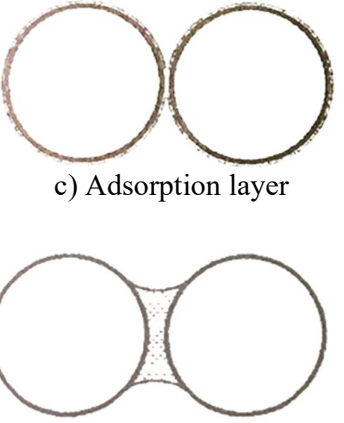
Material connection	Without material connection
<p>A) Solid material bridge</p>  <p>a) Sinter bridges, melt bridges</p> <p>b) Crystallized solid material, hardened binder</p>	<p>C) Attraction forces</p>  <p>e) Van-der- Waals- forces</p> <p><i>Electric conductor</i></p> <p><i>Electric isolator</i></p> <p>f) Electric forces</p>
<p>B) Liquid bridge</p>  <p>c) Adsorption layer</p> <p>d) Movable liquid bridge (Capillarity)</p>	<p>D) Form closed bond</p> 

Figure 2.3. Binding mechanism between solid particles (Stieß 1997)

2.2.2. Binding forces

Binding forces are transmitted at the coordination points of the primary particles forming the agglomerate Pietsch (2002). Some equations for estimating binding forces are presented by Pietsch (2005): The most important of all is that any environmental forces (gravity, inertia, drag, etc.) must be smaller than the binding forces between the adhering partners. The ratio of all binding forces $B_i(x)$, and the sum of the active components of the environmental forces $F_{jy}(x)$, involved is a measure of the adhesion tendency T_a .

$$T_a = \sum B_i(x) / \sum F_{jy}(x) > 1 \quad (1)$$

Both the binding and the environmental forces are mainly dependent on the size x of the powder particles. To cause adhesion, T_a has to be bigger than unity. To keep the particle adhering the sum of all moments $M_j(x)$ must also be zero in most cases.

$$M_j(x) = \frac{x}{2} \sum_j F_{jx}(x) = 0 \quad (2)$$

According to Schubert (1984), considering the moisture of a bulk material independently of its origin, it can be generally said, that a small quantity of liquid saturation causes the formation of a bridge between the individual particles (Figure 2.4a). Here, the liquid bridges co-exist with adsorbed water layers, but their contribution to the moisture content is usually much greater. This region is called the pendular state (Figure 2.4a). By increasing the amount of liquid, we first get the funicular state (Figure 2.4b), where both liquid bridge and pores filled with liquid are present, and then the capillary state (Figure 2.4c), where the pores are completely filled.

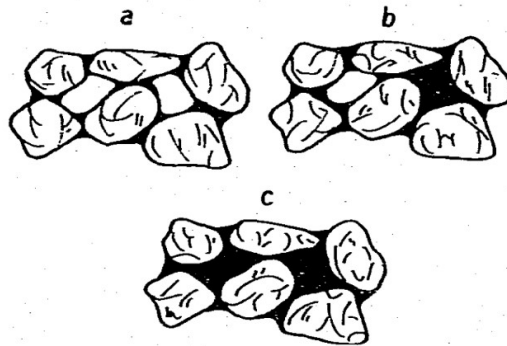


Figure 2.4. States of liquid bonding in a bulk material; (a) Pendular state; (b) Funicular state; (c) Capillary state (Schubert 1984)

2.2.3. Binders and binder-less of agglomeration

Binders are components which are added prior or during agglomeration to increase the strength of the agglomerated product at otherwise unchanged processing conditions. They can affect strength directly or after a curing step. Binder selection depends on many considerations which are specific for the particular application. They must be compatible with the materials to be agglomerated and the proposed uses of the product and environmental friendliness of the binders (Pietsch 2002; Tabil 1996; Marrero 1999).

Binders improve the cohesive characteristic of biomass by forming a gel with water, helping produce a more durable product. Binders also help reduce the wear on production equipment and increase the abrasion resistance of the fuel. In general, binders are allowed in a fuel feedstock but need to be specified as part of the final product (Tumuluru et al. 2011).

Many materials can be briquetted without adding a binder (binder-less agglomeration). Some of these already contain natural binders, such as bituminous substances in some coals. Others utilize partial melting resulting from direct preheating or from the residual heat in the material obtained from a drying or reducing process that immediately preceded the briquetting operation. Increasing the material temperature may also generally reduce the required machine mechanical force and energy requirements. When mechanical forces are used without the benefit of a binder substance, the binding mechanism consists of the plastic and elastic deformation of the particles in a manner in which the particles closely wrap around and interlock with each other, attaining extensive contact between the mating surfaces of the adjacent particles, thus employing van der Waals binding forces (Mcketta 1995).

2.2.4. Binding process in the case of biomass

In some European countries, the addition of binders is prohibited. In Austria, biological additives rich in starch content (e.g., maize and rye flour) of only 2 % (by weight) are allowed for wood pellet production (Oberberger and Thek 2004).

Pfost and Young (1973) found that addition of bentonite (2.4 % by weight) improved the durability of feed pellets by about six percentage points. Hill and Pulkinen (1988) concluded that addition (by weight) of any of the following six binders did not improve the alfalfa pellet durability over the control: 4 % bentonite, 1.5 % lignosulfonate, 1.5 % lignosite, 4 % of neutralized liquid lignosite, 4 % of liquid molasses, and 40 % of ground barley grain.

The most commonly used binders in pellet making are lignosulphonates or sulfonate salts made from the lignin in pulp mill liquors (Tabil et al. 1997; Tabil and Sokhansani 1996c). Lignosulfonates, considered the most effective binders, are used in animal feeds. (Macmhon 1984; Anonymous 1983a). The general quantity to include for effective binding ranges from 1-3 % (Anonymous 1983b).

Bentonite, or colloidal clay, is commonly used as a binder in feed pelleting and is made up of aluminum silicate composed of montmorillonite. As mentioned previously, proteins are natural binders that are activated through interactions with other biomass compositions, such as lipids and starches, and the heat produced in the dies. Some agricultural biomass, like alfalfa, has a high protein content and can be used as a binder to improve the durability of pellets made from lower lignin content biomass materials (Tumuluru et al. 2011).

2.3. Agglomeration of biomass

2.3.1. Biomass

Biomass sources with different chemical compositions require different process parameters for their densification (Kashaniejad and Tabil 2011; Stelte et al. 2011; Samuelsson et al. 2012; Stahl et al. 2012).

Biomass composition: Biomass is generally composed of three main groups of natural polymeric materials: cellulose (around 50 % on dry basis), hemicellulose (10- 30 % in woods and 20 - 40 % in herbaceous biomass on dry basis). Other typical components are grouped as extractives (generally smaller organic or polymers like protein, acids, salts) and minerals (Yaman 2004). Inorganic compounds like alkali metals mainly potassium, calcium, sodium, silicon, phosphorus and magnesium and also chlorine in herbaceous biomass (Zabaniotou 1999). The contents of these inorganic compounds vary from being less than 1 % in woods

to 15 % in herbaceous biomass and feedstock and up to 25 % in agricultural and forestry residues (Fitz et al. 1996).

Lignocellulosic biomass (Figure 2.5) is mainly composed of three organic constituents: lignin, cellulose and hemicellulose. The ratio of these three components varies, depending on the type of biomass and the part of the plant sampled (Yu 2017).

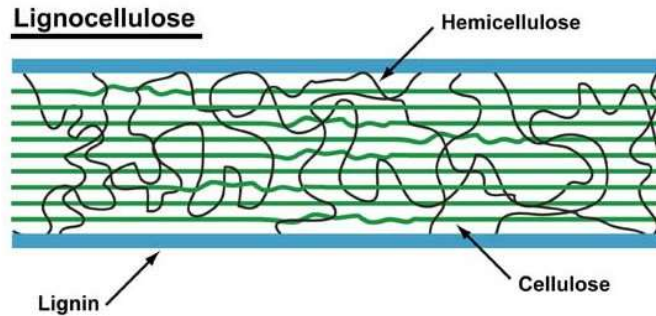


Figure 2.5. Lignocellulose and its components (Image: USDA Agricultural Research Service)

Yu (2017) defined lignin as a random, three-dimensional network polymer which is difficult to decompose due to the presence of linked phenylpropane units. Cellulose is defined as a linear polysaccharide, typically consisting of thousands of D-glucose monomers, and the largest single component of lignocellulosic biomass. According to (Sjöström 1993a), the most important constituent of the wood cell wall is cellulose, as it is the main component in both the native wood fiber and the processed pulp and has a concentration of about 40 % (on dry weight), depending on the species.

Cellulose is the load-bearing element of the pulp fiber and therefore its chemical degradation results in fibers having inferior strength properties (Gurnagul et al. 1992). The cellulose in a plant consists of parts with a crystalline (organized) structure, and parts with a, not well-organized, amorphous structure. The cellulose strains are ‘bundled’ together and form so-called cellulose fibrils or cellulose bundles. These cellulose fibrils are mostly independent and weakly bound by hydrogen bonding (Laureano-Perez et al. 2005).

The word hemicellulose was first used in 1891 (Schulze 1891). It originated due to the assumption that polysaccharides were precursors to cellulose (Fengel and Wegener 1984a), however, this assumption has been proved wrong (Sjöström 1993b). Hemicellulose is a polysaccharide composed of numerous carbohydrate monomers in varying ratios depending on the biomass sample. Its main constituents are xylose, arabinose, mannose and glucose. The degree of polymerization of hemicellulose is very low, about 50-200 monomers, compared to the much higher value for cellulose (Li 2014).

Table 2.1. Lignin and cellulose content in % of beech and spelt chaff

Materials	Cellulose content [%]	Lignin content [%]	References
Beech	35.6 %	21.8 %	Mahendra 2011
Spelt chaff	30.2 % - 42.5 %	5.7 % - 7.6 %	Escarnot 2011; Lequart 1999; Mani 2006

2.3.2. Binding by lignocellulose

The agglomeration of the lignocellulosic materials to form pellets occurs due to different inter-particle bonding mechanisms favoured by the softening of different components at the condition of high pressure and temperature (Castellano et al. 2015). In the field of hardboard manufacture, Back (1987) has found that at these conditions, hydrogen bonds between adjacent hemicellulose and amorphous cellulose play a major role in the inter-fiber bonding process. According to his work covalent bonds also occur in the inter-fiber bonding area of particles, lignin being the most reactive wood polymer in these auto-crosslinking reaction.

Kaliyan and Morey (2010) described the creation of “solid bridge” type bonding between particles in corn stover and switchgrass pellets. According to their results, the potential natural binding component in these materials are water-soluble carbohydrates, lignin, protein, starch, and fat.

Stelte et al. 2011 studied the bonding and failure mechanisms of pellets from beech, spruce and straw. In the case of wood pellets, they signaled Van der Waals forces and hydrogen bonds being mainly responsible for agglomeration; solid bridge formation was observed in beech pellets but not in spruce one. The presence of waxes on the straw surface produced a weak waxy boundary layer, resulting in a lower strength. They found that temperature played an important role in the bonding mechanisms, obtaining in every case higher compression strength for pellets produced at higher temperatures.

Biomass raw materials with high percentages of lignin and low extractives contents reached higher durability values. Extractive has a double effect in the pelletization process: they form a weak boundary layer preventing particles from bonding strongly together and they also produce a lubricating effect resulting in a lower friction inside the die channels. Lignin seems to favor the agglomeration of the biomass particles due to its thermoplastic behavior (Castellano et al. 2015).

The presence of lignin in feed material enhances the binding characteristics of densified pellets during the preheating of the material. Lignin has a low melting point of about 140°C. When biomass is heated, lignin becomes soft and sometimes melts and exhibits thermosetting properties (Van Dam 2004).

Physically, cellulose micro-fibrils are coated with hemicellulose, whose empty spaces are filled up with lignin (Lee et al. 2014). Lignin plays a binding role between hemicellulose and cellulose within the cell wall. It has been suggested that hemicellulose is hydrogen-bonded to cellulose, while lignin and hemicellulose are covalently bonded, more specifically, via ester bonds (Rowell 2012).

2.3.3. Particle shrinkage

Shrinkage and fragmentation are two processes that reduce the size and alter the shape of the parent wood particle during devolatilization. Shrinkage is the reduction in physical size of the parent particle while fragmentation is the breaking up of parent particle into small pieces. Fragmentation of the wood particle may occur during or at the end of devolatilization due to the buildup of volatile pressure and/or induced thermal stresses within the particle. While shrinkage affects the size and shape of the fuel particle during the devolatilization process, fragmentation breaks the particle at any instant, usually at the end. Both these phenomena decide the shape and size of the char particle that remains at the end of the devolatilization process. Shrinkage of wood due to loss of moisture is a common

phenomenon, however, little is known about the shrinkage that occurs during the devolatilization process (Kumar et al. 2006).

2.3.4. Particle size distribution

Particle size distribution plays an important role in the production of pellets (Stasiak et al. 2017). Bergstrom et al. 2008 studied the influence of raw material particle size distribution on the process and the physical and thermomechanical characteristics of produced fuel pellets. The study results indicated that particle size distribution had some effect on energy and compression strength, but no effect on single-pellet or bulk density, moisture content, or moisture content absorption during storage and abrasion.

2.3.5. Effect of moisture content

The effect of raw material moisture content on the pelletizing properties and product quality has been the subject of several studies (Andreiko and Grochowicz 2007; Arshadi et al. 2008; Carone et al. 2011; Filbakk et al. 2011; Kaliyan and Morey 2009b; Mani et al. 2006; Nielsen et al. 2009b, 2010; Odogherty and Wheeler 1984; Rhen et al. 2005; Ryu et al. 2008; Serrano et al. 2011; Smith et al. 1977; Stelte et al. 2011b). In these studies, biomass was pelletized at different levels of moisture content, and its impact on the pellet quality (durability or compression stability) was analyzed. In general, the optimum moisture content for wood species was found to be between 5 to 10 wt.%, while it was slightly higher for agricultural grasses was found to be between 10 to 20 wt.%. However, Zhang et al. 2016 reported that excess water that cannot be absorbed by particles attaches to the biomass surface, which impedes particle compaction and reduces pellet quality.

2.3.6. Effect of temperature

The increase in mechanical properties of the pellets with an increase in temperature was reported for spruce (Rhen et al. 2005), corn stover (Kaliyan and Morey 2009b), switchgrass (Gilbert et al 2009), pine (Nielsen et al. 2009a), olive (Carone et al. 2011), beech (Nielsen et al. 2009a), and wheat straw (Stelte et al. 2012a). Furthermore, it was reported that an increase in temperature reduces the friction in the press channel of the mill (Stelte et al. 2011b) and lowers the energy required for different components of the pelletizing process (Nielsen et al. 2009a). However, water hyacinth pellets were slightly discolored and charred at process temperatures above 110°C, which was unfavorable to the densification process. These imperfections may have lowered water hyacinth pellets quality (Zhang et al. 2016).

2.4. Description of pressure agglomeration

2.4.1. Pressure agglomeration principle

During pressure agglomeration (Figure 2.6), new, enlarged entities (tablets, briquettes, etc.) are formed by applying external forces to particulate solids in more or less closed systems that define the shape of the agglomerated product (Pietsch 2005).

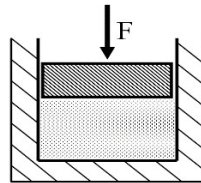


Figure 2.6. *Pressure agglomeration principle*

Figure 2.7 shows with four model sketch the structural change of a bulk mass of particulate matter during densification in a die, the attendant change in volume, and an indication of the modifications of particle shape and size that occur at high pressure (Pietsch 2005).

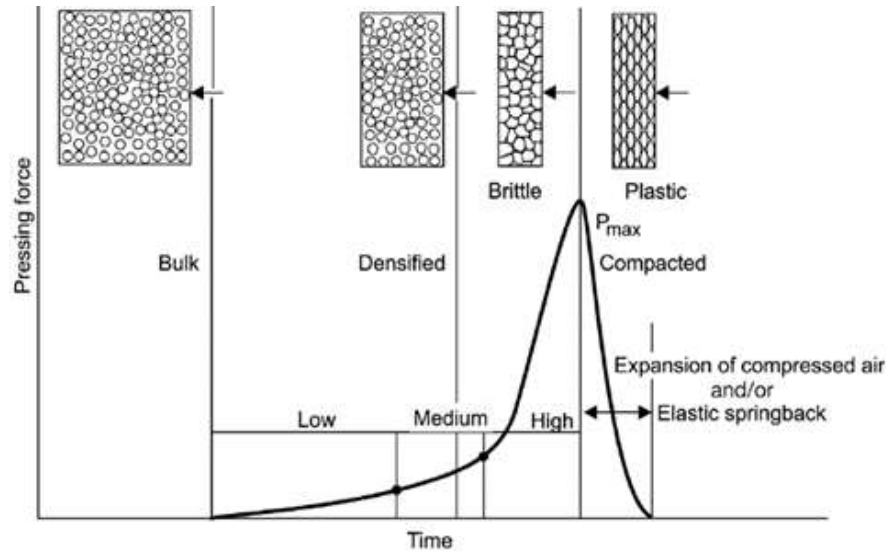


Figure 2.7. Sketches explaining the mechanism of pressure agglomeration (Pietsch 2005)

2.4.2. Compressibility - Theoretical background

Different approaches have been taken in order to calculate the connection between applied pressure and agglomerate density. The Johanson equation (1965) can take two forms:

$$\frac{\rho}{\rho^*} = \left(\frac{p}{p^*}\right)^{1/\kappa} ; \frac{F}{F_0} = \left(\frac{V_0}{V}\right)^\kappa \quad (3)$$

where κ is compressibility factor, ρ is agglomerate density, p is tableting pressure, F is tableting force, V is tablet volume, and p^* , ρ^* , F_0 , V_0 are reference values (if surface perpendicular to force and mass of tablet are constant) (Stieß 1997).

Liu and Wassgren (2016) modified the Johanson model for improved relative density predictions

$$\frac{P}{P_{\text{initial}}} = \left(\frac{\eta}{\eta_{\text{initial}}}\right)^\kappa \quad (4)$$

where η_{initial} is the inlet relative density, P_{initial} is the corresponding pressure according to the fit data; η is the powder's relative density.

Walker reported a series of an experiment on the compressibility of powder. He expressed the volume ratio V as a function of applied pressure P :

$$V = a_1 - K_1 \ln P \quad (5)$$

where a_1 and K_1 are constants (Adapa et al. 2009; Walker 1923).

Heckel proposed a model to express the compaction behaviour of compressed powder. The equation expresses the density of powdered materials in terms of packing fractions as a function of applied pressure:

$$\ln \frac{1}{1-\rho_f} = mP + n \quad \text{and} \quad \rho_f = \frac{\rho}{\rho_1 X_1 + \rho_2 X_2} \quad (6)$$

where ρ_r is packing fraction or relative density of the material after particle rearrangement, P is applied pressure (MPa); m, n are Heckel model constants, ρ is bulk density of compacted powder mixture (kg/m^3); X_1, X_2 are mass fraction of components of the mixture (Heckel 1961; Mani et al. 2004).

Kawakita and Lüdde performed compression experiments and proposed an equation compaction of powders based on an observed relationship between pressure and volume:

$$\frac{P}{C} = \frac{1}{a_2 b_2} + \frac{P}{a_2} \quad (7)$$

where P is applied pressure, a_2 and b_2 are constants, and C is relative volume decrease or engineering strain given by the equation:

$$C = \frac{V_0 - V_P}{V_0} \quad (8)$$

where V_0 is the initial volume and V_P is volume measured at any given pressure (Kawakita and Lüdde 1971; Chevanan et al. 2010).

The model developed by Sone (1969) is used for understanding the compaction characteristics by tapping. The Sone model has a close resemblance to the Kawakita and Lüdde model and the pressure term in the Kawakita and Lüdde model is replaced with a number of tappings.

$$\frac{n}{\gamma_n} = \frac{1}{a_3 b_3} + \frac{n}{a_3} \quad (9)$$

where γ_n is volume reduction ratio, n is number of tapping and a_3 and b_3 are constants. The volume reduction ratio γ_n calculated using

$$\gamma_n = \frac{V_0 - V_n}{V_0} \quad (10)$$

where V_0 is initial volume, and V_n is volume after n taps.

A compression equation was proposed by Panelli and Filho given as:

$$\ln \frac{1}{1 - \rho_r} = A\sqrt{P} + B \quad (11)$$

where ρ_r is the relative density of compactness, A is a parameter related to densification of the compacted agglomerate by particle deformation and B is a parameter related to powder density at the start of compression (Panelli and Filho 2001).

2.4.3. Compactibility

Compactibility is the ability of a powder to form coherent compacts (Sonnergaard 2006). Compactibility was estimated using two different approaches, tensile strength versus the compression pressure relationship was drawn and the slope of the linear curve was estimated using linear regression (Ilic et al. 2009). The tensile strength (σ) was calculated according to the Fell and Newton (1970) equation:

$$\sigma = \frac{2F}{\pi dh} \quad (12)$$

where F is the crushing strength, d is the diameter and h is the tablet height.

Compactibility was also estimated using the model proposed by Révész et al. 1991, in which tensile strength is normalized with the specific work (W_{spec}) needed to compress the tablet. This is called the compressibility factor (P_r). However, because this parameter is derived from the crushing strength of the tablet, it is more closely associated with compactibility than compressibility.

$$P_r = \frac{\sigma}{W_{\text{spec}}} = \frac{\sigma}{E/m} \quad (13)$$

where σ is the tensile strength of tablet and W_{spec} is the specific or mass-normalized work, which is expressed as the effective work (E) invested in the compression of the unit mass of the substance (m). Effective work represents the area of hysteresis between the compression and the decompression curves in force-displacement measurement during tablet manufacturing. P_r was calculated from tablets with compression pressures ranging from 120 to 300 MPa. The P_r values of various materials were compared using analysis of variance for statistically significant (non) equality.

For the purpose of compacting very fine powders without any binding material an experimental pilot-scale technological set up with press-rolls have been built with systematical tests have been carried out by Csőke and Faitli (2003). The results showed that the obtained briquette density was a little bit higher with gravity feed with 60 % pre-compacting, but the specific compacting work, as well as the powder ratio in the product, were better with screw feeder, even with 100 % fresh powder feed.

According to (Tarján et al. 1999) the airing out occurs during the compacting of fine granular material in press-roll in the non-sliding material zone because of the fast decrease of porosity. For the calculation of airing out in the non-sliding zone, a method has been developed with the distribution of the air pressure along the cylinder jacket was introduced by Tarján and Csőke 1997. Using non-linear rheological models, a more generally valid description of the compaction process was developed and used for sawdust and chips (Sitkei, 1994; Sitkei, 1997).

2.5. Equipment of pressure agglomeration

2.5.1. Piston press

2.5.1.1. General concept of piston press

The piston press acts in a discontinuous mode with the material being fed into a cylinder, which is compressed by a piston into a slightly tapering die (Mishra 1996). Basically, there are two main types of piston press, these are the mechanical and hydraulic piston presses (Grover and Mishra 1996B).

2.5.1.2. Tabletizer

A tabletizer tightly presses biomass with a hydraulic motor and ram in a 4 to 6-inches diameter cylindrical mold with biomass, shrinking the material from about 10 to 2-inches (Vanengelenhoven 2011). The application of about 140 MPa in the mold is sufficient to force the material to adhere together without adding binders. Long, coarse-cut feedstocks are favorable in the process, as they stick together more easily. Tablet densities average 900 kg/m³ compared to bale at 160 kg/m³ and pellets at 730 kg/m³. However, the tableting process uses more energy than pelletization. The tablets have not been tested extensively for various biomass resources (Tumuluru et al. 2011). Figure 2.8 illustrates a tablet press machine and its product with power 7.5 kW, weight 1500 kg.



Figure 2.8. *Illustration tablet press machine and products (Source: www.wood-pelletsmachine.com; www.wibbfuel.com)*

2.5.2. Roll press

2.5.2.1. General concept of roll press

Roll pressing of particulate matter is traditional of greatest interest for all industries in which large quantities of finely divided solids, both valuable and worthless (wastes), must be handled. Originally developed as an economic method to agglomerate coal fines, today this size enlargement technology is applied for a large number of materials in the chemical, pharmaceutical, food processing, mining, minerals and metallurgical industries (Pietsch 1991).

Roller-press machines were installed in a coal briquetting plant at Port Richmond, USA, in the late 1870s (Franke 1909). Johanson (1965) and Pietsch (1991) first proposed the theoretical analysis and operation of roll pressing machines. The Johanson (1965) analysis was based on understanding the behavior of granular solids within a roller press, which involves the interaction between the particles of the material itself as well as the interaction between the material and the machine (roller surface). The typical working principle of a roller press is shown in Figure 2.9. The roller presses consist of two cylindrical rollers of the same diameter, rotating horizontally in opposite directions on parallel axes, allowing feed to be drawn in one side and densified product to be discharged out the opposite. The two rollers are arranged in such a way that a small gap exists between them. The distance between the two rollers, which is normally referred to as “the gap” depends on many factors such as the type of biomass, the particle size, the moisture content, and the addition of binders. The shape of the densified biomass depends upon the type of die used (Yehia 2007).

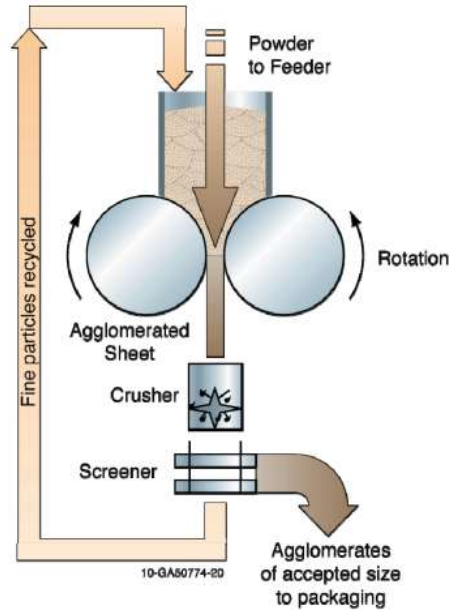


Figure 2.9. Roller press technology (Yehia 2007)

2.5.2.2. Briquetting

Briquetting applying sufficient pressure to an aggregate filled into a mold (with or without a binder) produces briquettes, pills blocks or bricks. The pressure required depends on the nature of the material to be briquetted (Tarján 1986). Briquetting is the process of compaction of residues into a product of higher density than the original raw materials (Kaliyan and Morey 2008). Figure 2.10 shows during briquetting the granular materials compacted between two counter-currently rotating rolls.

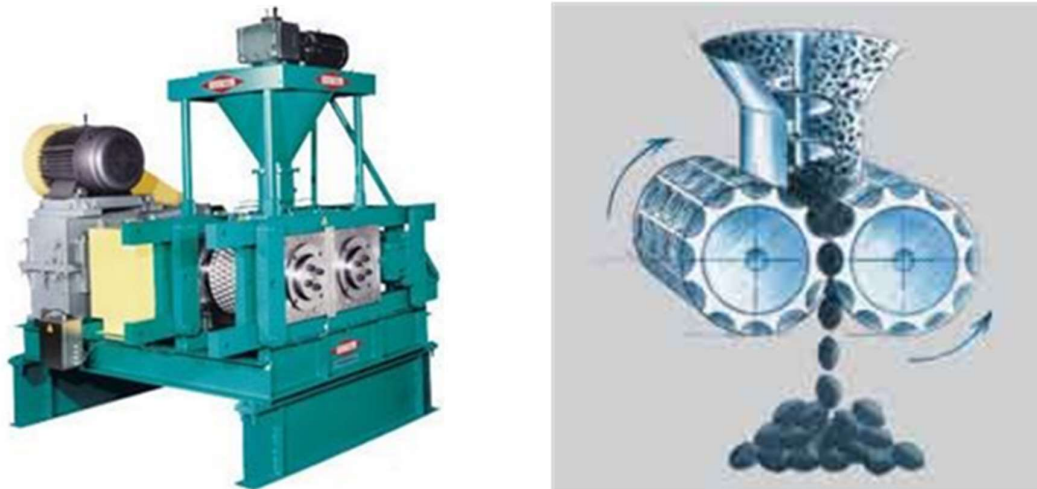


Figure 2.10. Briquetting machine (Source: www.koeppern.de)

2.5.3. Extrusion (briquetting in open form)

Extrusion brings small particles < 4 mm close together so that the forces acting between them become stronger, providing more strength to the densified bulk material. During extrusion, biomass moves from the feed port, with a rotating screw, through the barrel and against a die, resulting in a significant pressure gradient and friction due to shearing of the biomass (Grover and Mishra 1996B).

The pressing (extrusion) of a material of sufficient plasticity through a suitably shaped orifice (a die) can produce practically endless lengths of products whose cross-section is the same as that of the die aperture. These can be cut down to the desired size by a suitable cutting device. The machines performing this type of pressing are an extrusion or band presses. Plasticity is adjusted to the desired value by heating (in the plastics industry) or by an admixture of water (in the silicate industry). The pressure driving the material through the orifice may be transmitted by a piston, a spiral or pair of rolls (Tarján 1986).

Figure 2.11 shows the screw extrusion briquette machine for biomass and products with technical data following: rated electric power 30 kW, screw diameter 225 mm, capacity 1.5 - 2.5 t/h, weight 1.8 tonnes.



Figure 2.11. *Illustration biomass extrusion machine and products* (Source: <http://tmgreenbull.com.ua>)

2.5.4. Flat die pelletizer

The compression mechanism of the flat die is based on a round plane die and on press rolls on its surface (Figure 2.12). The number of rolls ranges 2-6, depending on the size of the machine. In some model, the die rotates and the rolls are stationary, in some other models the die is stationary and the rolls rotate, i.e.

The essential die is only the circumference of a circular plate, as the press rolls are rather narrow. The roll cannot rotate simultaneously at the speed required by different edges, and as a consequence, there is slipping between the roll and the die. In the plane die the material is fed onto the die simply downward by gravity. Compared to core roll machines, an advantage is ease of cleaning (Alakangas & Paju 2002).

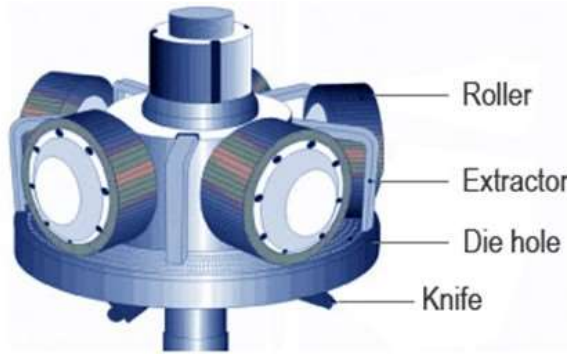


Figure 2.12. Roller and flat die (source: www.pellet-plants.com)

The material is fed to the dies in different ways depending on the machine type. A roll or rolls compress the material through the die holes and cutting knives cut then the extruded piece to pellets.

The pellet procedure is shown in (Figure 2.13 and Figure 2.15). The material is like a mat in front of the roll. The over rolling press roll tightens the mat and presses the material into the die holes. A tight raw material mat remains on the die. When over rolling the hole, the roll always presses new material into the pellet hole, and the pellet slides slightly forwards.

Six important issues affect the compression can be classified into: 1- connection between material characteristics, compression capacity of equipment, and tightening process, 2- Friction characteristics of die holes, 3- Hole length and diameter (Figure 2.14), 4- Thickness of raw material mat, and hence, thickness of the new material layer forced into the hole, 5- Frequency of compression, i.e., rolling speed, 6- Material and finishing of die and rolls (Kytö & Äijälä, 1981a).

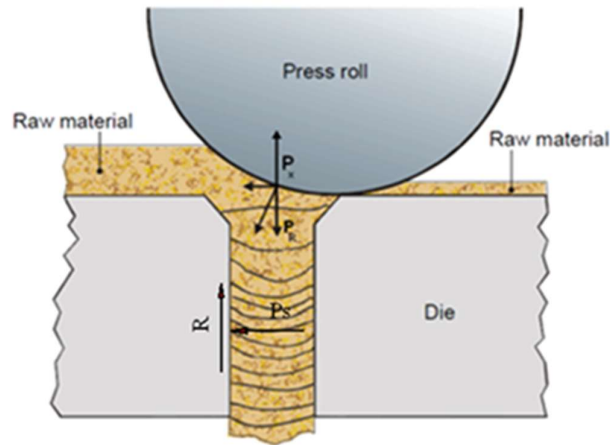


Figure 2.13. Pellet formation

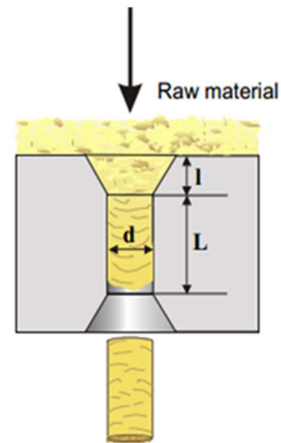


Figure 2.14. Compression ratio

According to Kytö & Äijälä (1981a) two different equations are introduced as following:

$$R = \mu P_s d \pi L < P_R \quad \text{and} \quad c = (L+2l)/d \quad (14)$$

where R is friction force [N], μ is friction coefficient, P_s is wall pressure [N/mm^2], d is diameter of hole [mm], L is length of hole [mm], P_R is pressure exerted by the rollers of the pellet press [N], P_x is the pressure build-up in the press channel and c is the aspect ratio (length/diameter) of the pellet. Single pellet press trials were done as aspect ratios between 0.1 and 5, and the model was used to estimate pressures that will likely occur in production size pellet mills with higher aspect ratios of about 8 to 10 (Holm et al. 2011).



Figure 2.15. Illustration biomass wood pellet machine (Source: www.ec21.com)

2.5.5. Ring die pelletizer

The most manufacturers make vertically mounted ring die machines, in which the compression mechanism is based on a solid die and in its inner rim rotating 1-3 compression rolls (Figure 2.16) or a rotating die and on-site rolling rolls. Today, there are also machines, in which rolls are rotated and the die rotates by friction strength. The friction strength is transmitted by the pelletized material.

In addition to the compression mechanism, the material feed is a decisive factor, when the aim is to reach a high output and a small and even wear of die. In a number of one-roll machines, the material flows into the die solely by the gravity or is carried by a screw conveyor. In a system of two or three on-site rolling rolls, a more effective feed is required and realised with a centrifugal feed by steering the material onto the rolls with adjustable ailerons. The aim is to spread the material as an even mat over the whole width of the die and on all rolls (Alakangas & Paju 2002).

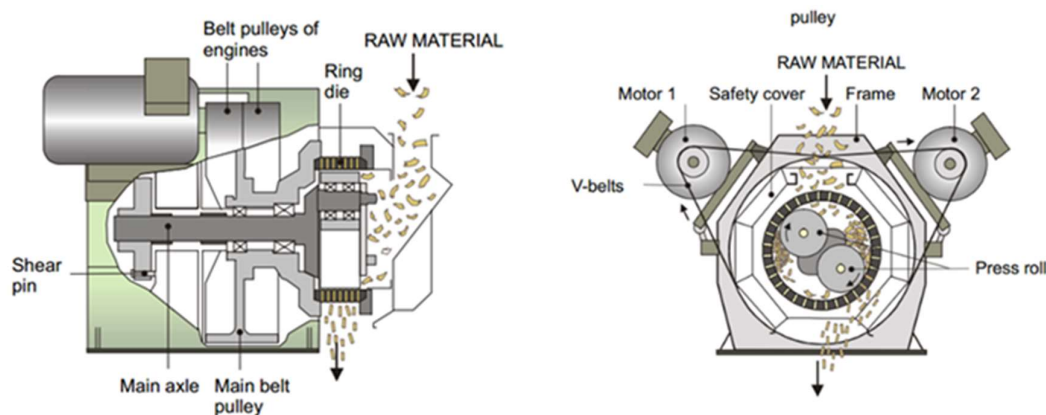


Figure 2.16. Vertical mounted ring die (Source: www.salmatec-gmbh.de)

2.6. Strength of agglomerates

2.6.1. Theory of the strength of agglomerates

The most important characteristic of all forms of agglomerates is their strength. For the investigation of agglomerate strength, stresses that occur in reality are often experimentally simulated. In addition to the frequently applied crushing, drop, and abrasion tests, methods for the determination of impact, bending, cutting, or shear strengths are employed. All values obtained by these methods are strictly empirical and cannot be predicted by theory because it is not known which stress component causes the agglomerate to fail. For the same reason, the experimental results from different methods can't be compared with each other (Pietsch 1991).

Therefore, Rumpf (1962) proposed to determine the tensile strength of agglomerates. It is defined as the tensile force at failure divided by the cross-section of the agglomerate. Because failure occurs with high probability as the result of the highest tensile strength in all stressing situations, this proposal is justified. Moreover, the tensile strength can be approximated by theoretical calculations. The durability index is a quality parameter defined as the ability of densified materials to remain intact when handled during storage and transportation. Thus, pellet durability is the pellet's physical strength and resistance to being broken up (Tumuluru et al. 2011).

2.6.2. Determination of agglomerate strength

For the practical determination of agglomerate strength, stresses occurring in processing, handling, storage, reclamation, shipping, etc., are simulated during testing. In addition to the most frequently used compression, drop abrasion tests and methods have been developed for the determination of impact and shear strength as well as the resistance to bending and cutting. The data defining. Strength obtained from these tests cannot be described by theories because stressing is not uniform and the specific strain leading to failure is normally not known (Pietsch 1991).

Armstrong and Palfrey (1989) suggested that differences in tablet tensile strength due to tableting speed could be accounted for by porosity changes. Hancock et al. 2003 found that the tablet strength and disintegration time for tablets made on an eccentric press and a rotary press were comparable when considering a comparable solid fraction. Maarschalk et

al. 1996 found that tensile strength as a function of tablet porosity for sorbitol was independent of compression speed.

The mechanical strength of agglomerates is one of the main features determining their further applicability or processing. There are many methods of defining and measuring the strength. Depending on needs, impact, wear, compression, bend and tensile tests are used (Schubert 1975; Kristensen et al. 1985; Gluba and Antkowiak 1988). In all these cases strength is determined by means of testing machines, so the theory and transfer of results of these measurements to other stresses are more or less hampered. Strength tests are, however, a significant source of information on the quality and structure of the granulated product.

2.7. Modelling of pelletizer

2.7.1. Previous research in the press channel model

The press channel model in experimental piston press has recently been studied by many research groups, such as Adapa et al. 2002; Mani et al. 2004; Holm et al. 2006; Nielsen et al. 2009a; Zafari et al. 2012. The studies (Adapa et al. 2002; and Mani et al. 2004) have focused on the compaction behavior of different biomass types by conducting a pelletizing test in a single pellet unit and fitting the obtained data to the different mathematical model found in the literature. The models having the best fit to the experimental data were identified and used to explain the compaction mechanism of biomass. According to Holm et al. 2006, the major force acting on the biomass in the press channel is the friction force between the press channel wall and the biomass. Assuming that the biomass is an orthotropic material, where the fibers align perpendicular to the direction of the press channel, and that the biomass also is an elastic material, the pressure build-up in the press channel of a pellet mill, can be described as a function of the friction coefficient, the Poisson ratio, press channel length, and its radius.

Nielsen et al. 2009a presented tools and methods that separate the pelletizing process into compression, flow and friction components, to measure the importance of raw material properties for the energy requirements of pelletizing, and pellet strength. Experimental materials were sawdust from European beech and Scots pine. Zafari et al. 2012 introduced in their research work about the experimental design to evaluate the effect of moisture content, the speed of piston, die length, and particle size on pellet density, and obtained maximum density. Experimental material was composted municipal solid waste, press channel had 10 mm diameter and the total length of the active part was 100 mm. Statistical analyses confirmed that the moisture content, speed of piston, and particle size significantly affected the pellet density.

2.7.2. Previous research in the applied pressure and backup pressure

The effect of pressure on biomass is exposed to during pelletizing and briquetting has a significant impact on the product density and durability, as well as on the process energy consumption. Therefore, this process parameter has been subjecting of various studies (Adapa et al. 2009; Carone et al. 2011; Gibert et al. 2009; Kaliyan and Morey 2009b; Mani et al. 2006; Odogherty and Wheeler 1984; Smith et al. 1977; Stelte et al. 2011b). In all the studies, there is a very clear agreement that concludes that pellet and briquette density increases with an increase in pressure. Maximum applied pressures ranged from 50 MPa (Odogherty and Wheeler 1984) to 600 MPa (Stelte et al. 2011b); the pressure typically used

in most studies was above 50 MPa in the case of open form (Adapa et al. 2009; Mani et al. 2006; Stelte et al. 2011b). Holm et al. 2007 measured the backup pressure needed to press pellets of different lengths out of the press channel, it is shown that the pelletizing pressure does increase exponentially as a function of the pellet length. The backup pressures were shown to be dependent on biomass species for all tested pellet lengths. Stelte et al. 2011b showed that the pelletizing pressure increases exponentially with the pellet length. An increasing pelletizing pressure is resulting in an increasing pellet density.

During continuous pelletization of biomass, a backup pressure is needed to initiate the process of pelletization. The backup pressure is created by the buildup of material in the press channel, which sets the requirement for a pressure (pre-stressing pressure) to overcome the friction within the channels. The initial pelletization pressure depends on die dimensions such as die hole, die length, friction coefficient, and pre-stressing pressure (Holm et al. 2006; Tumuluru et al. 2010).

CHAPTER 3. MATERIALS AND METHODS OF RESEARCH WORK

3.1. Materials

Biomasses (including spelt chaff raw material, ground post-agglomerated spelt chaff, beech sawdust, *Acacia mangium* sawdust one-month seasoned wood, *Acacia mangium* saw dust six-months seasoned wood and rice straw) were used for my experiments.

3.1.1. Spelt chaff and ground post-agglomerated spelt chaff

Biomass pellets made from spelt chaff were used industrial and household. Therefore, spelt chaff was being selected as the raw material for my experiments. It originated from Szendrő, Hungary (Natur Gold Farms Ltd.). It was dried and then ground using a cutting mill (Retsch SM2000) in one step (screen size 2 mm). The moisture content of spelt chaff biomass (< 1.6 mm) was determined as 5.3 wt.% and bulk density of 193 kg/m^3 . Raw material spelt chaff can be seen in Figure 3.1. It can be observed that spelt chaff is a homogeneous material and regular particle shape with elongated form.



Figure 3.1. Spelt chaff with particle size < 1.6 mm; (left) optical camera; (right) optical microscope: Zeiss AXIO Imager.M2m

Ground post-agglomerated (GPA) spelt chaff, the feed material was produced from agglomeration spelt chaff raw material at a temperature of 100°C (particle size < 1.6 mm) and then ground at screen size 1 mm. This material has particle size $x < 1$ mm, and bulk density of 354 kg/m^3 at a moisture content of 10 wt.% and the moisture content were then adjusted to 20 wt.%. Ground post-agglomerated spelt chaff can be seen in Figure 3.2. It can be observed that GPA-spelt chaff is an inhomogeneous material and irregularly shaped particle with spheroid and elongated form.

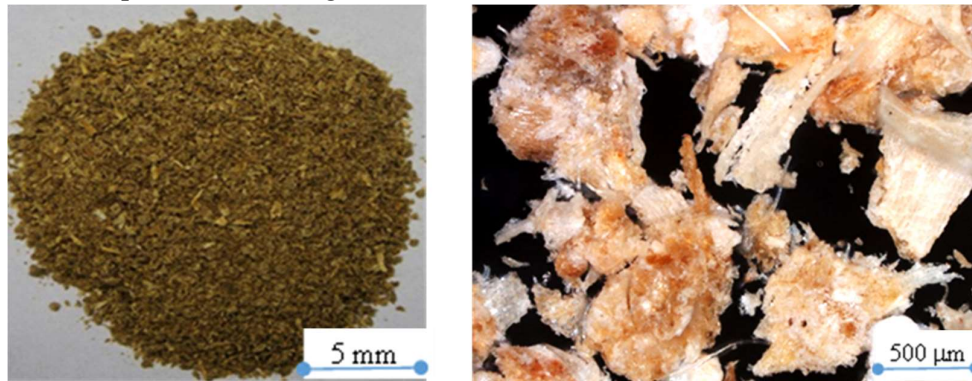


Figure 3.2. Ground post-agglomerated spelt chaff with particle size < 1 mm; (left) optical camera; (right) optical microscope: Zeiss AXIO Imager.M2m

Figure 3.3 shows the particle size distribution of spelt chaff raw material and ground post-agglomerated spelt chaff. Particle size < 1.6 mm were produced with cutting mill screen size 2 mm, in the case of spelt chaff. Particle size < 1 mm were produced with cutting mill screen size 1 mm, in the case of ground post-agglomerated.

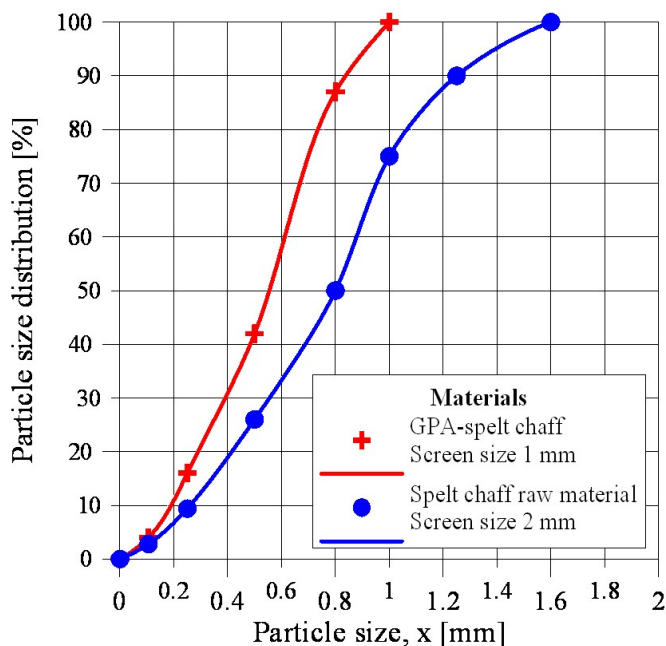


Figure 3.3. Particle size distribution of spelt chaff and GPA-spelt chaff

3.1.2. Beech sawdust

Tablets made from beech sawdust will be useful to the beech biomass industry. Thus, beech sawdust was chosen as the raw material for my experiments. It was originated from Miskolc, Hungary (Borsodwood Ltd.). It was dried and then ground using a cutting mill (Retsch SM2000) in one step (screen size 2 mm) and in two steps (screen sizes: 2 mm, 1 mm). The biomass was stored at room temperature (25°C), in closed plastic bags. The moisture contents and bulk density of beech biomass were determined to be 1.47 wt.%, 267 kg/m³ in the case of particle size < 1 mm, and 1.44 wt.%, 252 kg/m³ (particle size < 2 mm).

The raw material of beech sawdust can be seen in Figure 3.4. It can be observed that beech sawdust is a homogeneous material and regularly shaped particle with rectangular prism form.

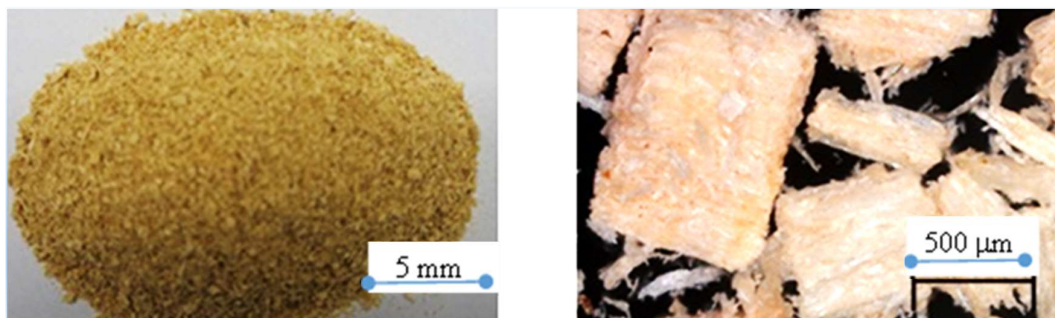


Figure 3.4. Beech sawdust with particle size < 2 mm; (left) optical camera; (right) optical microscope: Zeiss AXIO Imager.M2m

Figure 3.5 shows the particle size distribution of beech sawdust. Particle size < 1 mm were produced with cutting mill screen size 1 mm, and particle size < 2 mm were produced with cutting mill screen size 2 mm.

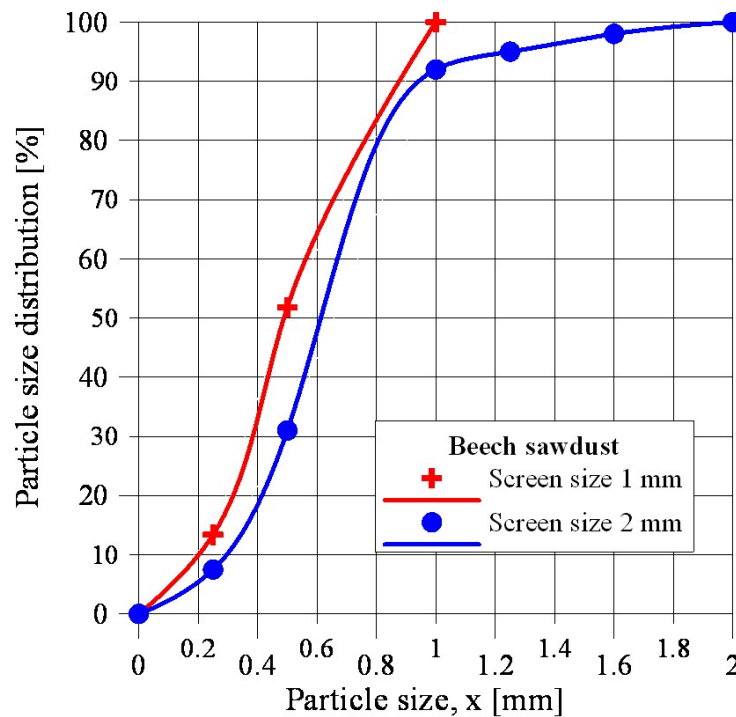


Figure 3.5. Particle size distribution of beech sawdust

3.1.3. *Acacia mangium* sawdust

The *A. mangium* is a potential and suitable source as a raw material for the production of particleboard with excellent dimensional stability (Korai and Nigel 2000; Nadhari et al. 2014). Therefore, an 8-year old *A. mangium* was chosen as the raw material for my experiments. It was obtained from Quang Ninh province, Vietnam. Half of it was seasoned for one month (from 25th August 2016 to 25th September 2016) by being covered outdoors, while the other half was seasoned for six months (From 25th August 2016 to 25th January 2017) in Vietnam.

In the case of the one month seasoned wood, it was comminuted by a cutting mill (Retsch SM2000) in one step (screen size 2 mm) and in two steps (screen sizes: 2 mm, 1 mm). Biomass was stored at room temperature (25°C), in closed plastic bags. The moisture contents and bulk density of *A. mangium* biomass were determined to be 5.1 wt.%, 143 kg/m³ for the case of particle size < 0.8 mm and 5.3 wt.%, 133 kg/m³ ($x < 1.6$ mm). Raw material

A. mangium sawdust is shown in Figure 3.6. It can be observed that *A. mangium* sawdust of one month seasoned wood is a homogeneous material and regularly shaped particle with elongated form.



Figure 3.6. *A. mangium* sawdust ($x < 1.6$ mm) in the case of one month seasoned wood; (left) optical camera; (right) optical microscope: Zeiss AXIO Imager.M2m

In the case of the six months seasoned wood, it was comminuted by a cutting mill (Retsch SM2000) in one step (screen size 2 mm). Biomass was stored at room temperature (25°C), in closed plastic bags. Therefore, the moisture contents (MC) and bulk density of *A. mangium* sawdust were determined, which were found to be 5.1 wt.% and 204 kg/m³ with particle size < 1.6 mm. Raw material *A. mangium* sawdust can be seen in Figure 3.7. It can be observed that *A. mangium* sawdust of six months seasoned wood is a homogeneous material and regularly shaped particle with elongated form.



Figure 3.7. *A. mangium* sawdust with ($x < 1.6$ mm) in the case of six months seasoned wood; (left) optical camera; (right) optical microscope: Zeiss AXIO Imager.M2m

Figure 3.8 shows the particle size distribution of *A. mangium* sawdust with the same particle size < 1.6 mm were produced with cutting mill screen size 2 mm, in the case of one month seasoned wood and six months seasoned wood. Particle size < 0.8 mm were produced with cutting mill screen size 1 mm. It can be observed that the same screen size 2 mm, but the particle size distribution was different. For instance, the particle size distribution of *A. mangium* sawdust with $x < 0.8$ mm were determined to be 85 % in the case of one month seasoned wood and 77 % (six months seasoned wood).

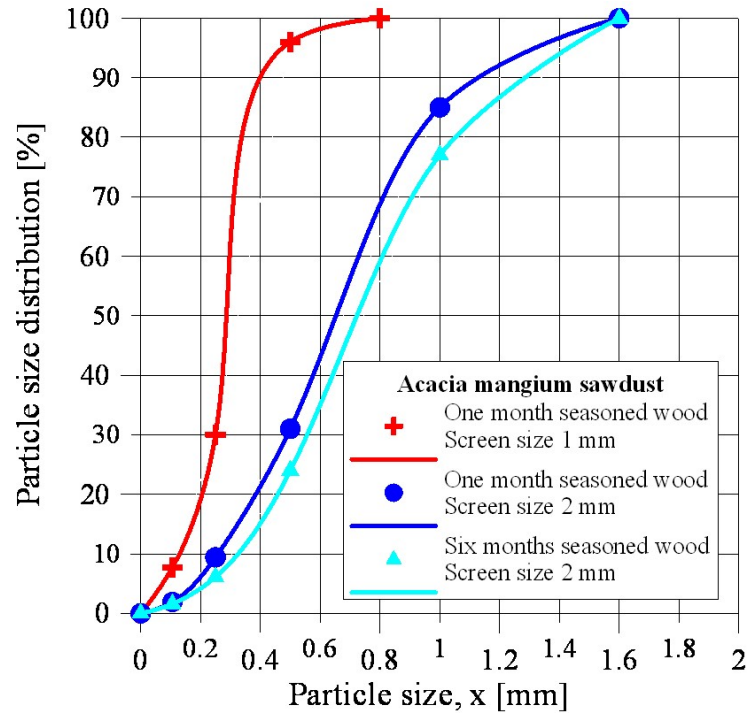


Figure 3.8. Particle size distribution of *A. mangium* sawdust

3.1.4. Rice straw

Rice straw is a major agriculture in Vietnam, the total annual average amount of rice straw was estimated 50 million tons/year (Le et al. 2011). The rice straw can be used for burning, burying, mushroom cultivation, breeding (Tran et al. 2014). Therefore, rice straw was chosen as the raw material for my experiments. It originated from Nam Dinh province, Vietnam. It was comminuted by a cutting mill (Retsch SM2000) in one step (screen size 2 mm). The moisture content, bulk density and particle size were determined to be 5 wt.%, 224 kg/m³ and $x < 1.6$ mm respectively. Rice straw is shown in Figure 3.9. It can be observed that rice straw is an inhomogeneous material and regularly shaped particle with elongated form.



Figure 3.9. Rice straw with ($x < 1.6$ mm); (left) optical camera; (right) optical microscope: Zeiss AXIO Imager.M2m

3.2. Hydraulic piston press at the University of Miskolc

The hydraulic piston press (Figure 3.10) was designed by the University of Miskolc. The hydraulic circuit diagram can be seen in Figure 3.11. The press is supported by a pump motor unit with a pressure limiter and a heat-able load cell (20-140°C). The maximum force is 200 kN, and the maximum velocity of the piston feed-rate is 30 mm/s (see Table 3.1). The measuring of the piston position is done with an incremental encoder. The relative deviation calculation can be seen in the appendix I.

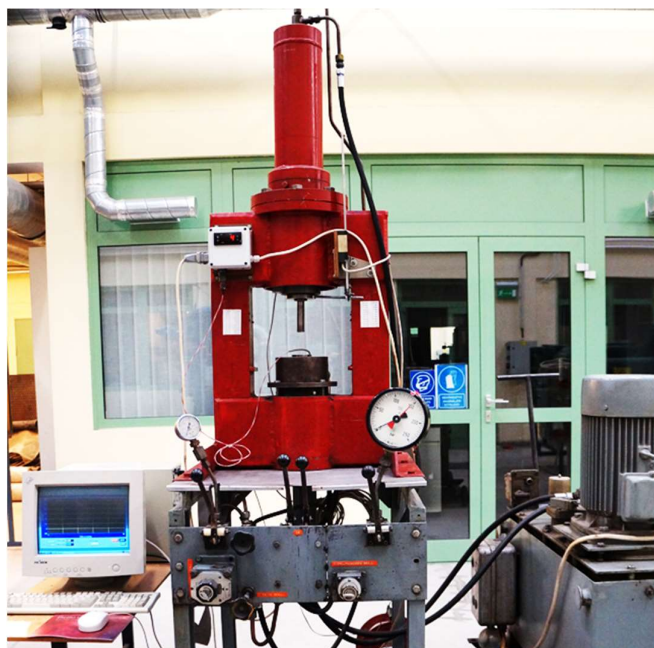


Figure 3.10. Hydraulic piston press

Table 3.1. Speed of piston

Pressure, p [MPa]	Value set on the equipment				
	2	4	6	8	10
	Speed [mm/s]				
100	5.63	12.81	20.15	28.08	34.76
150	5.84	11.69	19.9	27.28	36.57
200	5.54	12.4	19.41	28.4	32.85
250	5.58	12.47	20.19	28.74	33.74
Relative deviation [%]	2.36	3.81	1.8	2.22	4.63
Average values [mm/s]	5.65	12.34	19.91	28.13	34.48

Two hydraulic pistons are in the equipment. The one (1/a; $F_{max} = 200$ kN) is used for pressing, the other is for raising of the tablets. The pistons can be moved through control valves (4/a and 4/b). The pressure of the oil in the pistons can be set by the pressure controller (2/a and 2/b). The speed of pistons can be set by the volume stabilizer valves (3/a and 3/b). The following parts were installed on the equipment for my research work: incremental distance meter, force meter, heating unit, data acquiring system. The building of the equipment and the installing of different new units were made by the workshop of the institute (coordinated by Gábor Antal), the data acquiring system was developed by Dr. József Faitli.

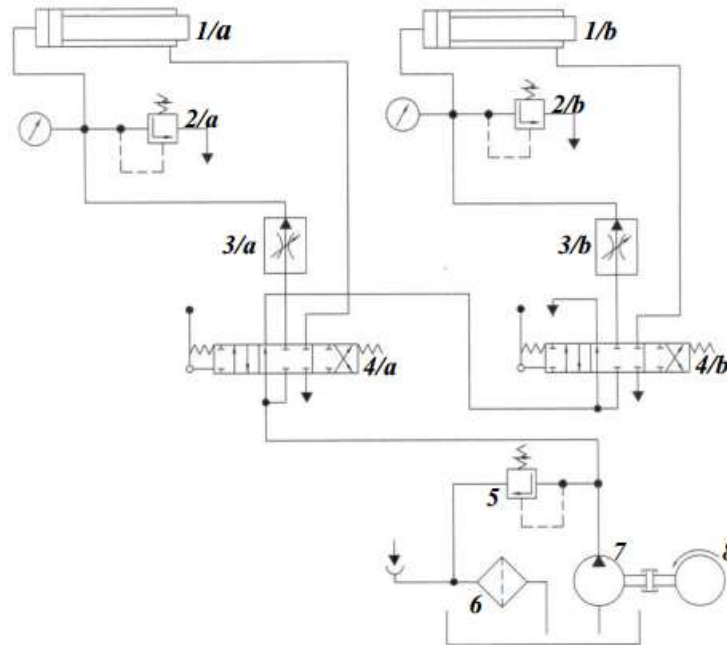


Figure 3.11. Simplified hydraulic circuit diagram of experimental equipment

3.3. Flat die pelletizer at the University of Miskolc

Flat die pelletizer (Figure 3.12): the system contains a press, mixing container, conditioning screw and a steam generator (Theobald TJ-Extra II, 19 kg/h steam). The capacity of the pelletizer is 50...100 kg/h depending on feed, during my experiments it was 60 kg/h. The diameter of the flat die is 200 mm, hole length is 28 mm and diameter is 8 mm.

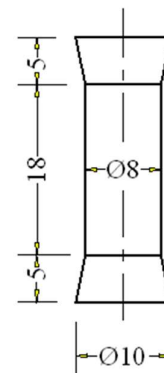


Figure 3.12. Flat die pelletizer (left), hole length (right)

3.4. Measurement of density

The density of each individual pellet was calculated by measuring the length and diameter of the pellet cylinder using an electronic caliper and by measuring the mass using an electronic scale with a precision of 0.01 g (type OHAUS-E1B120). To achieve a uniform length, the edges of the pellets were smoothed. Pellet density was calculated by dividing the mass of individual pellets by their volume calculated from length and diameter.

The quality of tablets can be described easily with the density. The diameters and heights of the tablets were measured by Vernier caliper (the tablet can be extended after agglomeration), mass was measured and density was calculated.

3.5. Spring-back ratio

The springback ratio (SBR) of a tablet can be determined by

$$\text{SBR} = \frac{H_t - H_{tp}}{H_{tp}} 100 \% \quad (15)$$

where H_t is the height of the produced tablet, H_{tp} is a minimum height of the tablet under pressure. The minimum height of tablets under pressure was measured by the incremental distance measurement method.

3.6. Structure of tablets and falling test method

The cross-sectional surfaces of tablets were investigated with an optical microscope Zeiss AXIO Imager.M2m. The determination of tablet strength was carried out by the well-known falling test method. Tablets were released by freefall from a height of 2 m onto a concrete floor repeatedly until they broke. The falling number is the number of falls the sample survived undamaged. In each experiment three tablets were tested, the results were calculated from the average of three independent tests.

CHAPTER 4. DEVELOPMENT OF EQUIPMENT

4.1. Single pelletizer unit 1

In this section, I have developed and implemented a pelletizing channel device (SPU 1) that is suitable for modeling the pelletizing process in the pressure channels of the flat pelletizer in the case of biomass with different production parameters. Afterwards, ground post-agglomerated spelt chaff was compressed using the single pelletizer unit 1 at various conditions based on an experimental design to evaluate the effect of moisture content (MC), the particle size of feed (x), temperature (T) are introduced. The compressibility of ground post-agglomerated spelt chaff by hydraulic piston press (25 mm diameter) and pellets produced by flat die pelletizer are also introduced.

4.1.1. Development of single pelletizer unit 1

The design of new press channel and piston are shown in Figure 4.1, which was mounted in the hydraulic piston press called single pelletizer unit 1 (Figure 4.2). Length of the active part was 55 mm, the diameter of the hole was 8 mm. A piston (diameter: 8 mm, length: 15 mm) limited by a cylinder (height: 26 mm) can force the raw material into the chamber. Above the piston, a force meter was built in (type: Kaliber 8923-1 ton, height 46 mm) to measure the actual force.

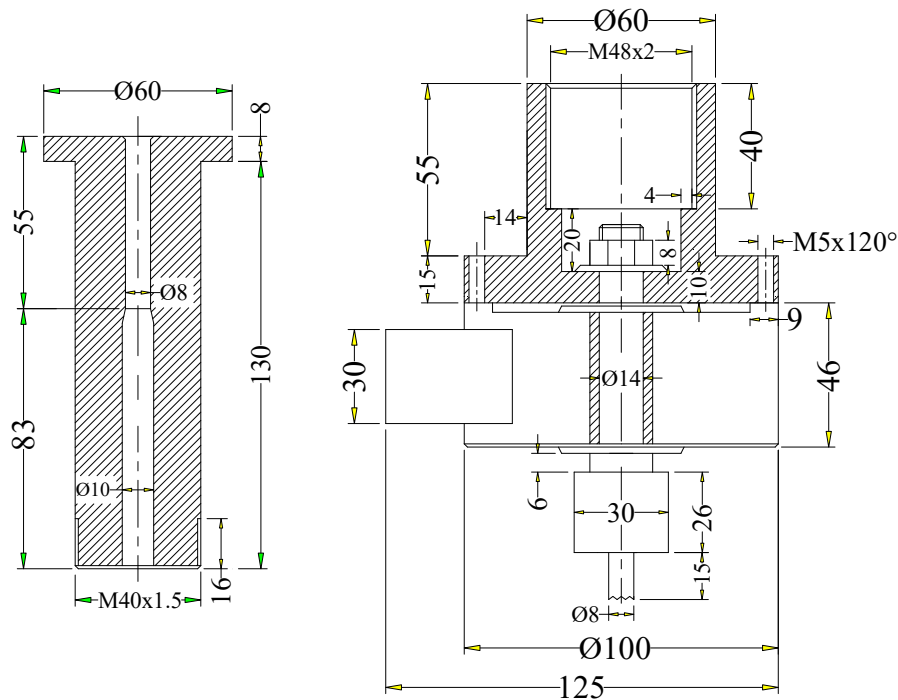


Figure 4.1. Design of new single pelletizer unit 1: press channel (left) and piston (right)



Figure 4.2. Single pelletizer unit 1

4.1.2. Determination of compressibility of ground post-agglomerated spelt chaff

Tablets were produced to determine the compressibility of the raw material. The hydraulic piston press with 25 mm diameter was used. The feed material was produced from ground post-agglomerated spelt chaff (GPA- spelt chaff) with particle size < 1 mm.

Table 4.1. Tablet density values for GPA-spelt chaff with particle size < 1 mm

Applied pressure, p [MPa]	Tablet density, ρ [kg/m ³]			
	ρ_1	ρ_2	ρ_3	$\bar{\rho}$
50	992	926	1010	952
100	966	952	956	957
150	948	949	997	964
200	969	977	1002	982
250	1002	989	971	986
300	1023	975	1002	999

Table 4.1 shows the tablet density values which are recorded as an average of three measurements with weight of sample 3 g, moisture content of 20 wt.% and temperature of 100°C. Figure 4.3 shows the relationship between applied pressure and density, described by the linear function.

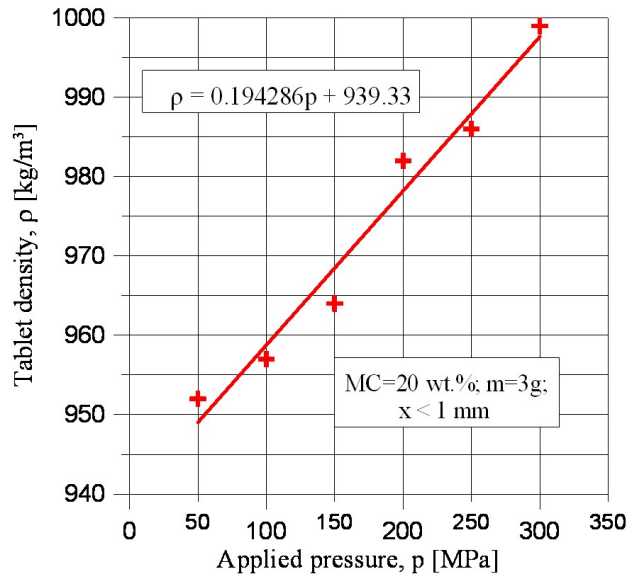


Figure 4.3. Applied pressure-tablet density diagram for GPA-spelt chaff ($x < 1$ mm)

4.1.3. Pellet production by flat die pelletizer

Ground raw material (spelt chaff) was fed five times (recirculated) into flat die pelletizer. Figure 4.4 shows the produced pellets, the moisture content of the raw material was 20 wt.%. Table 4.2 shows the geometrical parameters and density of pellets.



Figure 4.4. Pellets made from spelt chaff raw material by flat die pelletizer

Table 4.2. Measured geometrical parameters and density of pellets

Pellet	MC [wt.%]	x [mm]	Density of pellets, ρ_1 [kg/m³]			
			Diameter [mm]	Length [mm]	Weight [g]	Density [kg/m³]
1.	16	1	8.3	31	1.67	996
2.	16	1	8.3	33	1.84	1031
3.	16	1	8.4	33	1.81	990
$\bar{\rho}_1$						1005

The average pellet density could be calculated which is 1005 kg/m³ (see Table 4.2). According to the equation in Figure 4.3, using the average pellet density, the applied pressure of flat die pelletizer can be calculated of 338 MPa.

4.1.4. Pellet production by single pelletizer unit 1

During the process 0.2 g of ground post-agglomerated spelt chaff (*GPA-spelt chaff*) was fed into the channel. After that it was pressed and moved downwards 15 mm in the channel by the piston, then the piston was lifted. This was repeated until 20 g raw material was fed. The force limit was set to 350 MPa, and speed of piston was 6 mm/s. Figure 4.5 shows the pellets produced from single pelletizer unit 1 at temperature of 100°C and 20 wt.% moisture content.



Figure 4.5. Pellets produced by single pelletizer unit 1

Table 4.3 shows pellet densities made by single pelletizer unit 1. Experiments were carried out with GPA-spelt chaff and various conditions.

Table 4.3 Pellet process parameters

Original material	MC [wt.%]	x [mm]	T [°C]	Density of pellets, ρ_1 [kg/m ³]			
				Diameter [mm]	Length [mm]	Weight [g]	Density [kg/m ³]
Spelt chaff raw material	10	1	100	no pellets were formed			
	15	1	100	8.0	5.0	0.08	318
	15	1	80	no pellets were formed			
	15	1	60	no pellets were formed			
	15	1	40	no pellets were formed			
	20	1	100	8.2	7.0	0.12	341
	25	1	100	8.2	13.0	0.24	349
GPA- spelt chaff	10	1	100	8.2	18.0	0.57	599
	15	1	100	8.4	63.0	2.99	856
	15	1	80	8.4	47.0	1.74	668
	15	1	60	8.4	27.0	0.87	582
	15	1	40	no pellets were formed			
	20	1	80	8.4	36.6	1.85	913
	20	1	100	8.4	76.5	4.27	1008
	25	1	100	8.4	29.0	1.34	834

Figure 4.6 (left) shows the relationship between density of pellets and moisture content in the case of pellets made from spelt chaff and GPA-spelt chaff by single pelletizer unit 1 at a temperature of 100°C, applied pressure ($p = 350$ MPa), particle size < 1 mm with different moisture content. In the case of the same moisture content of 15 wt.% and different temperatures as shown in Figure 4.6 (right).

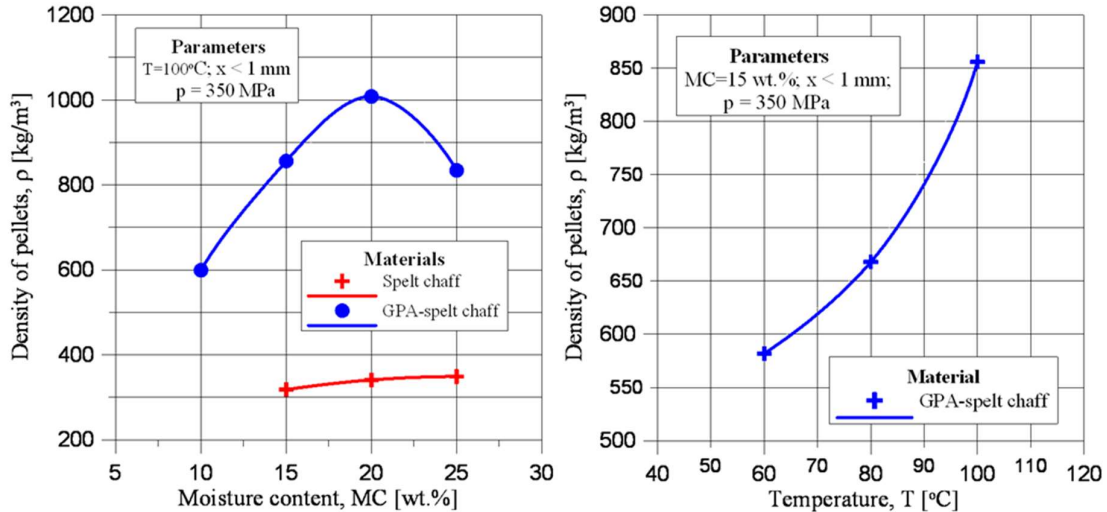


Figure 4.6. Relationship between density of pellets and moisture content (left) and temperature (right)

It is observed that at the same production conditions, pellets made from GPA-spelt chaff had a higher density than those made from spelt chaff raw material and have a maximum value at 20 wt.% moisture content. The increasing temperature has a higher density of pellets values.

4.2. Single pelletizer unit 2

4.2.1. Development of single pelletizer unit 2

I have designed and built a pelleting channel (SPU 2), which is divided into segments, one of which is a measuring segment, and I have developed a measurement method suitable for modeling pelletization in flat pelletizer pressure channels for biomasses with different properties, revealing the correlation between pellet density and channel wall pressure at different depths and temperatures.

4.2.1.1. The new design press channel of single pelletizer unit 2

The new design press channel is shown in Figure 4.7, which was mounted in the hydraulic piston press called single pelletizer unit 2 (Figure 4.8). The length of the active part was 55 mm, including three parts made from carbon steel, one part made from polyoxymethylene (POM), the length of each part was 13.75 mm and the diameter of the hole was 8 mm. Above the single pelletizer unit 2 a pressure transducer was built in (type: PU5402-100 bar- designed by Ifm electronic) to measure the backup pressure (solvent between membrane and pressure transducer: glycerin and alcohol). A piston (diameter: 8 mm, length: 15 mm limited by a cylinder (height: 26 mm)) can force the raw material to the chamber.

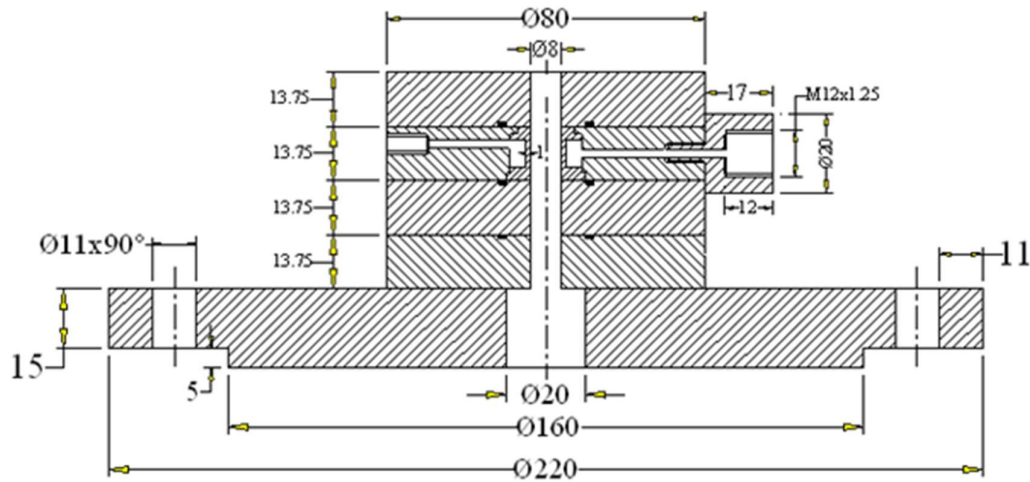


Figure 4.7. New design press channel of single pelletizer unit 2



Figure 4.8. Single pelletizer unit 2

4.2.1.2. Calibration of the equipment

Calibration is a process when the output signal of the sensor is compared to the value measured by a reference device, and the relationship between the measured and the reference value is determined.

Calibration of pressure transducer

From data sheet of Ifm Company Ltd. we have an analogue voltage output of the pressure transducer (type PU5402) from 0 to 10 V and measuring range from 0 to 100 bar. The use of the target pressure was from 0.08 bar to 6 bar in steps of 0.3 bar, compressed air was supplied to the air tank system (type EN286-1) for calibration. The reference pressure and voltage output of the transmitter from the display were read and it was repeated for all test points. Figure 4.9 shows the results of calibration using the air pressure calibration system and equation is fitted by the calibration results.

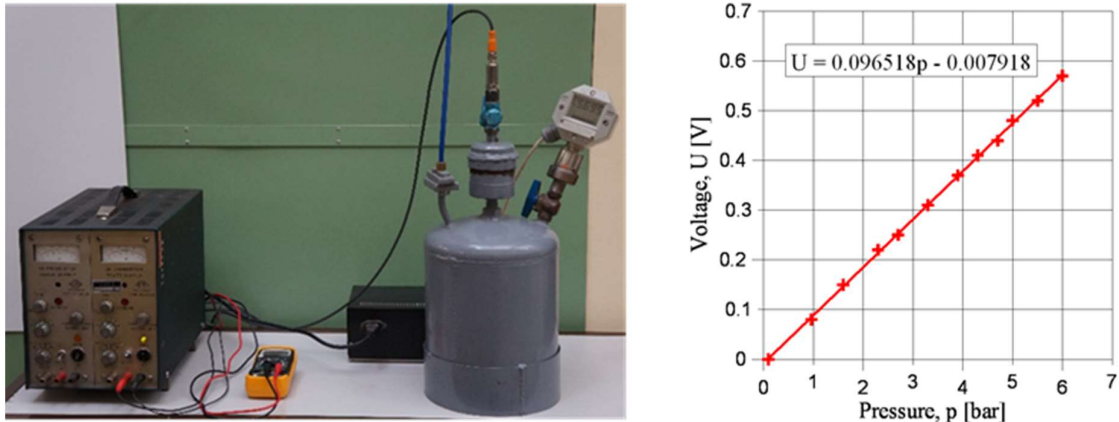


Figure 4.9. Air pressure calibration system (left); Calibration results for a PU5402 type pressure transducer (right)

Calibration of backup pressure in the chamber

The calibration of pressure in the chamber was performed by hydraulic pressure calibration. Before the beginning of the measurement, filling up of the test system. Filling of liquid (75 wt.% glycerin and 25 wt.% alcohol) through hole B when hole A is open when no air come through hole A, hole A is closed. The liquid is poured into the hole of the pressure transducer and then screw B is connected to pressure transducer when hole A is open, screw A is adjusted for liquid pressure of 3 bar as shown in Figure 4.10 and Figure 4.11 (left).

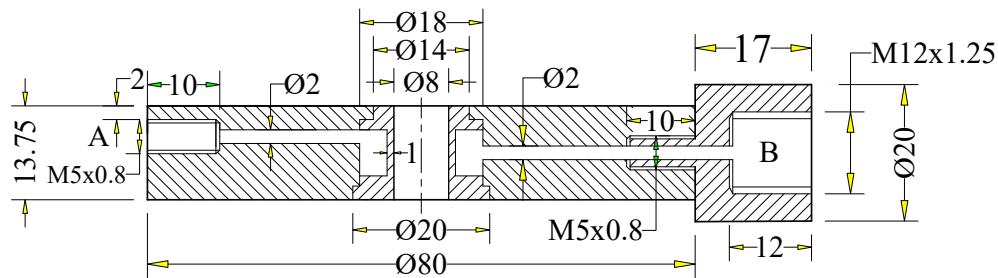


Figure 4.10. Design of backup pressure measurement disc (BPMD)

The backup pressure in the chamber was calibrated using the hydraulic pressure calibration system see Figure 4.11 (right). The calibration was carried out by adjusting the screw on the top of the system for liquid pressure increase, it was adjusted from 0 bar to 25 bar in steps of 1 bar and then the reference pressure and voltage output of the digital voltage meter were read and it was repeated for all test points. Figure 4.12 shows the results of calibration using the hydraulic pressure calibration system and the equation is fitted by the calibration results.



Figure 4.11. Set up pressure value in the backup pressure measurement disc (left) and hydraulic pressure calibration system (right)

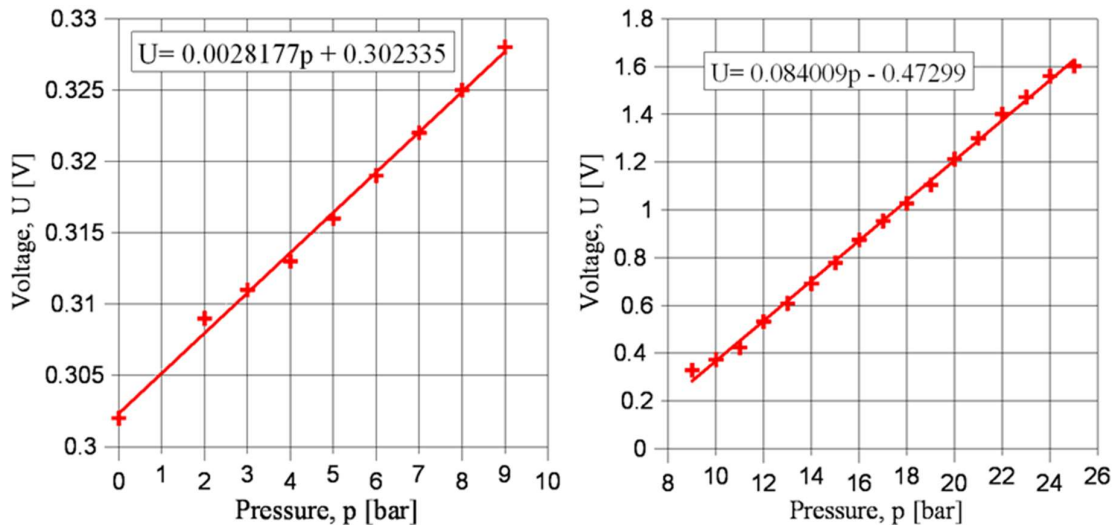


Figure 4.12. Calibration results for a backup pressure in the chamber; (left) 0 to 9 bar; (right) 9 to 25 bar

4.2.2. Determination of backup pressure distribution procedure

Single pelletizer unit 2 with diameter 8 mm was used for two kinds of press channel. During the process 0.3 g of GPA- spelt chaff with particle size < 1 mm and 20 wt.% moisture content was fed at the time into the channel. After that it was pressed and moved downwards 15 mm in the channel by the piston, then the piston was lifted. This was repeated until 10 g raw material had been fed into the channel and until the process of agglomeration stopped. The pressure limit was set at 350 MPa and the speed of the piston was 6 mm/s.

In the first press channel (including four parts without membrane), the applied temperature of 20°C in the case of four parts made from carbon steel, and three parts made from carbon steel and one part made from POM. In the second press channel, including three parts made from carbon steel and a backup pressure measurement disc. Each position of BPMD in the press channel was used to measure backup pressure at the temperature in the raw material of 20°C and 60°C respectively.

The backup pressure distributions were determined in the chamber by changing the pressure measurement points until the process of agglomeration stopped. The quality of pellets can be described easily by their density. The diameters and heights of the pellets product were measured by Vernier caliper. The mass was measured and density was calculated for each test.

The Jenike shear tester at the University of Miskolc (see Figure 4.13) was used to determine the coefficient of friction between GPA-spelt chaff, carbon steel and polyoxymethylene (POM). The results of this test showed that $\mu_{\text{GPA-cs}} = 0.299$ and $\mu_{\text{GPA-POM}} = 0.386$ respectively.



Figure 4.13. Jenike shear tester at the University of Miskolc

4.2.3. Backup pressure and pellet density distribution in the press channel

The piston was stopped after maximum 16 layers in the case of all active parts made from carbon steel and maximum 34 layers in the case of three small parts made from carbon steel and one part made from POM (without membrane). The first reason for that, the material doesn't flow continuously so it has time to stick on the wall of the active part may impede material movement, and temperature of the active part is smaller than temperature request of flat die pelletizer (100°C). The second reason for that according to Zhu et al. 2017, the Poisson ratio for POM (0.35) is higher than carbon steel (0.27-0.3) (Gercek 2007; Howatson et al. 1991). Although coefficient of friction between GPA-spelt chaff and POM (0.386) is higher than the coefficient of friction between carbon steel with the same material (0.299). The maximum layer number depending on the position of BPMD at the same temperature and moisture content, when BPMD at higher pressure position have higher maximum layer number. The reason for that at the same pressure, the hole diameter of BPMD have a higher plastic deformation than those other part made from carbon steel therefore the materials can be downward easily in the active part.

The pellets produced from single pelletizer unit 2 at 60°C and with 20 wt.% moisture content are shown in Figure 4.14 (with membrane).

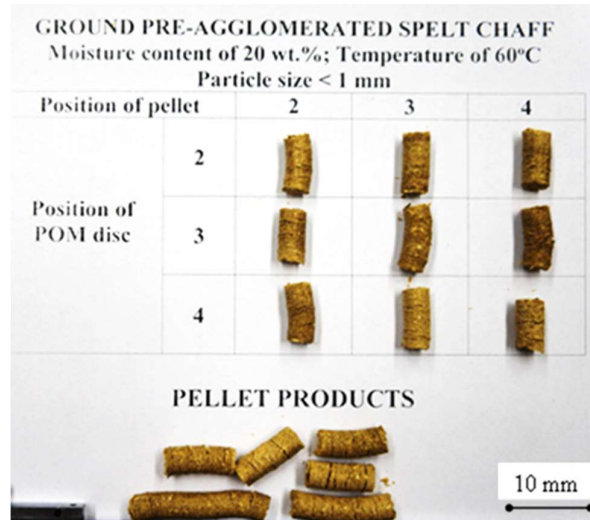


Figure 4.14. Pellets are produced by single pelletizer unit 2

Table 4.4 shows the density distribution in the pellet is reduced along the direction of the applied force in the active part, the pellets made at a temperature of 60°C have a higher density than those made at 20°C with the same moisture content of 20 wt.% and position of pellets in the active part. The weight of pellet in the active part is 2.5 g.

Table 4.4. Pellet density distribution

Density of pellets, ρ_1 [kg/m ³]							
Temperature [°C]		20°C			60°C		
Position of pellet		2	3	4	2	3	4
Position of backup pressure measurement disc	2	1080	971	901	1093	1021	902
	3	1056	959	907	1103	987	935
	4	1054	856	631	1095	886	773

The backup pressure distribution values can be seen Table 4.5, these values decrease along the direction of the applied force in the active part, the backup pressure distribution at 20 wt.% moisture content and temperature of 60°C in the range from 23.7, 14.9 and 9.6 bar. In the case of 20 wt.% moisture content and temperature of 20°C in the range from 21.1, 9.9 and 8.4 bar.

Table 4.5. Relationship between layer number and backup pressure

Backup pressure, p_B [bar]							
Temperature [°C]		20°C			60°C		
Layer number (L)		10	20	p_B (L _{max})	10	20	p_B (L _{max})
Position of backup pressure measurement disc	2	3.0	9.8	21.1 (33)	5.9	10.3	23.7 (34)
	3	2.7	9.1	9.9 (29)	3.4	9.8	14.9 (31)
	4	2.4	5.5	8.4 (24)	2.4	5.2	9.6 (29)

The relationship between the density of pellets and backup pressure at 20°C, 60°C temperature and different position of backup pressure measurement disc as shown in Table 4.6, and Figure 4.15 Illustrates the density of pellets and backup pressure distribution values along the active part at a temperature of 60°C.

Table 4.6. Relationship between density of pellets and backup pressure

Temperature [°C]		20°C		60°C	
Density/backup pressure		ρ_1 [kg/m ³]	p_B [bar]	ρ_1 [kg/m ³]	p_B [bar]
Position of backup pressure measurement disc	2	1080	21.1	1093	23.7
	3	959	9.9	987	14.9
	4	631	8.4	773	9.6

It is observed that, increasing backup pressure result in higher density at the same position of backup pressure measurement disc.

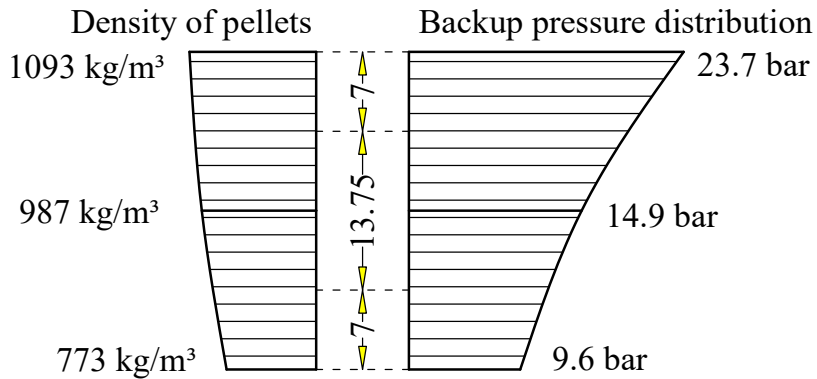


Figure 4.15. Pellet density and backup pressure distribution values along the active part at temperature of 60°C

4.3. Evaluation and discussion

4.3.1. Single pelletizer unit 1

It is possible to produce pellets with the developed single pelletizer unit 1 with different conditions, which can be set easily. The amount of the necessary feed material is low. Examination of compressibility was made by hydraulic piston press diameter 25 mm, showed that ground post-agglomerated is necessary for the good quality tablets. The densities of 3 g tablets are in a small range in the examined pressure range of 50, 100, 150, 200 and 250 MPa with (952, 964, 982, 986 and 999 kg/m³) respectively. Larger tablets (5 g) had fractures. The reason for that spelt chaff raw material (lower starch content: 0.5 %) could be poorly connected between particle sizes than ground post-agglomerated (higher starch content: 9.3 %). The pressure-density relationship can be described by a linear equation.

The systematic experiments with SPU showed pellets made from spelt chaff raw material were not strong enough (densities: 341 and 349 kg/m³). Pellets produced from GPA-spelt chaff fed into SPU1 had large densities (856 and 913 kg/m³). The maximal density was 1182 kg/m³, it was reached at 20 wt.% moisture content and 100°C temperature. The decreasing of temperature resulted in smaller density values both at 20 and 15 wt.% moisture content.

The pressure in the flat die pelletizer can be estimated from densities of produced pellets (1005 kg/m³) by the pressure density diagram. It can be assumed that the pressure was over 338 MPa.

4.3.2. Single pelletizer unit 2

Experiments found that if moisture content and temperature are kept constant, backup pressure values are reduced along the direction of the applied force in the active part. The highest backup pressure was observed at the second position of BPMD when the maximum pressure was 23.7 bar, and the minimum backup pressure was 9.6 bar at the fourth position of BPMD, it was reached at 20 wt.% moisture content and 60°C temperature.

If moisture content and position of BPMD are kept constant, the decreasing temperature resulted in smaller backup pressure values. For instance, in the case of the third position of BPMD, backup pressure value was 14.9 bar at 60°C and backup pressure value was 9.9 bar at 20°C temperature.

CHAPTER 5. EFFECT OF MOISTURE CONTENT AND PARTICLE SIZE ON BIOMASS AGGLOMERATION

5.1. Experimental procedure

The hydraulic piston press with diameter 25 mm was used for two different raw materials (beech sawdust and spelt chaff):

Each tablet was made by the compression of 5 g beech sawdust. Applied pressures on the surface of tablets were 50, 100, 150, 200, 250 and 275 MPa, the temperature of 20°C. In the first test, the applied moisture contents were 4.71, 9.27, 14.90 and 19.55 wt.% with particle size < 1 mm and 4.74, 9.68, 14.60 and 19.45 wt.% with the particle size < 2 mm. In the second test, spring-back ratio experiments were carried out with the particle size < 2 mm, moisture content 4.90, 9.60, 13.90 and 18.80 wt.%.

Each tablet was formed from the compression of 3 g spelt chaff with the same particle size < 1.6 mm. The applied pressure on the surfaces of tablets were 50, 100, 150, 200, 250 and 300 MPa for the six samples respectively. In the first test, the temperature was kept constant at 60°C and the moisture contents were 2.97, 5.30, 7.40, 10.50, 15.50 and 18.50 wt.% respectively. In the second test, spring-back ratio experiment was carried out, for different moisture content of (2.97, 5.30, 10.50 and 15.50 wt.%) at a constant temperature of 20°C.

Tablet density, spring-back ratio, the structure of tablets and tablet strength were defined according to chapter 3.

5.2. Tablet density

5.2.1. Tablets made from beech sawdust

Tablets produced by processes with different parameters are shown in Figure 5.1. The tablet density values are recorded as an average of three measurements with the particle size < 1 mm and also with the particle size < 2 mm (T = 20°C).



Figure 5.1. Tablets made from beech sawdust ($x < 2$ mm)

Figure 5.2 (left) shows the pressure density values and the fitted Johanson curves in the case of particle size < 1 mm raw material at 4.71, 9.27, 14.90 and 19.55 wt.%. Table 5.1 shows the constants of the fitted curves and coefficient of determination (R^2), residual mean square (σ) and calculated spread deviation (V_s) can be seen in the appendix II. Results for particle size < 2 mm are shown in Figure 5.2 (right) and Table 5.2.

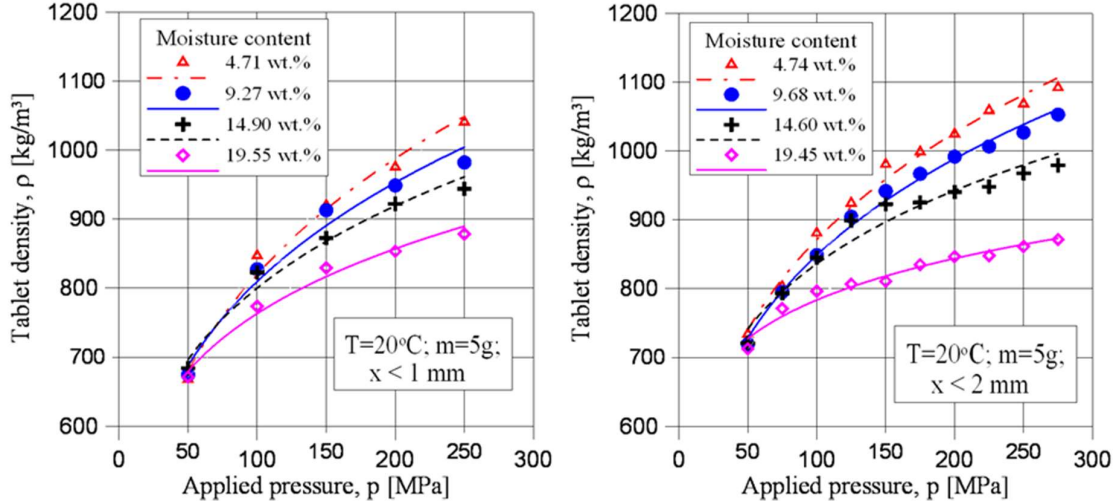


Figure 5.2. Compressibility data for beech sawdust with different moisture content; (left) particle size < 1 mm; (right) particle size < 2 mm

Table 5.1. Constants of Johanson’s equation ($\rho = a \cdot p^{1/\kappa}$) for beech sawdust with different moisture contents ($x < 1$ mm)

Moisture content [wt.%]	Constant a [$\text{kg}^{1-1/\kappa} \text{m}^{(1/\kappa)-3} \text{s}^{2/\kappa}$]	Constant κ [-]	Spread deviation: V_s [%]
			Coefficient of determination: R^2 [-] Residual mean square: σ [kg/m^3]
4.71	237.8374	3.7216	$R^2 = 0.9858$; $\sigma = 0.00055$; $V_s = 1.9$
9.27	273.9956	4.2517	$R^2 = 0.9782$; $\sigma = 0.00066$; $V_s = 3.0$
14.90	318.1958	4.9950	$R^2 = 0.9775$; $\sigma = 0.00049$; $V_s = 2.3$
19.55	352.8749	5.9737	$R^2 = 0.9835$; $\sigma = 0.00025$; $V_s = 1.9$

Table 5.2. Constants of Johanson’s equation for beech sawdust with different moisture contents ($x < 2$ mm)

Moisture content [wt.%]	Constant a [$\text{kg}^{1-1/\kappa} \text{m}^{(1/\kappa)-3} \text{s}^{2/\kappa}$]	Constant κ [-]	Spread deviation: V_s [%]
			Coefficient of determination: R^2 [-] Residual mean square: σ [kg/m^3]
4.74	293.8512	4.237	$R^2 = 0.9919$; $\sigma = 0.00015$; $V_s = 1.1$
9.68	307.3354	4.535	$R^2 = 0.9934$; $\sigma = 0.00011$; $V_s = 2.2$
14.60	377.0277	5.784	$R^2 = 0.9588$; $\sigma = 0.00044$; $V_s = 2.6$
19.45	478.6041	9.346	$R^2 = 0.9660$; $\sigma = 0.00013$; $V_s = 1.4$

Tablets compressed at lower pressure have a lower density. If pressure and particle size are kept constant, an increased moisture content resulted in lower tablet density (in the case of $x < 1$ mm raw material at 100 MPa tablet densities: $847.2 \text{ kg}/\text{m}^3$ (MC = 4.71 wt.%))

and 773.76 kg/m³ (MC = 19.55 wt.%). The reason for that could be the increasing SBR. Moisture content may have an effect on the strain-stress behavior of biomass particles and on the volume of particles, both of which affect SBR.

Tablets made from particle size < 2 mm have higher density than those made from particle size < 1 mm, at constant pressure, temperature and similar moisture content. For instance, at 200 MPa and T = 20°C, the tablet densities were 975 kg/m³ (particle size < 1 mm, MC = 4.71 wt.%) and 1024 kg/m³ (particle size < 2 mm, MC = 4.74 wt.%).

To describe the compressibility of beech sawdust, the Johanson equation was used. As the original equation for describing compressibility, it is universal. It is possible to insert other parameters in it, such as moisture content.

The spread deviation values (V_s) of fitted Johanson's equations are calculated (Table 5.1) and shown to have a value smaller than 3 %. At the same temperature, the higher moisture content results in higher constants a and κ . A linear equation can be found, that describes the moisture content dependence of values a and κ , and so compression can be described by an equation based on the original Johanson's equation and containing moisture content as a parameter.

Johanson's equation:
$$\rho = ap^{1/\kappa} = ap^b \quad (16)$$

Where

$$a = f(c_w) = a_1 c_w + a_2 \quad [\text{kg}^{1-1/\kappa} \cdot \text{m}^{(1/\kappa)-3} \cdot \text{s}^{2/\kappa}] \quad (17)$$

$$a_1 = 7.7639 \quad [\text{kg}^{1-1/\kappa} \cdot \text{m}^{(1/\kappa)-3} \cdot \text{s}^{2/\kappa}];$$

$$a_2 = 201.7242 \quad [\text{kg}^{1-1/\kappa} \cdot \text{m}^{(1/\kappa)-3} \cdot \text{s}^{2/\kappa}]$$

$$b = \frac{1}{\kappa} = f(c_w) = b_1 c_w + b_2 \quad [-] \quad (18)$$

$$b_1 = -0.0067 \quad [-]; \quad b_2 = 0.2995 \quad [-]$$

The new equation for particle size < 1 mm beech sawdust:

$$\rho = (7.7639c_w + 201.7242) p^{(-0.0067c_w+0.2995)} \quad [\text{kg/m}^3] \quad (19)$$

where c_w is moisture content [wt.%]

The new equation for particle size < 2 mm beech sawdust:

$$\rho = (12.7045c_w + 210.2576)p^{(-0.0088c_w+0.2913)} \quad [\text{kg/m}^3] \quad (20)$$

The processes were well described by the applied Johanson functions at each moisture content. The modified Johanson equation, which contains moisture content c_w as a parameter, provides only a small deviation of the density of approximately 0.7 %.

Thus, we conclude that the modified Johanson equation gives accurate results, particle size < 1 mm, MC = 4.71 wt.%, $p = 50$ MPa, density in the case of Johanson's equation 680 kg/m³; density in the case of modified Johanson's equation 679 kg/m³ and also for particle size < 2 mm, MC = 19.45 wt.%, $p = 75$ MPa, density in the case of Johanson's equation 765 kg/m³, density in the case of modified Johanson's equation 759 kg/m³.

5.2.2. Tablets made from spelt chaff

Tablets made from spelt chaff at the same temperature of 60°C and different moisture contents are shown in Figure 5.3. The values of the tablet density were recorded as an average of three measurements.



Figure 5.3. Tablets made from spelt chaff ($x < 1.6$ mm)

Figure 5.4 shows the pressure-density values and the fitted Johanson curves for the case of the following samples: 2.97, 5.30, 7.40, 10.50 and 15.50 wt.% moisture content, ($T = 60^\circ\text{C}$). Table 5.3 shows the constants of the fitted curves and coefficient of determination (R^2), residual mean square (σ) and calculated deviation (V_s).

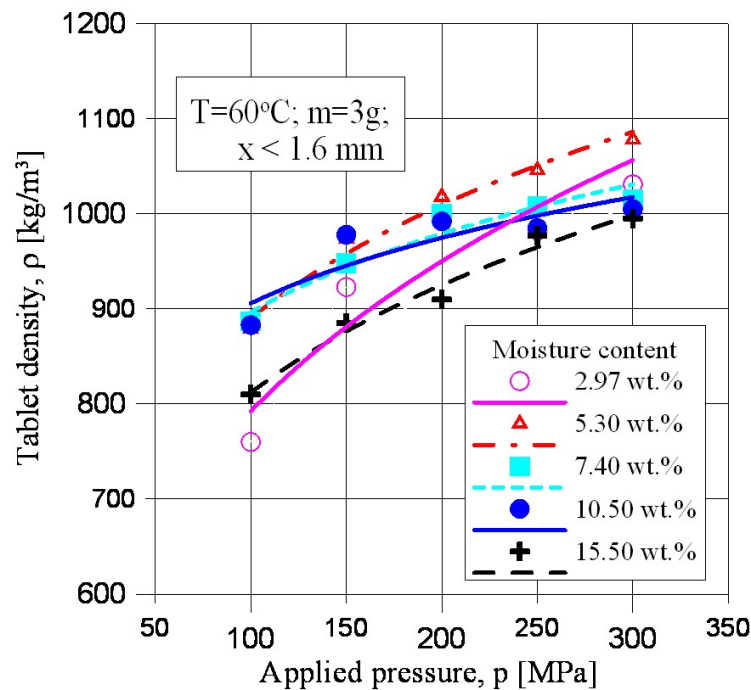


Figure 5.4. Compressibility data for spelt chaff with different moisture contents; $x < 1.6$ mm; temperature of 60°C

It is observed that at constant temperature and particle size, increasing moisture content resulted in lower density of tablets (except MC = 2.97 wt.%), and tablet density had a maximum value at 5.30 wt.% moisture content. (At a constant pressure of 200 MPa the tablet densities are: 994 kg/m³ (MC = 2.97 wt.%); 1018 kg/m³ (MC = 5.30 wt.%); 1000 kg/m³ (MC = 7.40 wt.%); 992 kg/m³ (MC = 10.5 wt.%) and 910 kg/m³ (MC = 15.50 wt.%)).

Table 5.3. Constants of Johanson's equation for spelt chaff at different moisture contents

Moisture content [wt.%]	Constant a [kg ^{1-1/κ} m ^{(1/κ)-3} s ^{2/κ}]	Constant κ [-]	Spread deviation: V_s [%] Coefficient of determination: R^2 [-] Residual mean square: σ [kg/m ³]
2.97	237.2621	3.8197	$R^2=0.8778$; $\sigma=0.0023$; $V_s = 4.10$
5.30	386.8001	5.5248	$R^2=0.9767$; $\sigma=0.0001$; $V_s = 1.10$
7.40	499.1618	7.8678	$R^2=0.9368$; $\sigma=0.0002$; $V_s = 1.40$
10.50	556.2694	9.4517	$R^2=0.7768$; $\sigma=0.0008$; $V_s = 2.40$
15.50	340.6957	5.3050	$R^2=0.9800$; $\sigma=0.0001$; $V_s = 1.10$

Spread deviation values (V_s) of fitted Johanson's equations are calculated in Table 5.3 and all the samples have values less than 4.10 %. It is also observed that at constant temperature, the increase in moisture content does not result to a higher values of the constants a and κ . A linear equation can't be found that described the moisture content dependence of values a and κ . Therefore, it cannot be described by modified Johanson's equation containing moisture content as a parameter.

5.3. Spring-back ratio of tablets

5.3.1. Tablets made from beech sawdust

Figure 5.5 shows the relationship between applied pressure and SBR in the case of different moisture contents of raw materials (4.90, 9.60, 13.90 and 18.80 wt.%). This relationship can be described by the following function: $SBR = dp^c$ the constants c and d are corresponding to each moisture content. Tablets made from the raw material with larger moisture content had larger SBR (at the same pressure, temperature and particle size). In the case of 18.80 wt.% moisture content, SBR of over 50 % was measured. Tablets with 4.90 wt.% moisture content had only 20.1 to 35.8 % SBR depending on pressure, in the examined pressure range.

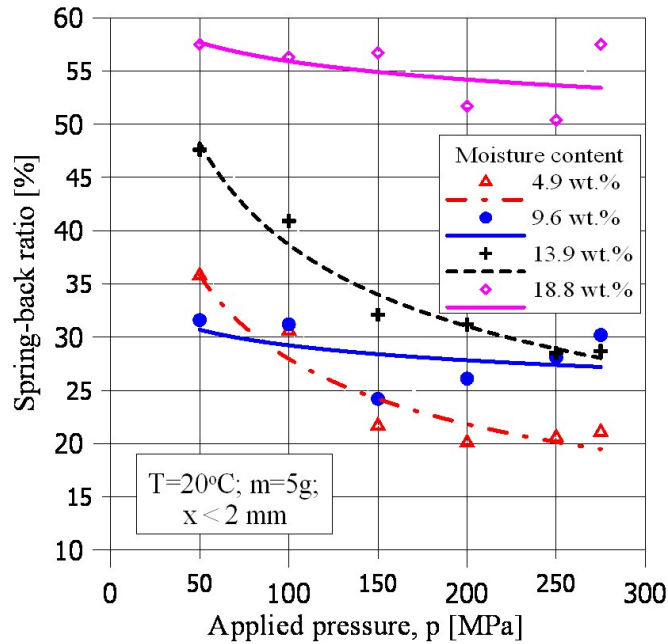


Figure 5.5. Relationship between spring-back ratio and pressure for different moisture content of beech sawdust ($x < 2$ mm)

5.3.2. Tablets made from spelt chaff

Figure 5.6 shows the relationship between applied pressure and spring-back ratio for different moisture contents of raw materials (2.97, 5.30, 10.50 and 15.50 wt.%). These relationships can be described by linear functions. At the same pressure and temperature, tablets made from the raw material with 5.30 wt.% moisture content had minimum spring-back ratio.

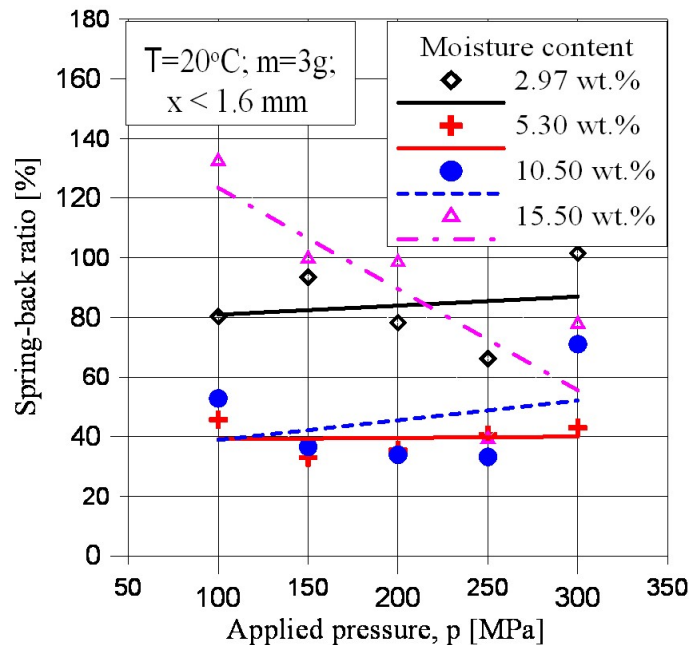


Figure 5.6. Relationship between spring-back ratio and pressure for different moisture contents of spelt chaff ($x < 1.6$ mm)

5.4. Structure of tablets

5.4.1. Tablets made from beech sawdust

The cross-sectional surfaces of tablets are shown in Figure 5.7. The tablets made at pressure 50 MPa had more space between particles (porosity is higher) than the tablet made at 250 MPa, with the same moisture content 4.71 wt.%. The same effect can be recognised in the case of MC = 19.55 wt.%. On the optical microscopy pictures no relevant differences can be seen between tablets made at 4.71 and 19.55 wt.% moisture content. The reasons for that the increasing external forces acting upon the particulate matter during size enlargement, porosity and characteristics related to this parameter decrease while density and strength increase (Pietsch 1991).

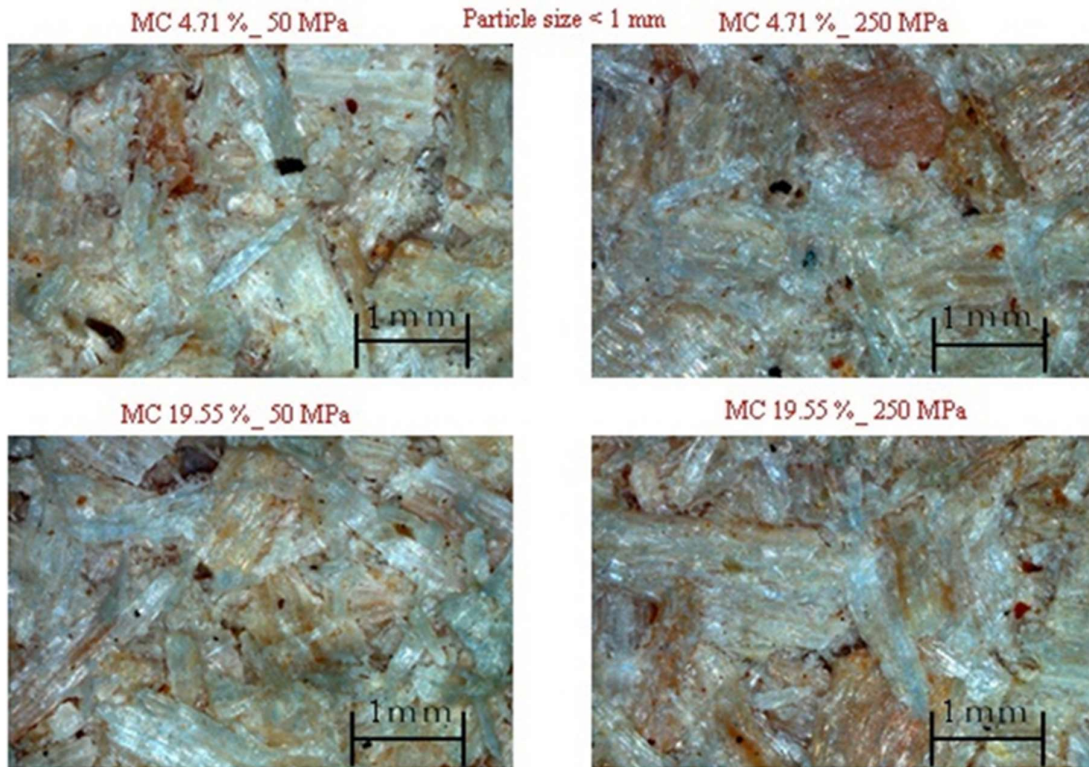


Figure 5.7. Cross sectional surface of tablets made from beech sawdust (optical microscope: Zeiss AXIO Imager.M2m)

5.4.2. Tablets made from spelt chaff

The cross-sectional surfaces of tablets were investigated with an optical microscope (Zeiss AXIO Imager.M2m), as shown in Figure 5.8. The tablets made at pressure 100 MPa had more space between particles (porosity is higher) than the tablets made at pressure 250 MPa, with the same moisture content 2.97 wt.% and $x < 1.6$ mm. The same effect is realized in the case of MC = 10.50 wt.%. In the optical microscopy pictures, no relevant differences can be seen between tablets made with 2.97 wt.% and 10.50 wt.% moisture content. The reason for this is that, generally, with increasing external forces acting upon the particulate matter during size enlargement, porosity and characteristics related to this parameter decrease while density and strength usually increase (Pietsch 1991).

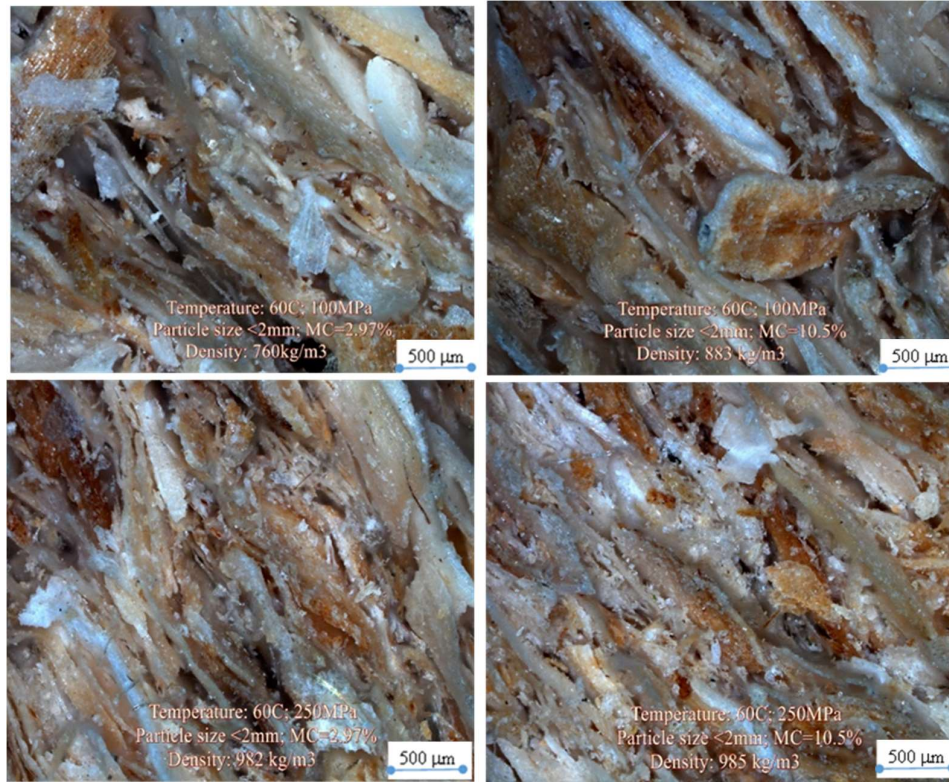


Figure 5.8. Cross sectional surface of tablets made from spelt chaff (optical microscope: Zeiss AXIO Imager.M2m)

5.5. Tablet strength

Falling number values in the case of tables made from beech sawdust are shown in Figure 5.9 as a function of moisture content at different pressures for both particle size < 1 mm and < 2 mm raw materials. Increasing moisture content resulted in lower tablet strength at the same pressure and with same particle size. Adsorbed moisture on the particle surface can also interfere with intermolecular forces, thus reducing the bond strength and resultant tablet strength (Herrmann 1971; Lordi 1983; Nyström et al 1993). Tablets made from particle size < 2 mm form tablets with higher strength (falling number: 5.66 at 250 MPa and 4.74 wt.%) than tablets made from particle size < 1 mm biomass (falling number: 4.33 at 250 MPa and 4.71 wt.%) if moisture content and pressure are constant. The reason for this may be that the larger particles size connects together better than small particles size under the same experimental conditions.

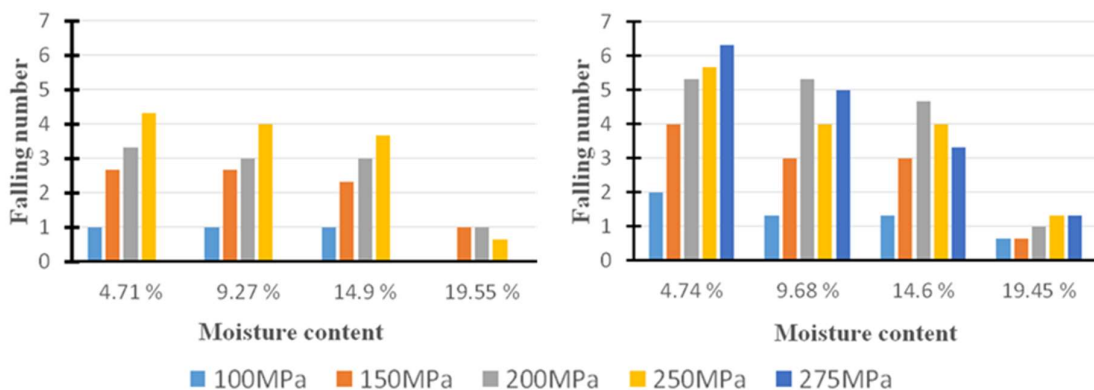


Figure 5.9. Falling number values in the case of tables made from beech sawdust with different moisture contents and pressures; (left) $x < 1$ mm; (right) $x < 2$ mm

5.6. Evaluation and discussion

The effect of moisture content, pressure and particle size on tablet density in the case of beech sawdust and spelt chaff are introduced as follows:

In the case of beech sawdust

The description of the agglomeration processes is essential to be able to determine the optimal production parameters. While the applied Johanson functions describe the processes well (at 9.27 wt.%, in the case of $x < 1$ mm raw material $V_s = 3.0$ %, when using $x < 2$ mm raw material $V_s = 2.2$ %) the modified Johanson's equation for compression introduced here contains also moisture content as a parameter.

Experiments found that if pressure and particle size are kept constant, increasing moisture content results in lower density and strength of tablets with the same particle size. An effect of particle size was also identified: tablets made from sawdust with particle size < 2 mm form tablets with higher strength than those made from the particle size < 1 mm biomass when moisture content and pressure are kept constant.

In the case of spelt chaff

Tablets were not formed in all cases, for 18.50 wt.% moisture content and also for a pressure of 50 MPa. If pressure and temperature are kept constant, tablet density had a maximum value at 5.3 wt.% moisture content in the examined range (2.97, 5.30, 7.40, 10.50, 15.50 and 18.50 wt.%).

CHAPTER 6. TEMPERATURE, PARTICLE SIZE AND SEASONING EFFECTS ON BIOMASS AGGLOMERATION

6.1. Experimental procedure

The hydraulic piston press with 25 mm diameter was used for three different kinds of raw material (beech sawdust, spelt chaff and *A. mangium*):

Each tablet was made by the compression of 5 g beech sawdust. The applied temperatures were 20, 40, 60, 80 and 100°C. The applied pressures on the surface of tablets were 50, 100, 150, 200 and 250 MPa. Experiments were carried out with two particle size fractions: < 1 mm and < 2 mm. The moisture content of beech sawdust was determined 1.47 wt.% in the case of $x < 1$ mm and 1.44 wt.% ($x < 2$ mm).

Each tablet was made by the compression of 3 g spelt chaff. The applied temperatures were 20, 40, 60, 80 and 100°C respectively, with the same moisture content of 2.97 wt.% and $x < 1.6$ mm. Applied pressure on the surface of tablets were 100, 150, 200, 250 and 300 MPa. Spring-back ratio experiment was carried with the same production conditions.

Each tablet was made by the compression of 3 g *A. mangium* sawdust. Applied pressures on the surface of tablets were 50, 100, 150, 200, 250 and 300 MPa with different temperature (20, 60, 100 and 120°C) respectively. Applied particle size < 0.8 mm (MC = 5.1 wt.%) and $x < 1.6$ mm (MC = 5.3 wt.%) in the case of one month seasoned wood, and $x < 1.6$ mm (MC = 5.1 wt.%) in the case of six months seasoned wood. Spring-back ratio experiments were carried out with *A. mangium* one month seasoned wood ($x < 1.6$ mm, MC = 5.3 wt.%), the applied temperatures were 20, 60, 100 and 120°C.

6.2. Tablet density

6.2.1. Tablets made from beech sawdust

Tablets produced by different parameters are shown in Figure 6.1. The tablet density values which are recorded as an average of three measurements with the particle size < 1 mm and also for the particle size < 2 mm.



Figure 6.1. Tablets made from beech sawdust ($x < 2$ mm)

Figure 6.2 (left) shows the pressure-density values and the fitted curves in the case of $x < 1$ mm raw material on 20, 40, 60, 80 and 100°C. Table 6.1 shows the constants of the fitted curves and coefficient of determination (R^2), residual mean square (σ) and calculated deviation (V_s). Results for particle size < 2 mm are introduced in Figure 6.2 (right) and Table 6.2.

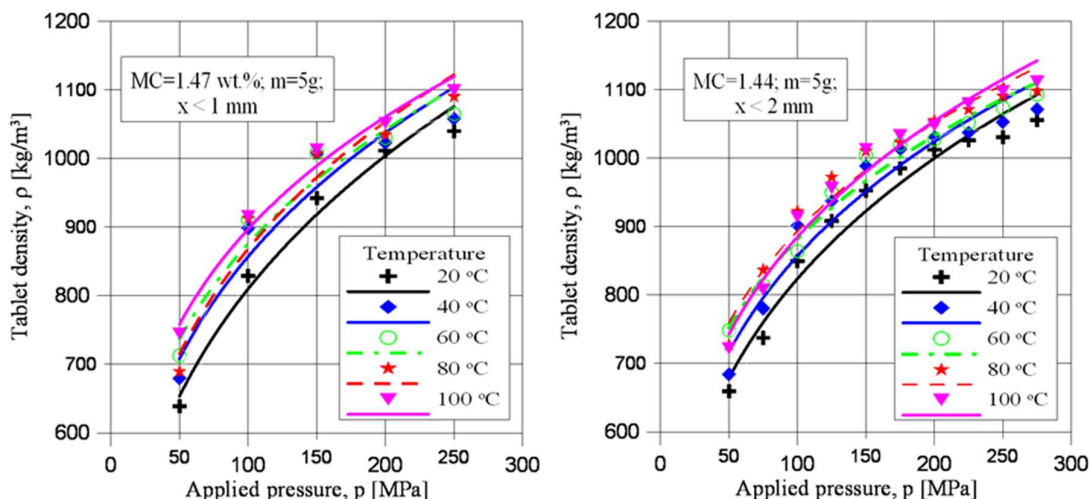


Figure 6.2. Compressibility data for beech sawdust with different temperatures; (left) particle size < 1 mm; (right) particle size < 2 mm

Table 6.1. Constants of Johanson's equation for beech sawdust with different temperatures ($x < 1$ mm)

Temperature [°C]	Constant a [$\text{kg}^{1-1/\kappa} \text{m}^{(1/\kappa)-3} \text{s}^{2/\kappa}$]	Constant κ [-]	Spread deviation: V_s [%] Coefficient of determination: R^2 [-] Residual mean square: σ [kg/m^3]
20	194.5093	3.2283	$R^2=0.9816$; $\sigma=0.00096$; $V_s = 2.78$
40	240.7600	3.6271	$R^2=0.9366$; $\sigma=0.00276$; $V_s = 4.53$
60	276.8318	3.9980	$R^2=0.9492$; $\sigma=0.00180$; $V_s = 3.64$
80	239.2337	3.5727	$R^2=0.9535$; $\sigma=0.00205$; $V_s = 3.79$
100	294.5099	4.1350	$R^2=0.9820$; $\sigma=0.00057$; $V_s = 2.00$

Table 6.2. Constants of Johanson's equation for beech sawdust with different temperatures ($x < 2$ mm)

Temperature [°C]	Constant a [$\text{kg}^{1-1/\kappa} \text{m}^{(1/\kappa)-3} \text{s}^{2/\kappa}$]	Constant κ [-]	Spread deviation: V_s [%] Coefficient of determination: R^2 [-] Residual mean square: σ [kg/m^3]
20	227.3821	3.5775	$R^2=0.9647$; $\sigma=0.00098$; $V_s = 4.18$
40	262.2798	3.8892	$R^2=0.9438$; $\sigma=0.00135$; $V_s = 4.24$
60	307.4255	4.3731	$R^2=0.9767$; $\sigma=0.00042$; $V_s = 3.00$
80	303.8298	4.2682	$R^2=0.9617$; $\sigma=0.00075$; $V_s = 3.10$
100	276.6470	3.9605	$R^2=0.9725$; $\sigma=0.00062$; $V_s = 3.40$

Spread deviation values (V_s) of fitted Johanson's equations are calculated in the Table 6.1 and 6.2, with all values smaller than 4.53 % ($x < 1$ mm) and 4.24 % ($x < 2$ mm) respectively. At the same moisture content the increasing of temperature results in not higher constants a and κ . A linear equation can't be found that described the temperature dependence of values a and κ . Therefore, it cannot be described by modified Johanson's equation containing temperature as a parameter.

6.2.2. Tablets made from spelt chaff

Tablets produced, using the same processes but with various parameters are shown in Figure 6.3. The values of the tablet density were recorded as an average of three measurements each; both for the case of different moisture content ($T = 60^\circ\text{C}$) and also for the case of different temperatures ($\text{MC} = 2.97$ wt.%).

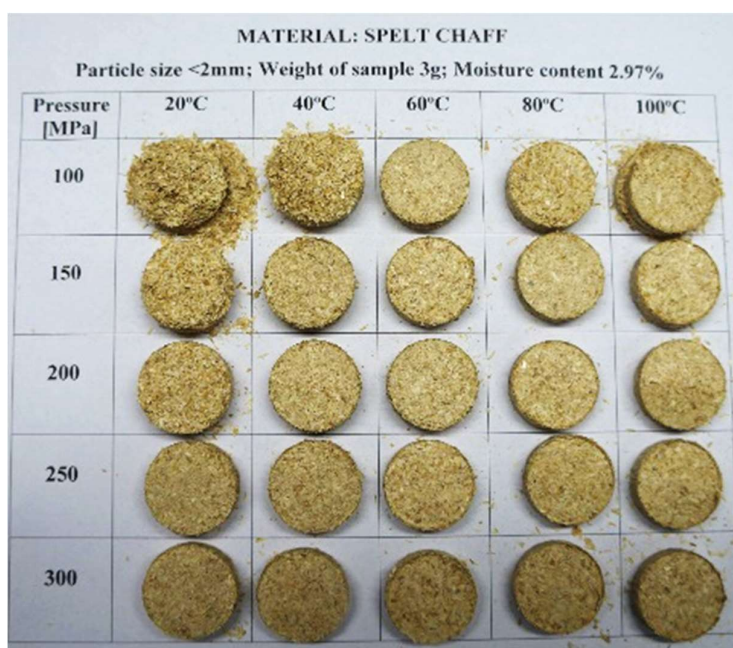


Figure 6.3. Tablets made from spelt chaff with different temperatures ($x < 1.6$ mm)

Results for the case of different temperatures are shown in Figure 6.4 and Table 6.3. It is observed that tablets formed using lower compacting pressures has smaller densities, while the reverse is the case for those produced using higher pressures.

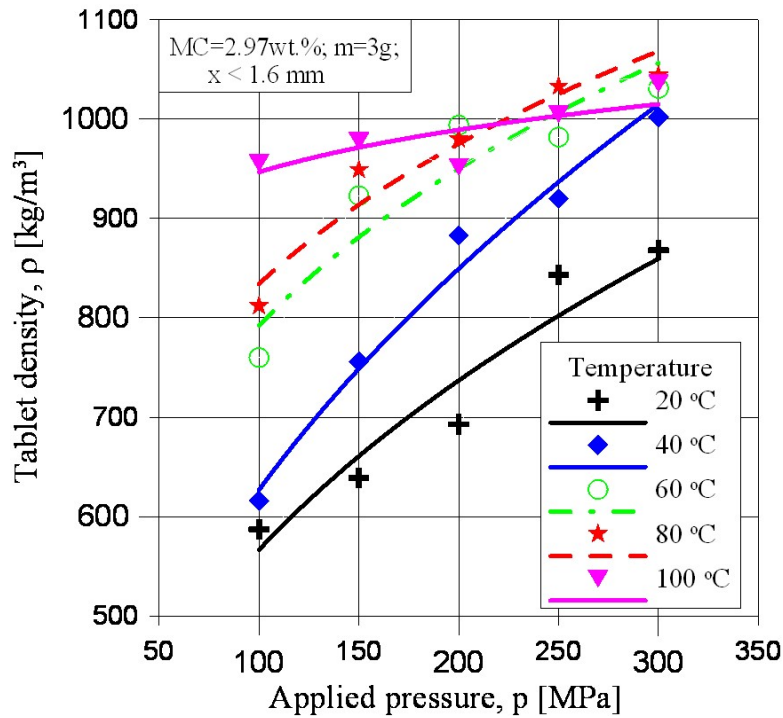


Figure 6.4. Compressibility data for spelt chaff with different temperatures ($x < 1.6$ mm)

If pressure and moisture content are kept constant, tablet density increases, as seen when the temperature increased from 20 to 80°C. Tablets made at 100°C resulted in increased densities, only at lower pressure values. (For instance, at 250 MPa the tablet densities are: 843 kg/m³ (T = 20°C); 1033 kg/m³ (T = 80°C); 1005 kg/m³ (T = 100°C)). The reason for this could be as a result of the temperature and pressure due to the shape of particle changing and binding between particle sizes better and then lower spring-back ratio. Tablets made from the raw material with lower spring-back ratio had smaller heights and higher densities.

Table 6.3. Constants of Johanson's equation for spelt chaff with different temperatures

Temperature [°C]	Constant a [kg ^{1-1/κ} m ^{(1/κ)-3} s ^{2/κ}]	Constant κ [-]	Spread deviation: V_s [%] Coefficient of determination: R^2 [-] Residual mean square: σ [kg/m ³]
20	98.6310	2.6350	$R^2=0.9254$; $\sigma=0.0029$; $V_s = 4.60$
40	83.1134	2.2841	$R^2=0.9838$; $\sigma=0.0007$; $V_s = 2.50$
60	237.2621	3.8197	$R^2=0.8778$; $\sigma=0.0023$; $V_s = 4.10$
80	295.3641	4.4365	$R^2=0.9328$; $\sigma=0.0009$; $V_s = 2.54$
100	707.1978	15.7977	$R^2=0.5973$; $\sigma=0.0006$; $V_s = 2.24$

Spread deviation values (V_s) of fitted Johanson's equations are calculated in Table 6.3 and they have a value smaller than 4.60 %. At the same moisture content the increasing of temperature results in not higher constants a and κ . A linear equation can't be found that described the temperature dependence of values a and κ . Therefore, it is not able to modified Johanson's equation which containing temperature as a parameter.

6.2.3. Tablets made from *Acacia mangium*

6.2.3.1. *A. mangium* one month seasoned wood

Tablets produced by processes with various parameters are shown in Figure 6.5. The tablet density values are recorded as an average of three measurements with the particle size < 0.8 mm (MC = 5.10 wt.%) and also with the particle size < 1.6 mm (MC = 5.30 wt.%).



Figure 6.5. Tablets made from *A. mangium* one month seasoned wood ($x < 1.6$ mm)

Figure 6.6 (left) shows the pressure-density values and the fitted Johanson curves in the case of $x < 0.8$ mm raw material at 20, 60, 100 and 120°C. Table 6.4 shows the values of the constants of the fitted curves, the coefficient of determination (R^2), residual mean square (σ) and calculated deviation (V_s). Results for particle size < 1.6 mm are introduced in Figure 6.6 (right) and Table 6.5.

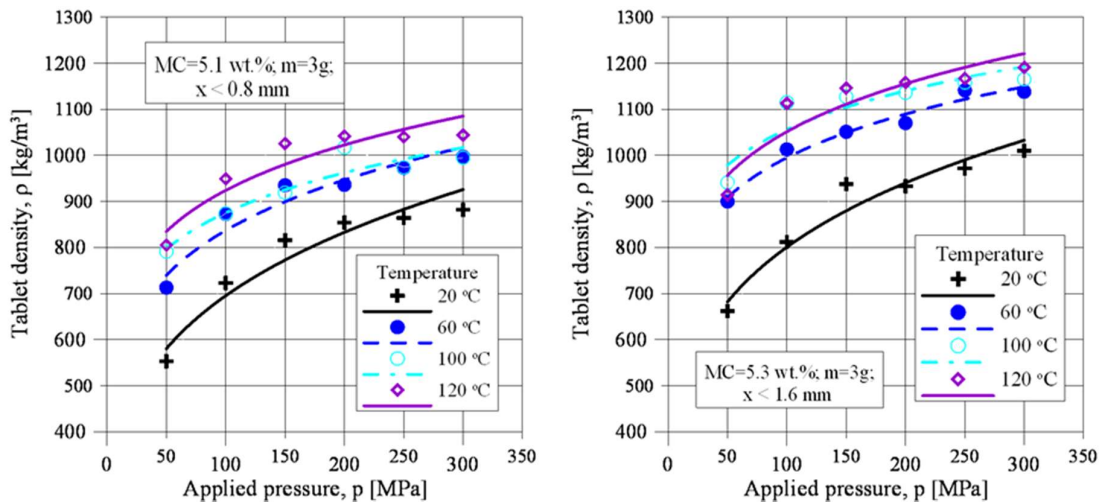


Figure 6.6. Compressibility data for *A. mangium* one month seasoned wood with different temperatures; (left) particle size < 0.8 mm; (right) particle size < 1.6 mm

Tablets compressed at lower pressure have lower densities. If pressure and particle size are kept constant, an increasing temperature resulted in higher tablet density (in the case of $x < 1.6$ mm raw material on 100 MPa the tablet densities: 1017 kg/m^3 ($T = 60^\circ\text{C}$) and 1123 kg/m^3 ($T = 100^\circ\text{C}$)). The reason for that can be increasing temperature results in lower spring-back ratio. Tablets made from raw material with larger spring-back ratio had higher heights and lower densities.

Tablets made from material particle size < 1.6 mm have higher density than tablets made from particle size < 0.8 mm, at constant pressure, temperature and moisture content (in the case of pressure 250 MPa, $T = 120^\circ\text{C}$, the tablet densities 1040 kg/m^3 ($x < 0.8$ mm, $\text{MC} = 5.10 \text{ wt.}\%$); 1167 kg/m^3 ($x < 1.6$ mm, $\text{MC} = 5.30 \text{ wt.}\%$)).

Table 6.4. Constants of Johanson's equation for *A. mangium* one month seasoned wood with different temperatures ($x < 0.8$ mm)

Temperature [°C]	Constant <i>a</i> [$\text{kg}^{1-1/\kappa} \text{m}^{(1/\kappa)-3} \text{s}^{2/\kappa}$]	Constant κ [-]	Spread deviation: V_s [%] Coefficient of determination: R^2 [-] Residual mean square: σ [kg/m^3]
20	209.4651	3.8388	$R^2 = 0.9355$; $\sigma = 0.0025$; $V_s = 4.4$
60	369.1054	5.6275	$R^2 = 0.9285$; $\sigma = 0.0013$; $V_s = 3.1$
100	467.4657	7.3421	$R^2 = 0.9112$; $\sigma = 0.0009$; $V_s = 3.0$
120	471.2722	6.8399	$R^2 = 0.8833$; $\sigma = 0.0015$; $V_s = 3.4$

The spread deviation values (V_s) of fitted Johanson's equations were calculated (Table 6.4) and they have a value smaller than 4.4 %. At the same moisture content, increase in temperature results in higher constants *a* and κ (except κ at 120°C).

Table 6.5. Constants of the Johanson equation for *A. mangium* one month seasoned wood with different temperatures ($x < 1.6$ mm)

Temperature [°C]	Constant <i>a</i> [$\text{kg}^{1-1/\kappa} \text{m}^{(1/\kappa)-3} \text{s}^{2/\kappa}$]	Constant κ [-]	Spread deviation: V_s [%] Coefficient of determination: R^2 [-] Residual mean square: σ [kg/m^3]
20	275.6347	4.3197	$R^2 = 0.9506$; $\sigma = 0.0015$; $V_s = 3.5$
60	544.2687	7.6394	$R^2 = 0.9710$; $\sigma = 0.0002$; $V_s = 1.5$
100	636.6259	9.0992	$R^2 = 0.8284$; $\sigma = 0.0013$; $V_s = 3.1$
120	561.5390	7.3475	$R^2 = 0.8474$; $\sigma = 0.0018$; $V_s = 3.6$

Spread deviation values (V_s) are calculated and it has all values smaller than 3.6 %. The processes were well described by the applied Johanson functions on each temperature.

6.2.3.2. *A. mangium* six months seasoned wood

Results for particle size < 1.6 mm, six months seasoned wood are introduced in Figure 6.7 and Table 6.6. Tablets compressed at lower pressure have a lower density. If the pressure is kept constant, an increasing temperature resulted in higher tablet density (in the case of tablets made at 100 MPa, the tablet densities: 594 kg/m^3 ($T = 20^\circ\text{C}$) and 715 kg/m^3 ($T = 60^\circ\text{C}$)). The reason for that can be the increasing temperature resulted in lower spring-back ratio. Tablets made from the raw material with larger spring-back ratio had higher heights and lower densities.

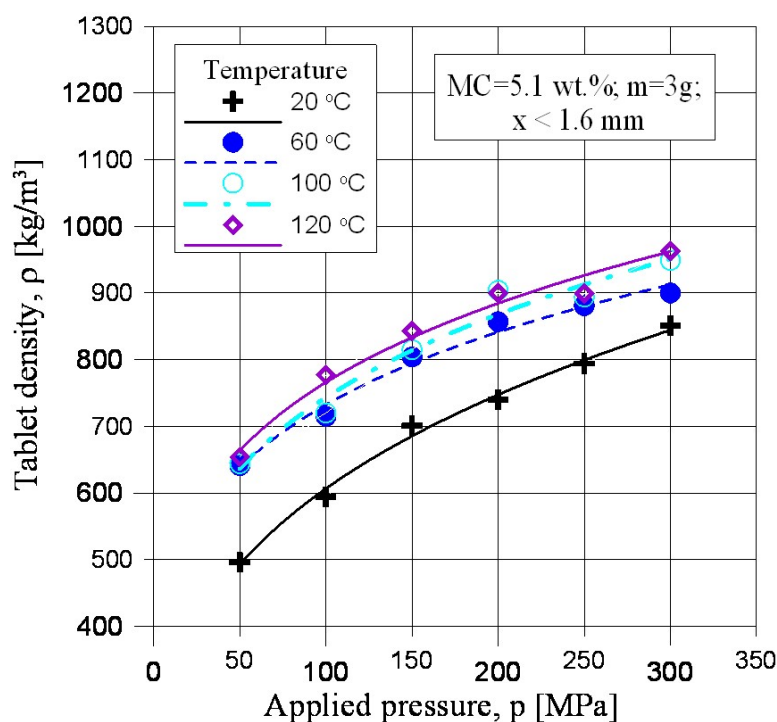


Figure 6.7. Compressibility data for *A. mangium* six months seasoned wood with different temperatures ($x < 1.6$ mm)

Tablets made from raw material (one month seasoned wood) have higher density than tablets made from raw material (six months seasoned wood), at constant pressure, temperature and moisture content (in the case of pressure 250 MPa, $T = 120^\circ\text{C}$, the tablet densities 1167 kg/m^3 (one month seasoned wood, $\text{MC} = 5.30\text{ wt.}\%$); 899 kg/m^3 (six months seasoned wood, $\text{MC} = 5.10\text{ wt.}\%$). The reason for this, *A. mangium* six months seasoned wood (lower lignin content: 23.7%) could be poorly connected between particle size than one month seasoned wood (higher lignin content: 26.6%) with the same particle size and starch content.

Table 6.6. Constants of Johanson's equation for *A. mangium* six months seasoned wood with different temperatures ($x < 1.6$ mm)

Temperature [°C]	Constant a [$\text{kg}^{1-1/\kappa}\text{m}^{(1/\kappa)-3}\text{s}^{2/\kappa}$]	Constant κ [-]	Spread deviation: V_s [%] Coefficient of determination: R^2 [-] Residual mean square: σ [kg/m^3]
20	151.7872	3.3244	$R^2 = 0.9939$; $\sigma = 0.0003$; $V_s = 1.4$
60	291.2331	4.9950	$R^2 = 0.9856$; $\sigma = 0.0003$; $V_s = 1.6$
100	265.0771	4.4682	$R^2 = 0.9715$; $\sigma = 0.0008$; $V_s = 2.5$
120	294.4848	4.8192	$R^2 = 0.9818$; $\sigma = 0.0004$; $V_s = 1.9$

6.3. Spring-back ratio of tablets

6.3.1. Tablets made from spelt chaff

Figure 6.8 shows the relationship between applied pressure and spring-back ratio for different temperatures of raw material (20, 40, 60, 80 and 100°C). The relationships can be described by linear functions. Tablets made from raw material at higher temperatures have a lower spring-back ratio. While for tablets made at 100°C, their spring-back ratio increase with an increase in pressure. At a constant pressure of 250 MPa, the following were obtained; at 100°C had 47.11 % SBR, at 80°C had 47.05 % SBR, and at 60°C temperature had 54.73 % SBR.

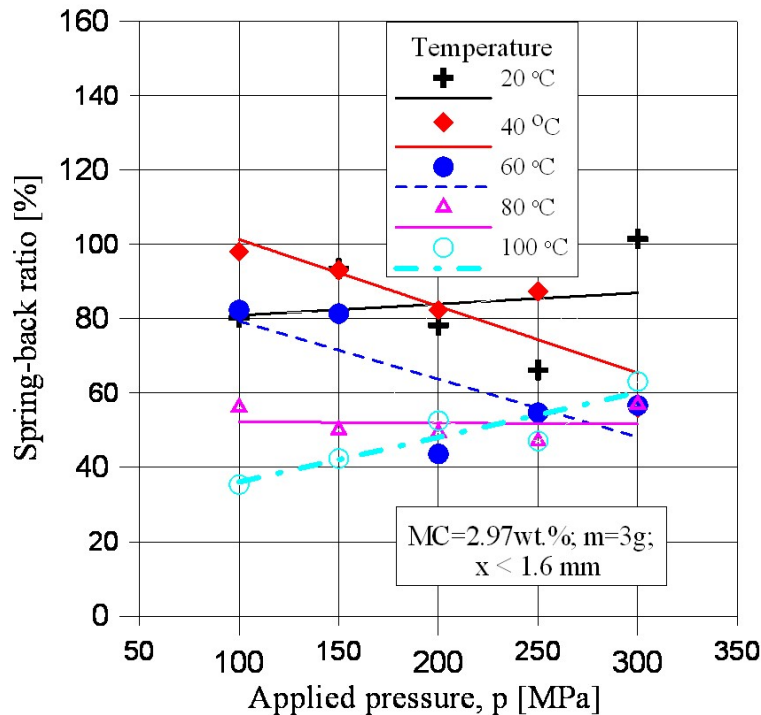


Figure 6.8. Relationship between spring-back ratio and pressure for the tablets made from spelt chaff at different temperatures ($x < 1.6$ mm)

6.3.2. Tablets made from *A. mangium* one month seasoned wood

Figure 6.9 shows the relationship between applied pressure and spring-back ratio in the case of one month seasoned wood, the same particle size < 1.6 mm and different temperature. This relationship can be well described by linear functions. Increasing of pressure with the same temperature resulted in higher SBR. Tablets made from the raw material with higher temperature had a lower spring-back ratio (at the same pressure, moisture content and particle size). In the case of $T = 120^{\circ}\text{C}$, less than 20 % SBR was measured. Tablets made at 20°C temperature had only 28.8 to 41.6 % SBR depending on pressure, in the examined pressure range.

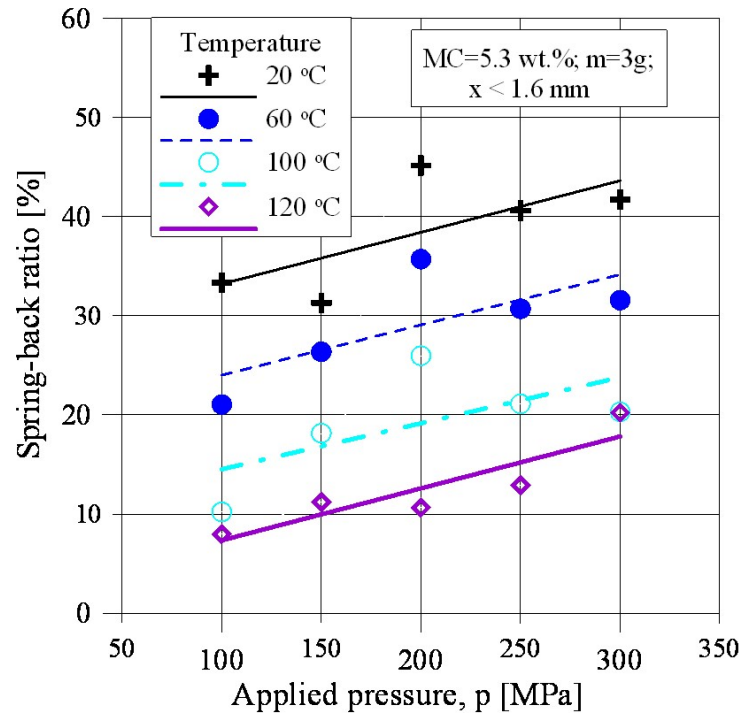


Figure 6.9. Relationship between pressure, spring-back ratio and temperature for the tablets made from *A. mangium* one month seasoned wood ($x < 1.6$ mm)

6.4. Structure of tablets

The cross-sectional surfaces of tablets made from *A. mangium* were investigated with an optical microscope (Zeiss AXIO Imager.M2m), as shown in Figure 6.10. The tablet made at pressure 250 MPa ($T = 100^{\circ}\text{C}$, six months seasoned wood) had more space between particles (porosity is higher) than the tablet made at pressure 250 MPa ($T = 100^{\circ}\text{C}$, one month season wood), with the same moisture content and particle size. The reasons for that generally, with increasing seasoning of time resulted in higher tablet swelling, thus higher porosity of the tablet with the temperature, moisture content, particle size and pressure are kept constant.

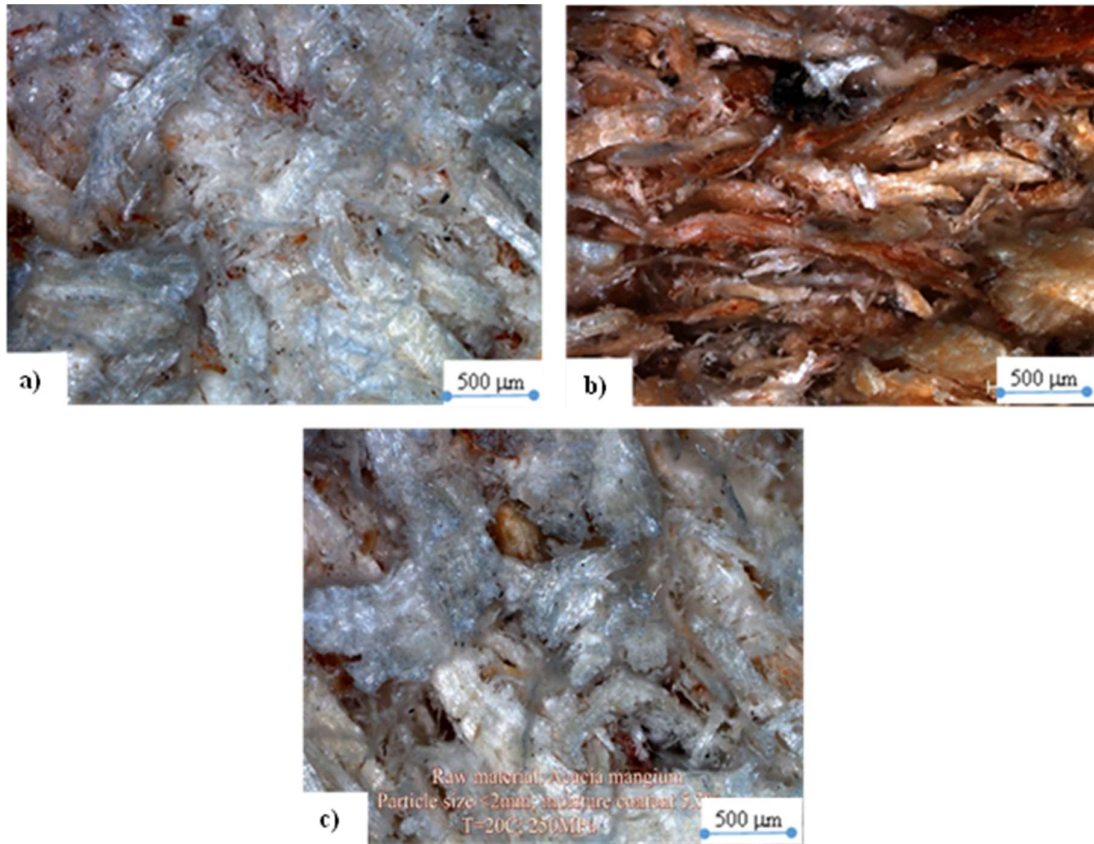


Figure 6.10. Cross sectional surface of tablets; (a) one month seasoned wood ($T = 100^{\circ}\text{C}$); (c) one month seasoned wood ($T = 20^{\circ}\text{C}$); (b) six months seasoned wood ($T = 100^{\circ}\text{C}$), (optical microscope: Zeiss AXIO Imager.M2m)

The tablets made at pressure 250 MPa ($T = 20^{\circ}\text{C}$) had more space between particles (porosity is higher) than the tablet made at pressure 250 MPa ($T = 100^{\circ}\text{C}$), with the same moisture content of 5.3 wt.% and particle size < 1.6 mm (in the case of one month seasoned wood). The reasons for that the increasing temperature resulted in lower swelling, thus the porosity of the tablet is lower at constant pressure, particle size and moisture content.

6.5. Tablet strength

6.5.1. Tablets made from *Acacia mangium*

Falling number values in the case of $x < 0.8$ mm and $x < 1.6$ mm raw materials (one month seasoned wood) are shown in Figure 6.11 (a) and (b) as a function of temperature on different pressures. Increasing temperature resulted in higher tablet strength at the same pressure and particle size. Tablets made from raw materials $x < 1.6$ mm have higher strength (falling number: 27.0 at 250 MPa and 120°C) than tablets made from $x < 0.8$ mm (falling number: 14.6 at 250 MPa and 120°C), if moisture content and pressure are kept constant. The reason for this can be more intensive binding in the case of larger particles ($x < 1.6$ mm).

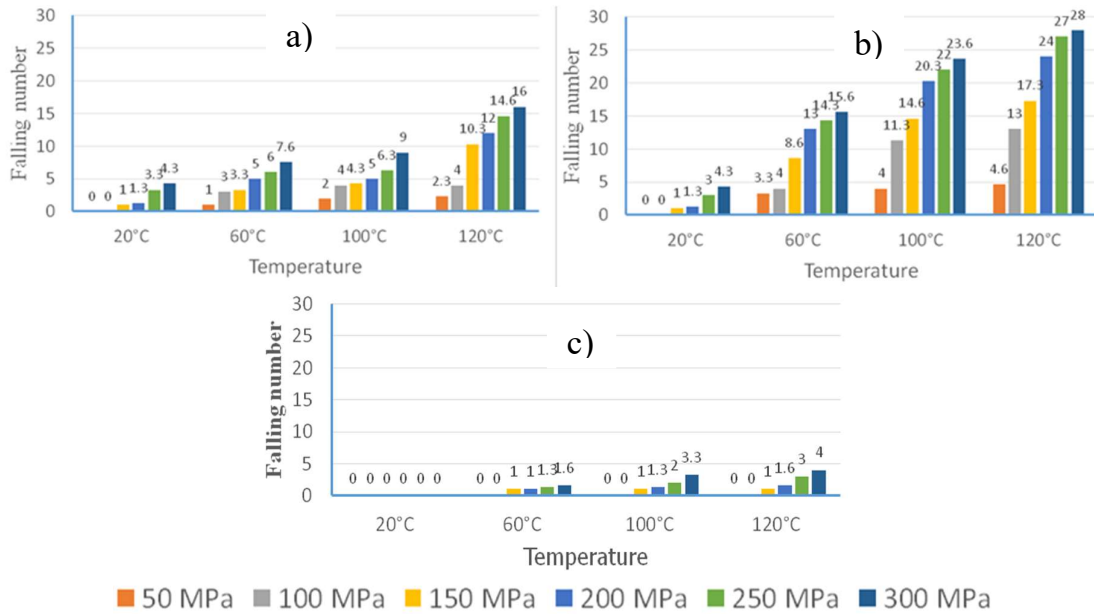


Figure 6.11. Relationship between falling number, temperature and pressure for tablets made from *A. mangium*; (a) Particle size < 0.8 mm - one month seasoned wood; (c) particle size < 1.6 mm - six months seasoned wood (b) Particle size < 1.6 mm - one month seasoned wood

Falling number values in the case of one month seasoned wood and six months seasoned wood raw materials with the same particle size < 1.6 mm are shown in Figure 6.11 (b) and (c). Increasing temperature resulted in higher tablet strength at the same pressure and particle size. Tablets made from raw materials one month seasoned wood had the higher strength (falling number: 27 at 250 MPa and 120°C than tablets made from six months seasoned wood biomass (falling number: 3 at 250 MPa and 120°C) if moisture content and pressure are constant. The reason for this can be more intensive form closing binding in the case of larger particles, and reduction in moisture content of wood, its surface to become inactivated, which results in poor bond (Unsal et al 2009).

6.5.2. Tablets made from beech sawdust

The result of the falling tests in the case of $x < 1$ mm and $x < 2$ mm raw materials ($m = 5$ g). Falling number is shown in Figure 6.12, as a function of temperature on different pressure values. Increasing temperature resulted in higher tablet strength at the same pressure and particle size. Tablets made from raw materials ($x < 2$ mm) form tablets with higher strength than tablets made from ($x < 1$ mm) if moisture content and pressure are constant.

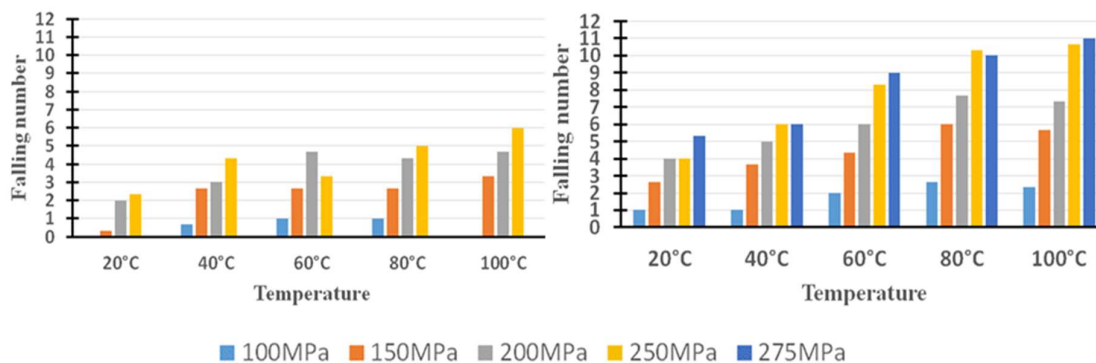


Figure 6.12. Relationship between falling number, temperature and pressure for tablets made from beech sawdust; (left) particle size < 1 mm; (right) particle size < 2 mm

6.6. Evaluation and discussion

The effect of temperature and pressure on tablet density in the case of beech saw dust ($x < 2$ mm), spelt chaff ($x < 1.6$ mm), and effect of temperature and seasoning with the same particle size < 1.6 mm in the case of *A. mangium* are introduced as follows:

In the case of beech sawdust: the description of the agglomeration processes is essential to be able to determinate the optimal parameters. The applied Johanson functions describes well the processes (at 60°C, in the case of $x < 1$ mm raw material $V_s = 3.64$ %, using $x < 2$ mm raw material $V_s = 3.0$ %). With the same pressure and particle size, increasing temperature resulted in a higher density of tablets (in the case of $x < 1$ mm raw material at 100 MPa the tablet densities: 829 kg/m³ (20°C) and 916 kg/m³ (100°C)). The small different tablet density between tablets made from particle size < 1 mm and tablets made from particle size < 2 mm (at 250 MPa, T = 60°C the tablet densities: 1065 kg/m³ ($x < 1$ mm) and 1073 ($x < 2$ mm)).

In the case of spelt chaff: at constant pressure and moisture content, tablets density increase was observed when the temperature increased from 20 to 80°C. Tablets made at 100°C resulted in increased densities, only at lower pressure values with the same particle size < 1.6 mm.

In the case of Acacia mangium: the description of the agglomeration processes is essential to be able to determine the optimal production parameters (100°C temperature and 300 MPa). While the Johanson functions describe the processes well (at 60°C temperature in the case of one month seasoned wood raw material $V_s = 1.5$ %, using six months seasoned wood raw material $V_s = 1.6$ %). When the pressure and particle size were kept constant, increasing temperature resulted in a higher density of tablets both in one month seasoned wood (MC = 5.1 wt.%) and six months seasoned wood (MC = 5.3 wt.%).

CHAPTER 7. CORRELATION OF LIGNIN, CELLULOSE AND STARCH WITH BIOMASS AGGLOMERATION

7.1. Determination of lignin, cellulose and starch content

For the biomass, the cellulose and lignin are generally recognized as main components in the biomass (Hajaligol et al. 2001). Therefore, I prepared biomass samples (including six samples: beech sawdust, *A. mangium* one month seasoned wood, *A. mangium* six months seasoned wood, spelt chaff, ground post-agglomerated spelt chaff and rice straw) and sent to Mezőlabor- Szolgáltató és Kereskedelmi Kft, Hungary for chemical analysis. The ADF content (Acid Detergent Fiber), ADL content (Acid Detergent Lignin) and starch content were determined. In this way, the lignin content is determined as ADL (in the case of small cutin), and cellulose can be calculated as ADF - ADL. The particle densities of the original form materials were determined in the range from 1205 to 1439 kg/m³ by using pycnometer, and also wood densities were investigated.

The result of lignin, cellulose, starch content and particle density are shown in Table 7.1. From this table it can be seen that all the biomass samples contain more cellulose than lignin. GPA-spelt chaff contains the highest amount of starch and the lowest lignin content compared to other materials. The lignin and cellulose contents varied from 3.9 to 26.6 % and from 25.1 to 52.1 % respectively.

Table 7.1. Lignin, cellulose, starch content and particle density of biomass materials

Components	Materials					
	Untreated				Treated	
	Beech	<i>A. mangium</i> 1 month	Rice straw	Spelt chaff	GPA-spelt chaff	<i>A. mangium</i> 6 months
Lignin [%]	15.4	26.6	4.7	8.8	3.9	23.7
Cellulose [%]	52.1	47.4	41.9	35.1	25.1	51.2
Starch [%]	< 0.5	< 0.5	< 0.54	< 0.5	9.3	< 0.5
Particle density ρ^* [kg/m ³]	1253	1340	1273	1364	1439	1205
Wood density, ρ^{**} [kg/m ³]	686	570	-	-	-	515

Reduction of lignin and increasing cellulose with the same starch content were observed in the *A. mangium* six months seasoned wood. The reason is that differently treated biomass materials strategies are currently available with variation in terms of temperature, types of catalyst, and treatment time. These variations affect the severity of the treated biomass and the biomass composition during its degradation (Pedersen and Meyer 2010).

While reduction of lignin, cellulose content and increasing starch content were observed in ground post-agglomerated spelt chaff. The reason for that is the glucose can be released from cellulose and lignin by heating material, while starch is proportional to glucose (Kaysu et al. 1885).

7.2. Tablet density

For tablets produced by the hydraulic piston press with 25 mm diameter, six different biomass samples (beech sawdust, *A. mangium* one month seasoned wood, *A. mangium* six months seasoned wood, spelt chaff, GPA-spelt chaff and rice straw) were used. Each tablet

was made by the compression of 3 g material. Applied pressure on the surface of tablets were 50, 100, 150, 200, 250 and 300 MPa at the same production conditions (temperature of 100°C, moisture content of 5 wt.%, particle size < 1.6 mm, compression time of 2 seconds) as shown in Figure 7.1. The tablet density values are recorded as an average of three measurements.

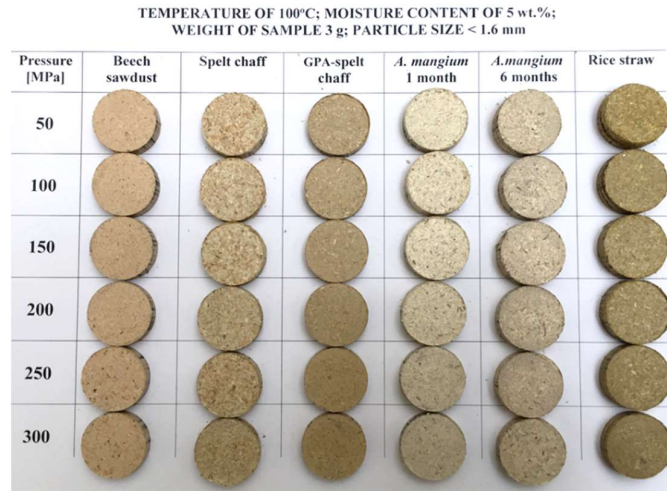


Figure 7.1. Tablets made from various materials and pressure with the same production conditions ($x < 1.6$ mm; $T = 100^\circ\text{C}$; $m = 3$ g; $MC = 5$ wt.%)

Figure 7.2 shows the pressure - density values and the fitted Johanson curves in the case of different materials and the same production conditions. Table 7.2 shows the constants of the fitted curves and coefficient of determination (R^2), residual mean square (σ) and spread deviation values (V_s) of fitted the Johanson equations are calculated and all the sample have valued less than 4.4 %.

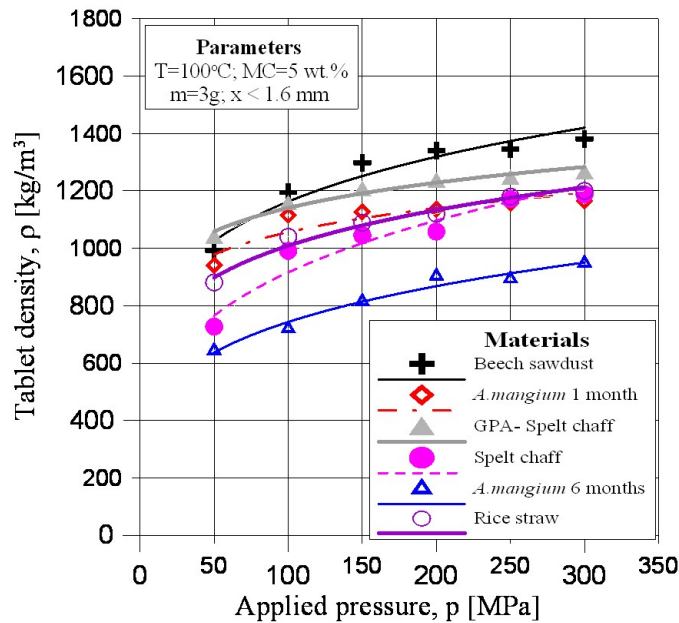


Figure 7.2. Compressibility data for various materials with the same production conditions ($x < 1.6$ mm; $T = 100^\circ\text{C}$; $m = 3$ g; $MC = 5$ wt.%)

Tablets compressed at higher pressure had a higher density. If the same production conditions had been applied, tablets made from beech sawdust resulted in the highest density values, while tablets made from *A. mangium* six month seasoned wood has the lowest density values. Tablets made from ground post-agglomeration spelt chaff have higher density than those made from spelt chaff raw material, and tablets made from *A. mangium* one month seasoned wood have a higher density than those made from six months seasoned wood. For instance at 200 MPa tablet densities: 1341 kg/m³ (beech sawdust), 1136 kg/m³ (*A. mangium* one month seasoned wood), 1058 kg/m³ (spelt chaff), 1238 kg/m³ (ground post-agglomerated spelt chaff), 904 kg/m³ (*A. mangium* six months seasoned wood) and 1120 kg/m³ (rice straw).

The reason for that could be the cellulose content effect on the compressibility of materials, an increasing cellulose content resulted in higher tablet densities (see Figure 7.3). If cellulose is smaller, it will increase the tablet porosity (Harmsen 2010; Karimi 2013), in the case of without treatment of materials with higher cellulose content have higher tablet densities. In the case of treated materials with higher starch content have higher tablet densities.

Table 7.2. Constants of Johanson’s equation for various materials with the same production conditions

Type of materials	Constant a [kg ^{1-1/κ} m ^{(1/κ)-3} s ^{2/κ}]	Constant κ [-]	Spread deviation: V_s [%] Coefficient of determination: R^2 [-] Residual mean square: σ [kg/m ³]
Beech sawdust	503.1176	5.5006	$R^2 = 0.9404$; $\sigma = 0.0011$; $V_s = 2.9$
<i>A. mangium</i> 1 month	636.6259	9.0992	$R^2 = 0.8284$; $\sigma = 0.0013$; $V_s = 3.1$
<i>A. mangium</i> 6 months	265.0771	4.4683	$R^2 = 0.9715$; $\sigma = 0.0008$; $V_s = 2.5$
Spelt chaff	276.8775	3.8489	$R^2 = 0.9280$; $\sigma = 0.0028$; $V_s = 4.4$
GPA- spelt chaff	695.6108	9.3197	$R^2 = 0.9621$; $\sigma = 0.0002$; $V_s = 1.3$
Rice straw	466.4309	5.9701	$R^2 = 0.9744$; $\sigma = 0.0004$; $V_s = 1.6$

Few values for the density of granular wheat starch appear in the literature, giving values around 1500 kg/m³ (Dengate et al. 1978). The density of cellulose in the crystalline region and amorphous region in the range of 1500 to 1588 kg/m³ respectively (Yang 2008). While the density of lignin range from 1348 to 1451 kg/m³ (Jiang 2001).

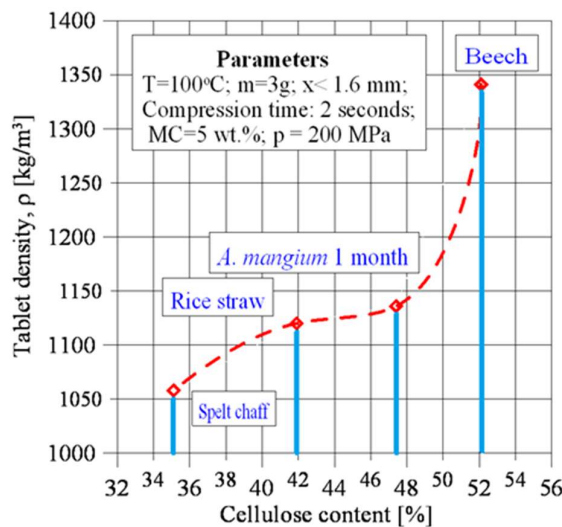


Figure 7.3. Relationship between cellulose content and tablet density

7.3. Spring-back ratio of tablets

Figure 7.4 shows the relationship between applied pressure and SBR in the case of different materials (beech sawdust, *A. mangium* one month seasoned wood, *A. mangium* six months seasoned wood, GPA-spelt chaff, spelt chaff, and rice straw) with the same production conditions (temperature of 100°C, moisture content of 5 wt.%, weight of sample 3g, particle size < 1.6 mm, compression time of 2 seconds). This relationship can be described by the following function: $SBR = dp^c$ the constant c and d are corresponding to each kind of material.

Spring-back ratio of tablets made from GPA-spelt chaff have the lowest values while those made from rice straw have the highest spring-back ratio. For instance, spring-back ratio of tablet at 200 MPa: 37.2 % (rice straw), 35 % (spelt chaff), 22 % (*A. mangium* one month seasoned wood), 16 % (beech sawdust), 30 % (*A. mangium* six months seasoned wood) and 14 % (GPA-spelt chaff).

Spring-back ratio of tablets made from *A. mangium* one month seasoned wood increases with higher pressure values. While the spring-back ratio of tablets made from other materials decreases with increasing pressure values.

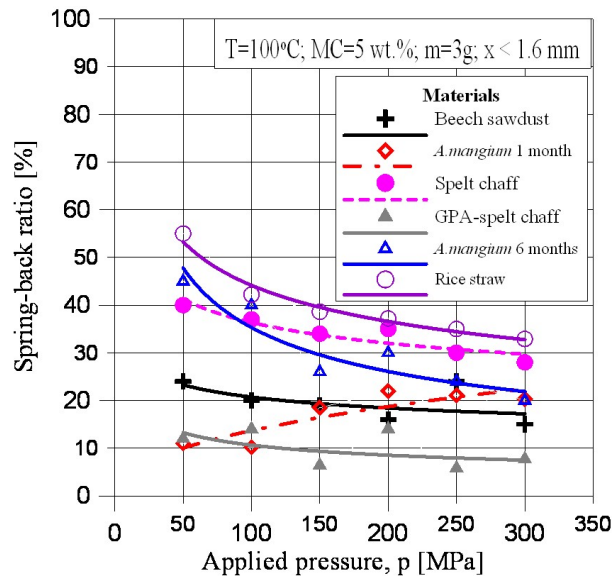


Figure 7.4. Spring-back ratio of various materials with the same production conditions ($x < 1.6$ mm; $T = 100^\circ\text{C}$; $m = 3\text{g}$; $MC = 5$ wt.%)

7.4. Structure of tablets

The cross-sectional surfaces of tablets made from four different kinds of material (Spelt chaff, rice straw, *A. mangium* six months seasoned wood and GPA-spelt chaff) at the same production conditions (temperature of 100°C, moisture content of 5 wt.%, particle size < 1.6 mm) were investigated with an optical microscope (Zeiss AXIO Imager.M2m) as shown in Figure 7.5.

In the case of untreated materials, tablets made from rice straw with the lower lignin content (4.7 %) have the smaller granules, smoother, smaller pores and higher densities than those made from spelt chaff with the same production conditions.

In the case of treated materials, tablets made from GPA-spelt chaff with highest starch content (9.3 %) had less space between particles than those made from *A. mangium* six months seasoned wood.

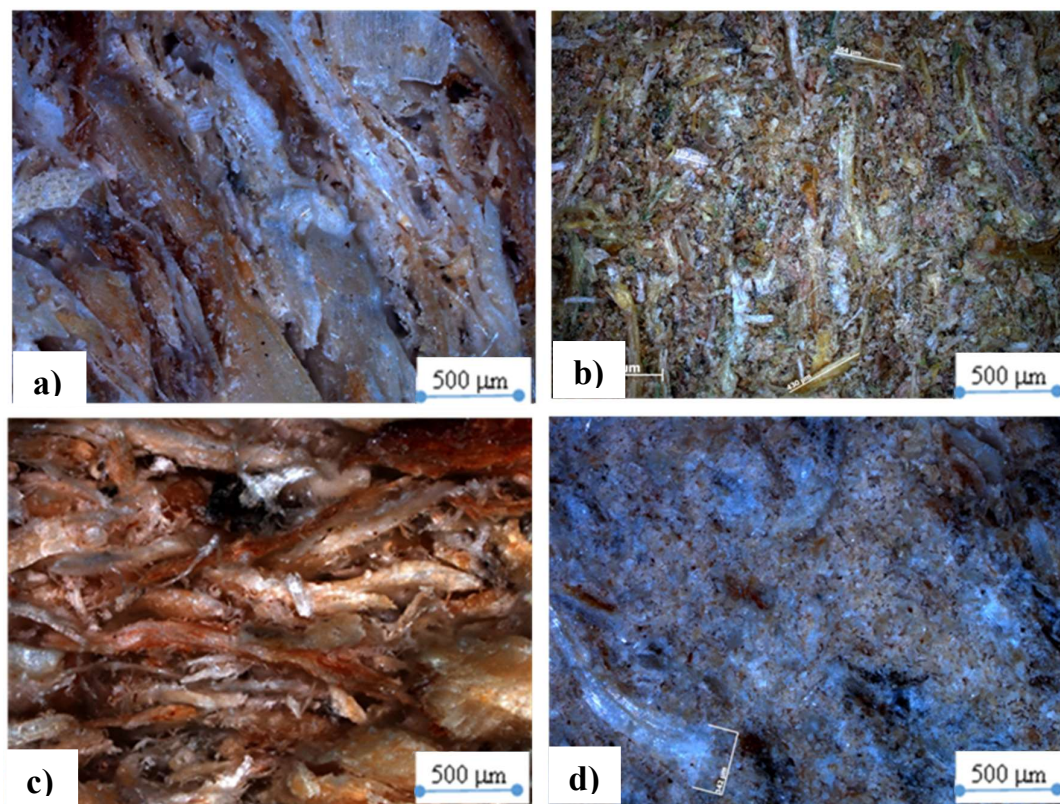


Figure 7.5. Cross sectional surface of tablets; (a) spelt chaff; (b) Rice straw; (c) *A. mangium* 6 months; (d) GPA-spelt chaff, at $x < 1.6$ mm; $T = 100^{\circ}\text{C}$, $\text{MC} = 5$ wt.%; $m = 3$ g (optical microscope: Zeiss AXIO Imager.M2m)

7.5. Tablet strength

Falling number values in the case of tablets made from different materials and the same produce conditions (temperature of 100°C , moisture content of 5 wt.%, particle size < 1.6 mm, a weight of sample 3 g, and a compression time of 2 seconds) are shown in Figure 7.6. In the case of untreated materials, the falling number of tablets made from *A. mangium* one month seasoned wood have the highest value and those made from rice straw have the lowest value. In the case of treated materials, the falling number of tablets made from *A. mangium* six months seasoned wood was lower than those made from the GPA-spelt chaff. For instance the falling number value at 200 MPa: 20.3 (*A. mangium* one month seasoned wood), 8.0 (beech sawdust), 3.0 (spelt chaff), 2.3 (rice straw), 1.3 (*A. mangium* six months seasoned wood) 7.3 (GPA-spelt chaff).

The reason for this may be tablets made from higher lignin content of material have higher tablet strength in the case of untreated materials and the same starch content (see Figure 7.7) and lignin is used as adhesives (Dai et al. 2017). In the case of treated materials, tablets made from higher starch content have higher tablet strength. The reason for this,

starch is already used as a biological binding agent to achieve higher abrasion resistance and strength (Stahl et al. 2012).

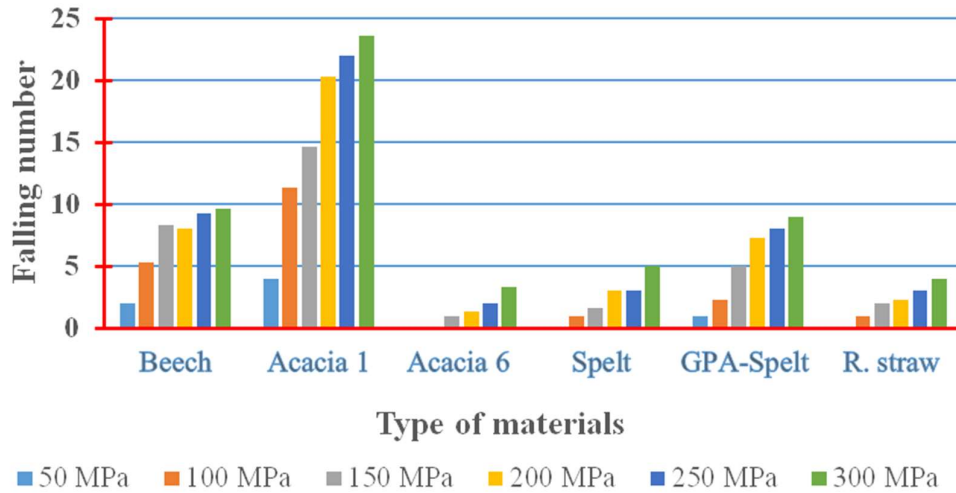


Figure 7.6. Falling number of tablets made from various materials with the same production conditions ($x < 1.6$ mm; $T = 100^{\circ}\text{C}$; $m = 3\text{g}$; $\text{MC} = 5$ wt.%)

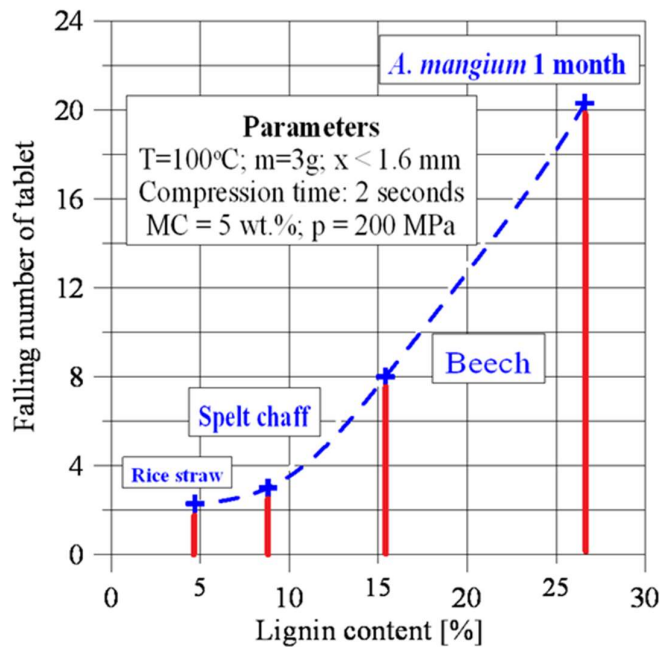


Figure 7.7. Relationship between lignin content and falling number of tablets

7.6. Evaluation and discussion

In the case of untreated materials, tablets made from various materials (beech sawdust, spelt chaff, *A. mangium* one month seasoned wood and rice straw) with reducing cellulose content have lower tablet density values and higher spring-back ratio. While tablets made from raw materials with higher lignin content had higher tablet strength with the same starch content. Tablets made from rice straw with the lower lignin content (4.7 %) have the smaller

granules, smoother, smaller pores and higher densities than those made from spelt chaff with the same production conditions.

In the case of treated materials, the biomass component ratios changed, for example, the lignin, cellulose content of spelt chaff decreased when heated and compressed simultaneously at 100°C and then ground again (ground post agglomerated spelt chaff). While its starch content (9.3 %) was higher than the spelt chaff raw material (< 0.5 %). The tablets made from the material with the higher starch content have the higher density, smooth surface, and lower spring-back ratio.

The determination of other components of biomass (for example: hemicellulose, proteins, lipid and fat) are to be studied in a further work.

CHAPTER 8. THE APPLICABILITY OF THE RESULTS AND FURTHER DEVELOPMENT OPPORTUNITIES

8.1. New model single pelletizer unit

A model and experimental procedures for pelletizing have been presented and also experimental procedures to measure backup pressure distribution among the chamber wall were shown. During compression of the pelletizing operation with an experimental equipment based on single pelletizer unit was mounted in the hydraulic piston press. The main results that can be drawn from this study are summarized in followings.

8.1.1. Single pelletizer unit 1

New design press channel model of flat die pelletizer has an 8 mm diameter hole, the length of the active part is 55 mm with experimental equipment based on hydraulic piston press (single pelletizer unit 1). Compressibility was determined, and pellets were produced by flat die pelletizer and results were compared with results of single pelletizer unit. During this modelling, the parameters could be changed easily, and the amount of the raw material is low for the experiment. This enables a fast estimation of key process parameters such as optimal moisture content, pressure, temperature, particle size and speed of the piston.

The systematic experiments with SPU showed pellets made from spelt chaff raw material were not strong enough. While pellets produced from the ground post-agglomerated spelt chaff feed by SPU had large densities. The maximal density was 1182 kg/m³, it was reached at 20 wt.% moisture content and 100°C temperature. The decreasing of temperature resulted in smaller density values both at 20 and 15 wt.% moisture content.

8.1.2. Single pelletizer unit 2

A design of a new measuring system for backup pressure distribution (perpendicular to chamber wall), whose length of an active part made from four parts, length of each part and hole diameter are 13.75 mm and 8 mm respectively. The results showed that the backup pressure of the ground post-agglomerated spelt chaff at 20 wt.% moisture content and temperature of 60°C were 23.7, 14.9 and 9.6 bar respectively, along with the direction of the applied pressure. If moisture content and position of BPMD are kept constant, the decreasing temperature resulted in smaller backup pressure values.

8.2. Relationship between moisture content and density of tablets

It was observed that tablets made from raw material at constant pressure and particle size, increasing moisture content resulted in lower density and strength of tablets. Furthermore, tablets made from the raw material with smaller particle size was observed to have lower strength than tablets made from the raw material with a larger particle size in the case tablet made from beech sawdust. While tablets made from spelt chaff had a maximum density value at 5.3 wt.% moisture content in the examined range (2.97, 5.30, 7.40, 10.50, 15.50 and 18.50 wt.%).

8.3. Relationship between temperature, seasoning and density of tablets

The effect of temperature, pressure on tablet density in the case of beech saw dust ($x < 2$ mm), spelt chaff ($x < 1.6$ mm), and effect of temperature, seasoning with the same particle size < 1.6 mm in the case of *A. mangium* are introduced. It was observed that tablets made from raw material at constant pressure with increasing temperature resulted in a higher density and strength of tablets. Tablets made from *A. mangium* one month seasoned wood was seen to have higher density and strength compared to those made from *A. mangium* six months of seasoning. Tablets made at 100°C resulted in increased densities, only at lower pressure values with the same particle size < 1.6 mm. The small different tablet density between tablets made from particle size < 1 mm and tablets made from particle size < 2 mm

8.4. Spring-back ratio, porosity and strength of tables

8.4.1. Spring-back ratio of tablets

The relationship between applied pressure and spring-back ratio in the case of beech sawdust, spelt chaff and *A. mangium* one month seasoned wood, with the same particle size < 2 mm as follows:

In the case of beech sawdust: tablets made from the raw material with larger moisture content had larger SBR (at the same pressure, temperature and particle size). In the case of 18.80 wt.% moisture content, SBR of tablets over 50 % was measured. Tablets with 4.90 wt.% moisture content had only 20.1 to 35.8 % SBR depending on pressure, in the examined pressure range.

In the case of spelt chaff: at the same pressure and temperature, tablets made from the raw material with 5.30 wt.% moisture content had minimum spring-back ratio. Tablets made from raw material at higher temperatures have lower spring-back ratios. While for tablets made at 100°C , their spring-back ratio increase with an increase in pressure. At a constant pressure of 250 MPa, the following were obtained: 100°C had 47.11 % SBR, 80°C had 47.05 % SBR, and the 60°C temperature had 54.73 % SBR.

In the case of *A. mangium*: increasing pressure with the same temperature resulted in higher SBR. Tablets made from *A. mangium* sawdust (one month seasoned wood) with higher temperature had a lower spring-back ratio (at the same pressure, moisture content and particle size). In the case of $T = 120^{\circ}\text{C}$, less than 20 % SBR was measured. Tablets made at 20°C temperature had only 28.8 to 41.6 % SBR depending on pressure, in the examined pressure range.

8.4.2. Porosity of tablets

The cross-sectional surfaces of tablets made from European beech sawdust, spelt chaff and *A. mangium* were investigated with an optical microscope (Zeiss AXIO Imager.M2m):

In the case of beech sawdust: the tablets made at pressure 50 MPa had more space between particles (porosity is higher) than the tablet made at 250 MPa, with the same moisture content 4.71 wt.%. The same effect can be recognised in the case of MC = 19.55 wt.%. In the optical microscopy, the pictures no relevant differences can be seen between tablets made with 4.71 wt.% and 19.55 wt.% moisture content.

In the case of spelt chaff: the tablets made at pressure 100 MPa had more space between particles (porosity is higher) than the tablets made at pressure 250 MPa with the same moisture content 2.97 wt.%. The same effect is realized in the case of MC = 10.50

wt.%. In the optical microscopy pictures, no relevant differences can be seen between tablets made at 2.97 wt.% and 10.50 wt.% moisture content.

In the case of *A. mangium*: the tablets made at pressure 250 MPa ($T = 100^{\circ}\text{C}$, six months seasoned wood) had more space between particles (porosity is higher) than the tablets made at pressure 250 MPa ($T = 100^{\circ}\text{C}$, one month seasoned wood), with the same moisture content and particle size. The tablets made at pressure 250 MPa ($T = 20^{\circ}\text{C}$) had more space between particles (porosity is higher) than the tablets made at pressure 250 MPa ($T = 100^{\circ}\text{C}$), with the same moisture content of 5.30 wt.% and particle size < 2 mm. The reasons for that generally, increasing temperature resulted in lower swelling, the thus lower porosity of the tablet at constant pressure, particle size and moisture content.

8.4.3. Tablet strength

Falling number values in the case of beech sawdust, spelt chaff, *A. mangium* one month seasoned wood and six months seasoned wood raw materials were investigated as a function of moisture content or temperature at different pressure for both particle size < 1 mm and < 2 mm:

In the case of beech sawdust: increasing temperature resulted in higher tablet strength on the same pressure and with same particle size. Tablets made from the raw material ($x < 2$ mm) have the higher strength (falling number: 7.33 on 200 MPa and 100°C) than tablets made from $x < 1$ mm biomass (falling number: 4.66 on 200 MPa and 100°C) if temperature and pressure are constant. Increasing moisture content resulted in lower tablet strength at the same pressure and with the same particle size (falling number: 1.33 on 250 MPa, 19.55 wt.%; falling number: 4.00 on 250 MPa, 9.27 wt.% with the same particle size < 1 mm).

In the case of *Acacia mangium*: increasing temperature resulted in higher tablet strength at the same pressure and particle size. Tablets made from raw material one month seasoned wood $x < 1.6$ mm form tablets with higher strength (falling number: 27.0 at 250 MPa and 120°C), than tablets made from raw material six months seasoned wood ($x < 0.8$ mm) (falling number: 14.6 at 250 MPa and 120°C), in the case of one month seasoned wood, moisture content and pressure are kept constant. Tablets made from raw material one month seasoned wood form tablets with higher strength (falling number: 27 at 250 MPa and 120°C) than tablets made from six months seasoned wood biomass (falling number: 3 at 250 MPa and 120°C) if moisture content and pressure are constant.

8.5. Correlation of lignin, cellulose and starch with biomass agglomeration

In the case of untreated materials, tablets made from the raw material with higher cellulose content have higher tablet density values and lower spring-back ratio. While tablets made from the raw material with higher lignin content have higher tablet strength with the same starch content.

In the case of treated materials, the biomass component ratios changed, for example, the lignin, cellulose content of spelt chaff decreased when heated and compressed simultaneously at 100°C and then ground again (ground post-agglomerated spelt chaff). While its starch content of that material (9.5 %) was higher than the spelt chaff raw material (< 0.5 %). The tablets made from the raw material with higher starch content have higher density, smooth surface and lower spring-back ratio.

8.6. Further development opportunities

The process optimization of pelletizing such as moisture content, particle size and temperature equivalent each type of biomass can be determined by single pelletizer unit 1 (SPU1).

The SPU2 can be used for other materials as well to find the optimal conditions of backup pressure, moisture content and particle size during the process of agglomeration. The membrane of the measurement disc should be made from a material the properties of which are equivalent to carbon steel properties.

The new equation (modified Johanson's equation) allow the forecasting of the effect of various production parameters on the quality of agglomeration. The lignin content - falling number relationship and cellulose content - density relationship allows the expected tablet parameters to be calculated which can be used in industry (e.g. forecast mixtures behavior).

The experimental method can be used for other materials as well to find the optimal conditions of pressure, temperature, moisture content and particle size during an agglomeration process. The ground post-agglomerated raw material (spelt chaff) should be investigated in a new research work.

The determination of other components of biomass (for example: hemicellulose, proteins, lipid and fat) and compression time are to be studied in a further work.

PUBLICATIONS RELATED TO THIS DISSERTATION

Paper in international journal

[1] Trinh, V. Q., Nagy, S., Csöke, B.: *Effect of Moisture Content and Particle Size on Beech Biomass Agglomeration*. Advances in Agriculture & Botany- International Journal of the Bioflux Society. Vol 9, issue 2 (2017), p79-89. Online ISSN 2067-6352; Print ISSN 2066-7639.

Paper in Hungarian Journal

[2] Trinh, V. Q., Nagy, S.: *Effect of Various Production Parameters on Biomass Agglomeration*. Journal of Geosciences and Engineering, Vol.4, No.7 (2015), p86-96. HU ISSN 2063- 6997.

Paper in Vietnamese Journal

[3] Trinh, V. Q., Nagy, S.: *Agglomeration of Acacia mangium Biomass*. Vietnam Journal of Science and Technology. 56 (2) (2018) p196-207. ISSN 2525-2518.

Papers in international conference proceedings

[4] Trinh, V. Q., Nagy, S.: *Effect of Temperature and Particle Size on Beech Biomass Agglomerates*. MultiScience - XXX. microCAD International Multidisciplinary Scientific Conference;University of Miskolc, Hungary, 21-22th April 2016, p A8_1-8. ISBN 978-963-358-113-1.

[5] Trinh, V. Q., Nagy, S.: *Development of Single Pelletizer Unit for Modelling Flat Die Pelletizer*. MultiScience - XXX. microCAD International Multidisciplinary Scientific Conference;University of Miskolc, Hungary, 21-22th April 2016, p A7_1-8. ISBN 978-963-358-113-1.

[6] Trinh, V. Q., Nagy, S.: *Effect of Temperature on Acacia mangium Biomass Agglomeration*. 19th Mining Metallurgy and Geology Conference; 30th March - 2th April, 2017; Cluj-Napoca, Romania; Publisher: Hungarian Technical Scientific Society of Transylvania, p155-159. ISSN 1842- 9440.

[7] Trinh, V. Q., Nagy, S.: *Effect of Temperature and Particle Size on Acacia mangium Biomass Agglomeration*. MultiScience - XXXI. microCAD International Multidisciplinary Scientific Conference;University of Miskolc, Hungary, 20-21th April 2017, pA1-6_1-9. ISBN 978-963-358-132-2.

[8] Trinh, V. Q., Nagy, S.: *Temperature and Seasoning Effects on Acacia mangium Biomass Agglomeration*. Geo-spatial technologies and Earth Resources, Publishing House for Science and Technology, Vietnam (2017), p429-435. ISBN 978-604-913-618-4.

[9] Nagy, S., Trinh, V. Q., Dóra, G.: *Compression Time and Temperature Effects on PUR Agglomeration*. International V4 Waste XXI Recycling conference, University of Miskolc, Hungary (2018) ISBN 978-963-358-173-5.

[10] Nagy, S., Trinh, V. Q., Bokányi, L., Pintér., A., Fábrik, T.: *Influence of Moisture Content and Temperature on Briquetting of Solar Dried Sewage Sludge*. International V4 Waste XXI Recycling conference, University of Miskolc, Hungary (2018) ISBN 978-963-358-173-5.

Papers in Hungarian conference proceedings

[11] Trinh, V. Q., Nagy, S., Csöke, B.: *Compressibility of Spelt Chaff as a Function of Moisture Content and Temperature*. Doktoranduszok Fóruma, University of Miskolc, 16th November **2016**, p 42-51. ISBN 978-963-358-129-2.

[12] Trinh, V. Q., Nagy, S.: *Agglomeration of Various Biomasses*. RING - Fenntartható Nyersanyag-gazdálkodás Tudományos Konferencia Pécs, 8 - 9th November **2018**.

[13] Nagy, S., Trinh, V. Q., Dóra, G.: *Influence of Temperature on PUR Briquetting*. RING - Fenntartható Nyersanyag-gazdálkodás Tudományos Konferencia Pécs, 8 - 9th November **2018**.

REFERENCES

- [1] Adapa, P. K., Tabil, L. G., Schoenau, G. J., 2009.: *Compression Characteristics of Selected Ground Agricultural Biomass*. Agricultural Engineering International. The CIGR Ejournal, manuscript 1347, Vol. XI.
- [2] Adapa, P. K., Tabil, L. G., Schoenau, G. J., Crear, B., and Sokhansanj, S., 2002.: *Compression characteristics of fractionated alfalfa grinds*. Powder Handl. Process 14 (4), p252-259.
- [3] Alakangas, E., and Paju, P., 2002.: *Wood pellets in Finland-technology, economy and market*. Organisations for the Promotion of Energy Technologies Finland Report 5, p1-62.
- [4] Andreiko, D., and Grochowicz, J., 2007.: *Effect of moisture content on compression energy and strength characteristic of lupine briquettes*. J. Food Eng 83 (1), p116-120.
- [5] Anonymous., 1983a.: *Special report, Binders*. Milling 166 (2), p31-33.
- [6] Anonymous., 1983b.: *Conditioning mixed feeds for higher quality*. Milling 166 (10): p22-23.
- [7] Armstrong, N. A, Palfrey L. P., 1989.: *The effect of machine speed on the consolidation of four directly compressible tablet diluents*. J Pharm Pharmacol 41, p149-151.
- [8] Arshadi, M., Gref, R., Geladi, P., Dahlgvist, S., and Lestander, T., 2008.: *The influence of raw material characteristics on the industrial pelletizing process and pellet quality*. Fuel Process. Technol 89 (12), p1442 -1447.
- [9] Back, E. L., 1987.: *The bonding mechanisms in hardboard manufacture- review report*. Holzforschung 41, p247-258.
- [10] Bergström, D., Israelsson, S., Ohman, M., Dahlgvist, A. S., Gref, R., Boman, C., Wasterlund, I., 2008.: *Effect of raw material particle size distribution on the characteristic of Scot pine sawdust fuel pellets*. Fuel Process. Technol, p1324-1329.
- [11] Carone, M. T., Pantaleo, A., and Pellerano, A., 2011.: *Influence of process parameters and biomass characteristics on the durability of pellets from the pruning residues of Olea europaea L*. Biomass Bioenergy 35 (1), p402-410.
- [12] Castellano, M. J., Gómez, M., Fernández, M., Esteban, S. L., Earrasco, E. J., 2015.: *Study on the effect of raw materials composition and pellets obtained from different woody and non woody biomasses*. Fuel 139, p629-636.
- [13] Chevanan, N., Womac, A. R., Bitra, V. S. P., Igathinathane, C., Yang, Y. T., Miu P. I., Escarnot, E., Aguedo, M., Paquot, M., 2011.: *Characterization of hemicellulosic fractions from spelt hull extracted by different methods*. Carbohydrate Polymers 85, p419-428.
- [14] Cocchi, M., Nikolaisen, L., Junginger, M., Goh, C. S., Heinimö, J., Bradley, D., Hess, R., Jacobson, J., Ovard, L. P., Thrän, D., 2011.: *Global Wood Pellet Industry Market and Trade Study*. International Energy Agency, Paris, p7.
- [15] Csöke, B and Faltli, J., 2003.: *Experimental Study of the Compacting Phenomena in Roll Presses Using Screw Feed*. Advances in Incremental Petroleum Production. Akadémiai Kiadó, Budapest. Vol.5, p413-424.

- [16] Dai, Z., Shi, X., Liu, H., Li, H., Han, Y., Zhou, J., 2017.: *High-strength lignin-based carbon fibers via a low-energy method*. The Royal Society of Chemistry, p1218-1224.
- [17] Dengate, H.N., Baruch, D.W., and Meredith, P., 1978.: *The Density of Wheat Starch Granules: A Tracer Dilution Procedure for Determining the Density of an Immiscible Dispersed Phase*. Starch/Starke 30 Nr 3, p80-84.
- [18] Fell, J. T., Newton, J. M., 1970.: *Determination of tablet strength by the diametral compression test*. J. Pharm Sci 59, p688-691.
- [19] Fengel, D., and Wegener, G., 1984a.: *Wood chemistry, ultrastructure, reactions*. Berlin/New York, Walter de Gruyter p106.
- [20] Filbakk, T., Skjevraak, G., Hoibo, O., Dibdiakova, J., and Jirjis, R., 2011.: *The influence of storage and drying methods for scots pine raw material on mechanical pellet properties and production parameters*. Fuel Process. Technol 92 (5), p871-878.
- [21] Fitz, H. C., Debellevue, E. B., Costanza, R., Boumans, R., Maxwell, T., Waigner, L., 1996.: *Development of general ecosystem model for a range of scales and ecosystems*. Ecol Modell 88, p263-295.
- [22] Franke, G., 1909.: *Handbuch der Briкетtbereitung*. Vol. 1, Die Briкетtbereitung aus Steinkohlen, Braunkohlen und Sonstigen Brennstoffen, Verlag Ferdinand Enke, Stuttgart, Germany.
- [23] Gercek, H., 2007. *Poisson's ratio values for rocks*. International Journal of Rock Mechanics & Mining Sciences 44, p1-13.
- [24] Gilbert, P., Ryu, C., Sharifi, V., and Swithenbank, J., 2009.: *Effect of process parameters on pelletisation of herbaceous crops*. Fuel 88 (8), p1491-1497.
- [25] Gluba, T., Antkowiak, W., 1988.: *Effect of wetting on granule abrasion resistance*. Aufbereitungs Technik 2, p76-80.
- [26] Grover, P. D., and Mishra, S. K., 1996B.: *Biomass briquetting: Technology and practices, in Regional Wood Energy Development Program in Asia, Tech. Report GCP/RAS/154/NET*. Food and Agricultural Organization of the United Nations, Bangkok, Thailand.
- [27] Gurnagul, N., Page, D. H., and Paice, M. G., 1992.: *The effect of cellulose degradation on the strength of wood pulp fibres*. Nord. Pulp Pap. Res. J., 7, 3, p152-154.
- [28] Hajaligol, M., Waymack, B., Kellog, D., 2001.: *Low temperature formation of aromatic hydrocarbon from pyrolysis of cellulosic materials*. Fuel 80, p1799-1807.
- [29] Hancock, B. C., Colvin, J.T., Mullarney, M. P., Zinchuk, A. V., 2003.: *The relative densities of pharmaceutical powders, blends, dry granulations, and immediate-release tablets*. Pharm Technol 27 (4), p64-80.
- [30] Harmsen, P., 2010.: *Literature Review of Physical and Chemical Pretreatment Processes for Lignocellulosic Biomass*. Wageningen UR, Food & Biobased Research.
- [31] Heckel, R. W., 1961.: *Density-Pressure Relationships in powder compaction*. Transactions of the Metallurgical Society of AIME 221, p1001-1008.

- [32] Herrmann, W., 1971.: *The effect of water vapour on the shear strength of briquettes*. Powder Technology 5, p25-30.
- [33] Hill, B., Pulkinen, D. A., 1998.: *A study of the factors affecting pellet durability and pelleting efficiency in the production of dehydrated alfalfa pellets*. Saskatchewan, Canada: Saskatchewan Dehydrators Association.
- [34] Holm, K. J., Henriksen, B. U., Hustad, E. J., and Sorensen, H. L., 2006.: *Toward an understanding of controlling parameters in softwood and hardwood pellets production*. Energy Fuels 20 (6), p2686-2694.
- [35] Holm, K. J., Stelte, W., Posselt, D., Ahrenfeldt, J., and Jenriksen, B. U., 2011.: *Optimization of a multiparameter model for biomass palletization to investigate temperature dependence and to facilitate fast testing of pelletization behavior*. Energy Fuels 25 (8), p3706-3711.
- [36] Holm, K. J., Henriksen, B. U., Wand, K., Hustad, E. J., and Posselt, D., 2007.: *Experimental Verification of Novel Pellet Model Using a single Pelleter Unit*. Energy & Fuels 21, p2446-2449.
- [37] Howatson, A. M., Lund, P. G., Todd, J. D., 1991.: *Engineering tables and data*. 2nd edition. London: Chapman & Hall.
- [38] Ilic, I., Kása, P., Dreu, R., Hódi, P. K., Srcic, S., 2009.: *The compressibility and compactibility of different types of lactose*. Drug Development and Industrial Pharmacy, 35 (10), p1271-1280.
- [39] Jiang, T.D., 2001.: *Lignin*. Beijing: Chemical Industry Press.
- [40] Johanson, J. R., 1965.: *A rolling theory for granular solids*. American Society of Mechanical Engineers 32, p842-848.
- [41] Kaliyan, N., Morey, R. V., 2009.: *Factors affecting strength and durability of densified biomass products*. Biomass Bioenergy 33, p337-359.
- [42] Kaliyan, N., and Morey, R. V., 2008.: *Densification characteristics of corn cob*. American Society of Agricultural and Biological Engineers, St. Joseph Michigan.
- [43] Kaliyan, N., and Morey, R. V., 2009b.: *Densification characteristics of corn stover and switchgrass*. Trans. ASABE 52 (3), p907-920.
- [44] Kaliyan, N., Morey, R. V., 2010.: *Natural binder and solid bridge type binding mechanisms in briquettes and pellets made from corn stover and switchgrass*. Bioresour Technol 101, p1082-1090.
- [45] Karimi, K., Shafei, M., and Kumar, R., 2013.: *Progress in physical and chemical pretreatment of lignocellulosic biomass*. In Biofuel Technologies, V. K. Gupta and M. G. Tuohy, Eds., p53-96, Springer, Berlin, Germany.
- [46] Kashaniejad, M, and Tabil, L. G., 2011.: *Effect of microwave- chemical pre-treatment on compression characteristics of biomass grinds*. Biosystems Engineering 108 (1), p36-45.
- [47] Kayisu, K., Hood, F. L., Vansoest, J. P., 1885.: *Characterization of starch and Fiber of Banana Fruit*. Journal of Food Science, Volume 46, p1-6.

- [48] Kawakita, K., and Lüdde, K. H., 1971.: *Some consideration on Powder Compression Equation*. Powder Technology 4, p61-68.
- [49] Korai, H., Nigel, T. P., 2000.: *Properties of Acacia mangium particle board II*, in: Paper Presented at the Proceedings the Fourth Pacific Rim BioBased Composite Symposium., Bogor, November 2-5, p189-194.
- [50] Kristensen, H. G., Holm, P., Schaefer, T., 1985.: *Mechanical Properties of Moist Agglomerates in Relation to Granulation Mechanisms*. Powder Technology 44, p227-237.
- [51] Kumar, R.R., Kolar, K. A., Leckner, B., 2006.: *Shrinkage characteristics of Casuarina wood during devolatilization in a fluidized bed combustor*. Biomass and Bioenergy 30, p153-165.
- [52] Kytö & Äijälä, M., 1981a.: *Use and conversion of wood energy. Part 3. Equipment technology for biomass pelletisation*. Espoo: Technical Research Centre of Finland Research Notes 38/1981.46p. (In Finnish).
- [53] Laureano-Perez, L., Teymouri, F., Alizadeh, H., Dale, B.E., 2005.: *Understanding factors that limit enzymatic hydrolysis of biomass*. Appl. Biochem. Biotechnol., p1081-1099
- [54] Le, Q. D., Doan, T. H., Nguyen, T. M. P., Nguyen, T. M. N., 2011.: *Rice straw and corn stalk in the northern Vietnam as potential lignocellulosic sources for production of bioethanol and other value added products*. Conference paper, 8th Biomass-Asia Workshop.
- [55] Lee, H. V., Hamid, S. B. A., Zain, S. K., 2014.: *Conversion of lignocellulosic biomass to nanocellulose: structure and chemical process*. Sci Word 20.
- [56] Lequart, C., Nuzillard, J., 1999.: *Hydrolysis of wheat bran and straw by an endoxylanase: Production and structural characterization of cinnamoyl- oligosaccharides*. Carbohydrate Research 319, p102-111.
- [57] Li, Y., 2014.: *Studies on cellulose hydrolysis and hemicellulose monosaccharide degradation in concentrated hydrolysis acid*. University of Ottawa.
- [58] Liu Y., Wassgren C., 2016.: *Modifications to Johanson's roll compaction model for improved relative density predictions*. Powder Technology 297, p294-302.
- [59] Lordi, N., Shiromani, P., 1983.: *Use of sorption isotherms to study the effect of moisture on the hardness of aged compacts*. Drug Development and Industrial Pharmacy 9, p1399-1416.
- [60] Maarschalk, K. V., Zuurman, K., Vromans, H., Bolhuis, G.K., Lerk, C.F., 1996.: *Porosity expansion of tablets as a result of bonding and deformation of particulate solids*. Int J Pharm 140 (2), p185-193.
- [61] Macmahon, M. J., 1984.: *Additives for physical quality of animal feed, in Manufacturing of Animal Feed*, ed by Beaven DA. Turret-Wheatland Ltd, Herts, England, p69-70.
- [62] Mahendra, V., Shiro, S., 2011.: *A comparative study of oil Palm and Japanese Beech on Their fractionation and Characterization as Treated by Supercritical Water*. Waste Biomass Valor 2, p309-315.

- [63] Mani, S., Tabil, L. G., and Sokhansanj, S., 2004.: *Evaluation of compaction equations applied to four biomass species*. Can. Biosyst. Eng 46, p355-361.
- [64] Mani, S., Tabil, L. G., and Sokhansanj, S., 2006.: *Effect of compressive force, particle size and moisture content on mechanical properties of biomass pellets from grasses*. Biomass bioenergy 30 (7), p648-654.
- [65] Marrero, T. R., 1999.: *Theory and application of binders: an update*. Proceedings of the Institute for Briquetting and Agglomeration (IBA) 26, p103-109.
- [66] Mcketta, J. J., 1995.: *Encyclopedia of Chemical Processing and Design (Volume 52)*. Published by CRC Press, ISBN 10: 0824726030.
- [67] Mishra, S. K., 1996.: *Hard facing of screw for wear resistance*. Proceedings of the international workshop on Biomass Briquetting, New Delhi.
- [68] Nadhari, W. N. A. W., Hashim, R., Hizirolu, S., Slulaiman, O., Boon, J. G., Salleh, K. M., Awaludin, M. F., Sato, M., Sugimoto, T., 2014. *Measurement of some properties of binderless composites manufactured from oil palm trunks and Acacia mangium*. Measurement 50, p250-254.
- [69] Nielsen, N. P. K., Gardner, D. J., and Felby, C., 2010.: *Effect of extractives and storage on the pelletizing process of sawdust*. Fuel 89 (1), p94-98.
- [70] Nielsen, N. P. K., Gardner, D. J., Poulsen, T., and Felby, C., 2009a.: *Importance of temperature, moisture content, and species for the conversion process of wood residues into fuel pellets*. Wood Fiber Sci 41 (4), p414-425.
- [71] Nyström, C., Alderborn, G., Duberg, M., Karehill, P. G., 1993.: *Bonding surface area an bonding mechanism - two important factors for the understanding of powder compactability*. Drug Development and Industrial Pharmacy 19, p2143-2196.
- [72] Obernberger, I., Thek, G., 2004.: *Physical characterisation and chemical composition of densified biomass fuels with regard to their combustion behavior*. Biomass and Bioenergy 27, p653-669.
- [73] Odogherty, M. J., and Wheeler, J. A., 1984.: *Compression of straw to high-densities in closed cylindrical dies*. J. Agric. Eng. Res 29 (1), p61-72.
- [74] Pedersen, M., and Meyer, A. S., 2010.: *Lignocellulose pretreatment severity-relating pH to biomatrix opening*. New Biotechnology, vol. 27, No. 6, p739-750.
- [75] Pfof, H. B., and Young, L. R., 1973.: *Effect of colloidal binders and other factors on pelleting*. Feedstuffs 45 (49), p21-22.
- [76] Pietsch, W., 1991.: *Size Enlargement by Agglomeration*. John Wiley & Sons Ltd, p115.
- [77] Pietsch, W., 2002. *Agglomeration Processes (Phenomena, Technologies, Equipment)*. Federal Republic of Germany, ISBN 3-527-30369.3.
- [78] Pietsch, W., 2005.: *Agglomeration in Industry Occurrence and Applications*. WILEY-VCH Verlag GmbH & Co. KGaA, Weinheim p 47.

- [79] Pöyry., 2011.: *Pellets - Becoming a global commodity Perspectives on the global pellet market to 2020*. View point report, Pöyry, Vantaa, Finland, p4.
- [80] Révész, P., Hódi, K., Miseta, M., Selmeczi, B., 1991.: *Production of tablets by direct compressing, compressibility of active ingredients and auxiliary materials*. *Gyógyszerészet* 35, p215-218.
- [81] Rhen, C., Gref, R., Sjostrom, M., and Wasterlund, I., 2005.: *Effects of raw material moisture content, densification pressure and temperature on some properties of Norway spruce pellets* *Fuel Process. Technol* 87 (1), p11-16.
- [82] Rowell, R. M., 2012.: *Handbook of wood chemical and wood composites*. 2nd ed. Taylor & Francis.
- [83] Rumpf, H., 1962.: *The strength of granules and agglomerates*. In *Agglomeration* (Knepper, W.A editor), *Proceedings of First International Symposium on Agglomeration*, Philadelphia, Pa., John Wiley and Sons, New York, USA, and London, UK, p379-418.
- [84] Ryu, C., Finney, K., Sharifi, V. N., and Swithenbank, J., 2008.: *Pelletizes fuel production from coal tailings and spent mushroom compost- Part I - Identification of pelletisation parameters*. *Fuel Process. Technol* 89 (3), p269-275.
- [85] Samuelsson, R., Larsson, S. H., Thyrel, M., and Lestander, T. A., 2012.: *Moisture content and storage time influence the binding mechanisms in biofuel wood pellet*. *Applied Energy* 99, p109 - 105.
- [86] Schulze, E., 1891.: *Zur Kenntniss der chemischen Zusammensetzung der pflanzlichen Zellmembranen*. *Ber.Dtsch.Chem.Ges.* 24, p2277-2287.
- [87] Schmidt, M., Pohle, D., Rechtenwald, T., 2007.: *Selective Laser Sintering of PEEK*. *CIRP Annals - Manufacturing Technology* 56 (1), p205-208.
- [88] Schubert, H., 1975.: *Tensile strength of agglomerates*. *Powder Technology* 11, p107-119.
- [89] Schubert, H., 1984.: *Capillary Forces - Modelling and Application in Particulate Technology*. *Powder Technology* 37, p105-116.
- [90] Serrano, C., Monedero, E., Lapuerta, M., and Portero, H., 2011.: *Effect of moisture content, particle size and pine addition on quality parameters of barley straw pellets*. *Fuel Process. Technol* 92 (3), p699-706.
- [91] Sikkema, R., Steiner, M., Junginge, M., Hiegl, W., Hansen, M. T., and Faaij, A., 2011.: *The European wood pellet markets: Current status and prospects for 2020*. *Biofuels Bioprod. Bioref.* 5 (3), p250-278.
- [92] Sjöström, E., 1993b.: *Wood Chemistry*. London, Academic Press 63.
- [93] Sitkei, G., 1994.: *Non-linear rheological method describing compaction processes*. *Int. Agrophysics*, pp.137- 142.
- [94] Sitkei, G., 1997.: *A non-linear viscoelastic-plastic model describing compaction processes*. *Proc. of the 2nd Int. Conf. of IMACS/IFAC Budapest*, pp.105-112.

- [95] Smith, I. E., Probert, S. D., Stokes, R. E., and Hansford, R. J., 1977.: *Briquetting of wheat straw*. J. Agric. Eng. Res 22 (2), p105-111.
- [96] Sokhansanj, S., 2010.: *Bulk density and compaction behavior of knife mill chopped switchgrass, wheat straw, and corn stover*. Bioresource Technology 101, p207-214.
- [97] Sone, T., 1969.: *Consistency of Foodstuffs*. Reidell Publishing Company, Dordecht, Holland.
- [98] Sonnergaard, J. M., 2006.: *Quantification of the compactibility of pharmaceutical powders*. Eur J Pharm Biopharm 63 (3), p270-277.
- [99] Speltter, H., Toth, D., 2009.: *North America's Wood Pellet Sector*. Research Paper FPL-RP-656. Madison, WI: U.S. Department of Agriculture, Forest Service, Forest Products Laboratory, p1.
- [100] Stahl, M., Berghel, J., Frodeson, S., Granstrom, K., and Renstrom, R., 2012.: *Effect on pellets properties and energy use when starch is added in the wood-fuel pelletizing process*. Energy and Fuel 26 (3), p1937-1945.
- [101] Stasiak, M., Molenda, M., Bańda, M., Wiącek, J., Parafiniuk, P., Gondek, E., 2017.: *Mechanical and combustion properties of sawdust-Straw pellets blended in different proportions*. Fuel Processing Technology 156, p366-375.
- [102] Stelte, W., Clemons, C., Holm, K. J., Sanadi, A. R., Shang, L., Ahrenfeldt, J., and Henriksen, B. U., 2012a.: *Fuel pellets from wheat straw: The effect of lignin glass transition and surface waxes on pelletizing properties*. Bioenerg. Res 5 (2), p450-458.
- [103] Stelte, W., Holm, K. J., Sanadi, R. A., Ahrenfeldt, J., and Henriksen, B. U., 2011b.: *Fuel pellets from biomass: The importance of the pelletizing pressure and its dependency on the processing conditions*. Fuel 90 (11), p3285-3290.
- [104] Stelte, W., Holm, K. J., Sanadi, R. A., Barsberg, S., Ahrenfeldt, J., Henriksen, B. U., 2011.: *A study of bonding and failure mechanisms in fuel pellets from different biomass resources*. Biomass Bioenergy 35, p910-918.
- [105] Strauss William., 2017.: *Overview of Global Pellet Markets*. Future Metrics LLC USA, p1-12.
- [106] Stieß, M., 1997.: *Mechanische Verfahrenstechnik 2*. Springer Lehrbuch.
- [107] Tabil, L. G., and Sokhansanj, S., 1996c.: *Process conditions affecting the physical quality of alfalfa pellets*. Am Soc Agric Eng 12 (3), p345-350.
- [108] Tabil, L. G., 1996.: *Binding and pelleting characteristics of alfalfa*. Ph.D. dissertation. Saskatoon, Saskatchewan, CA: Department of Agricultural and Bioresource Engineering, University of Saskatchewan.
- [109] Tabil, L. G., Sokhansanj, S., and Tyler, R. T., 1997.: *Performance of different binders during alfalfa pelleting*. Can Agric Eng 39 (1), p17-23.
- [110] Tarján, G., 1986.: *Mineral Processing (Volume II)*. Akadémiai Kiadó, Budapest, p.606.

- [111] Tarján, I and Csőke, B., 1997.: *The investigation of airing out at compacting fine granular material in press-rolls*. Compernicus, European Economic community, CEEC N₀. CIPA-CT 93-0151 (DG 12 HSMU), p71-90.
- [112] Tarján, I., Csőke, B and Jaitli, J., 1999.: *Investigation of Airing out at Compacting Fine Granular Material*. Challenges of an Interdisciplinary Science - Akadémiai Kiadó, Budapest. Vol 1, p275-284.
- [113] Tran, S. N., Nguyen, T. H. N., Nguyen, H. C., Nguyen, V. C. N., Le, H. V., and Ingvorsen, K., 2014.: Ước tính lượng và các biện pháp xử lý rom rạ ở một số tỉnh đồng bằng sông cửu long. Tạp chí Khoa học Trường Đại học Cần Thơ, 32, p87-93.
- [114] Tumuluru, S. J., Wright, T. C., Hess, R. J and Kenney, L. K., 2010.: *A Review on Biomass Densification Technologies for Energy Application*. Idaho National Laboratory Biofuels and Renewable Energy Technologies Department Energy Systems and Technologies Division Idaho Falls, Idaho 83415, p1-96.
- [115] Tumuluru, S. J., Wright, T. C., Hess, R. J and Kenney, L. K., 2011.: *A review of biomass densification systems to develop uniform feedstock commodities for bioenergy application*. Biofuels, Bioprod. Bioref 5, p683-707.
- [116] Unsal, O., Kartal, S. N., Candan, Z., Arango, R. A., Clausen, C. A., Iii, F. G., 2009.: *Decay and termite resistance, water absorption and swelling of thermally compressed wood panels*. Int. Biodeter. Biodegrad 63 (5), p548-552.
- [117] Van Dam, J. E. G, Van Den Oever, M. J. A., Teunissen, W., Keijsers, E. R. P., Peralta, A. G., 2004.: *Process for production of high density/high performance binder-less boards from whole coconut husk Part I: lignin as intrinsic thermosetting binder resin*. Industrial Crops and Products 19, p207-216.
- [118] Vanengelenhoven, J., 2011.: *Energy tablet-making machine for biomass*. [Online]. US Department of Energy. Available at: <http://www.columbiamissourian.com> [June 22, 2011].
- [119] Walker, E. E., 1923.: *The Properties of Powders-Part VI: The compressibility of powder*. Transactions of the Faraday Society 19, p73-82.
- [120] Yang, S. H., 2008.: *Plant fiber chemistry*. Beijing: China Light Industry Press.
- [121] Yehia, K. A, 2007.: *Estimation of roll press design parameters based on the assessment of a particular nip region*. Powder Technol 177, p148-153.
- [122] Yman, S., 2004.: *Pyrolysis of biomass to produce fuels and chemical feedstocks*. Energy Convers Manage 45, p651-671.
- [123] Yu, J., Paterson, N., Blamey, J., Millan, M., 2017.: *Cellulose, xylan and lignin interactions during pyrolysis of lignocellulosic biomass*. Fuel 191, p140-149.
- [124] Zabaniotou, A. A., 1999.: *Pyrolysis of forestry biomass by-products in Greece*. Energy Sources Part A: Recovery Util Environ Eff 21, p395-403.
- [125] Zafari, A., Kianmehr, H. M., 2012.: *Effect of raw material properties and die geometry on the density of biomass pellets from composted municipal solid waste*. Bio-Resources 7 (4), p4704- 4714.

[126] Zhang, X., Cai, Z., Chen, L., Zhang, D., and Zhang, Z., 2016.: *Effect of Moisture content and Temperature on the Quality of Water Hyacinth Pellets*. *Bio-Resources* 11 (1), p1407-1416.

[127] Zhu, F., Zhang, Y., Wang, W. Z., 2017.: *Study on the thermal expansion coefficient of athermalization infrared lens' thermal compensation element*. *Advances in Materials Science, Energy Technology and Environmental Engineering- Patty& Zhou (Eds)*. Taylor & Francis Group, London, ISBN 978-1-138-19668-1, p93-98.

APPENDIX I: Reproducibility examination

Speed of piston: v [mm/s]

Average of piston speed: \bar{v} [mm/s]

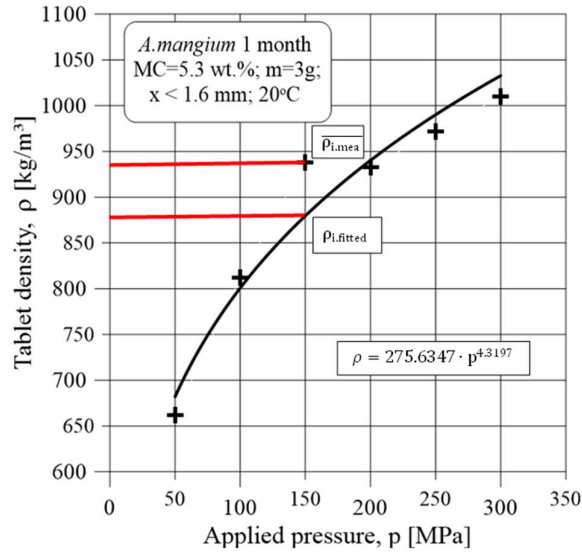
Standard deviation in the case of different speed of piston: V_T [mm/s]

$$V_T = \sqrt{\frac{\sum_{i=1}^n (v_i - \bar{v})^2}{n-1}} \text{ [mm/s]}$$

Relative deviation: V'_s [%]

$$V'_s = 100 \cdot \frac{V_T}{\bar{v}} \text{ [%]}$$

APPENDIX II: Correlation examination



The tablet density values $\overline{\rho_{i.meas}}$ are recorded as an average of three measurements

Standard deviation in the case of different tablet parameters: ρ_s [kg/m³]

$$\rho_s = \sqrt{\frac{1}{n-1} \sum_{i=1}^n (\rho_{i.fitted} - \overline{\rho_{i.meas}})^2} \text{ [kg/m}^3\text{]}$$

n is the number of data points

The tablet density fitted values: $\rho_{i.fitted}$ [kg/m³]

Spread deviation: V_s [%]

$$V_s = 100 \cdot \frac{\rho_s}{\overline{\rho_{i.fitted}}} \text{ [%]}$$

Coefficient of determination: R^2 [-]

Residual mean square: σ [kg/m³].